

**A STUDY ON THE EFFECT OF HEAT ON PROPERTIES
OF REINFORCING STEEL BARS MADE FROM SCRAP
METAL**

JOSEPHAT OBWOGE BANGI

**MASTER OF SCIENCE
(Mechanical Engineering)**

**JOMO KENYATTA UNIVERSITY OF
AGRICULTURE AND TECHNOLOGY**

2015

A Study on the Effect of Heat on Properties of Reinforcing Steel Bars
made from Scrap Metal

Josephat Obwoye Bangi

A thesis submitted in partial fulfilment of the requirements for the award of the
Degree of Master of Science in Mechanical Engineering in the Jomo Kenyatta
University of Agriculture and Technology

2015

DECLARATION

This thesis is my original work and has not been presented for a degree in any other university.

Sign.....Date.....

Josephat O. Bangi

This thesis has been submitted for examination with our approval as the University supervisors:

Sign.....Date.....

Prof. S. M. Maranga (JKUAT-Kenya)

Sign.....Date.....

Prof. S. P. Ng'ang'a (JKUAT-Kenya)

Sign.....Date.....

Prof. Stephen M. Mutuli (UoN- Kenya)

Dedication

I dedicate this work to my family.

My Wife Alice

My Children: Joanne Obwoye, Angela Obwoye, and Alpha Obwoye

For their unchanging love and pride in me

ACKNOWLEDGEMENTS

The author wishes to record his appreciation for the support and guidance provided by Prof. Eng. S. M. Maranga, Prof. Eng. S. P. Ng'ang'a and Prof. Eng. S. M. Mutuli, while supervising this project. Their encouragement, suggestions and time spent in discussion have been much appreciated.

I also extend my gratitude to Dr. Li Rongfeng and Dr. Peng Wenjie both from Wuhan Iron and Steel, China for the use of their facilities and their role in fatigue testing, Mr. S. Njue of the UoN for guidance in microscopy, several working colleagues at KEBS for their various roles as follows; Mr. T. Atacha and Mr. J. Kimani from the engineering workshop for the preparation of test specimens, Mr. G. Onguso for his role in tensile testing and Ms Tabitha Orwa for her assistance in the chemical analysis.

Special thanks to my employer, Kenya Bureau of Standards, who granted me leave to pursue my graduate studies, funded my trip to China to conduct fatigue experiments, and made available testing facilities for tensile, hardness, and chemical analysis. Special thanks also go to the steel mills responsible for providing the steels that were used in this study.

My thanks also go to my fellow postgraduate students and staff in the School of Mechanical, Manufacturing and Materials Engineering for all

the mind stimulating discussions we had and assistance in various issues regarding this work.

To my parents, Bangi and Truphena, this work is actually an answer to your encouragement and unfailing prayers. Thank you also for teaching me the value of hard work by your own example.

Finally, I would like to thank the most important people of my life, my wife Alice, my two daughters, Joanne and Angela and my son Alpha for their friendship, constant love, support which has always kept me striving to reach my goals.

TABLE OF CONTENTS

DECLARATION	ii
DEDICATION	iii
ACKNOWLEDGEMENTS	iv
TABLE OF CONTENTS	vi
LIST OF TABLES	xiv
LIST OF FIGURES	xvii
LIST OF PLATES	xx
LIST OF APPENDICES	xxi
LIST OF ABBREVIATIONS	xxi
NOTATIONS	xxiv
ABSTRACT	xxvi
Introduction	1
1.1 Preface	1
1.2 Overview on steels	1
1.3 Uses of steel	2

1.4 Sources of Iron and steel scrap	3
1.5 Heat treatment of steel	3
1.6 Alloy steels	5
1.7 The steel market	6
1.8 Scrap Market Description	7
1.8.1 Scrap Metal Act, 2014	8
1.8.2 Benefits of using scrap metal	9
1.9 Quality Control in the steel industry	10
1.10 Use of scrap in other economies	10
1.11 Problem Statement	11
1.12 Justification of the study	14
1.13 Objectives of the study	14
1.13.1 Main Objective	14
1.13.2 Specific objectives/tasks	14
1.14 Scope of the research	15
1.15 Research Questions	15
1.16 Outline of thesis	16
Literature Review	17
2.1 Introduction	17
2.2 Fatigue failure	17
2.2.1 How to determine the fatigue strength of a metal	19

2.3	Definitions of terms related to fatigue	21
2.4	Factors affecting fatigue life	22
2.4.1	Effect of average stress on fatigue	23
2.4.2	Effect of stress concentrators	24
2.4.3	Effect of the level of inclusions	25
2.4.4	Effect of grain size and grain direction	26
2.4.5	Effect of the microstructure on fatigue strength	27
2.4.6	Initiation of microcracks	27
2.4.7	Crack propagation	28
2.5	Review of the previous work on fatigue in rebars	28
2.6	Steel production processes	40
2.6.1	Steel Production from Iron Ore	42
2.6.2	Steel Production from Scrap Metals	42
2.7	Effects of Chemical Composition on Mechanical Properties	43
2.8	Effect of heat on mechanical properties of rebars	45
	Methodology	51
3.1	Introduction	51
3.2	Survey	51
3.3	Sampling and Number of Specimens	52
3.4	Heating and cooling of the specimens	53
3.5	Chemical composition analysis	55

3.5.1	Microstructure Characterization	56
3.5.2	Metallographic Sample Preparation	56
3.5.3	Grain Size Measurements	58
3.6	Tensile testing	58
3.6.1	Test equipment	58
3.6.2	Test Specimens	60
3.6.3	Test Procedure	63
3.7	Brinell hardness test (HBW)	64
3.7.1	Test equipment	64
3.7.2	Test Specimen	65
3.7.3	Test Procedure	65
3.8	Impact test	66
3.8.1	Test equipment	66
3.8.2	Test specimens	66
3.8.3	Test Procedure	68
3.9	Fatigue Testing	69
3.9.1	Introduction	69
3.9.2	Test equipment	69
3.9.3	Test specimens	70
3.9.4	Test procedure	71
3.9.5	Challenges in gripping of as received rebars	72

3.9.6	Criterion of failure and test termination	73
3.9.7	S-N Plots of Stress versus Fatigue Life	74
3.10	Data Acquisition	74
Results and Discussion	79
4.1	Introduction	79
4.2	Results from the Survey	79
4.2.1	Quality Control	79
4.2.2	Production Methods	80
4.2.3	Survey results from KEBS	83
4.2.4	Industrial Visits	83
4.3	Chemical compositions	85
4.4	Comparison of test results from Mill A and Mill B - Air cooling	87
4.5	Effect of Heat on Mechanical Properties and Microstructure - Air cooling	88
4.5.1	Yield stress (R_e)	89
4.5.2	Tensile Strength (R_m)	91
4.5.3	Elongation	92
4.5.4	Modulus of Elasticity (E)	93
4.5.5	Brinell Hardness (HBW)	94
4.5.6	Effect of Heat on Microstructure and grain size	95

4.6	Comparison of test results from Mill A and Mill B -Water Quenching	96
4.6.1	Yield Stress Vs Temperature for water quenched re- bars from Mills A and B	96
4.7	Effect of Heat on Mechanical Properties and Microstructure - Water quenching	97
4.7.1	Yield stress (R_e)	98
4.7.2	Tensile Strength (R_m)	100
4.7.3	Elongation	101
4.7.4	Modulus of Elasticity (E)	102
4.7.5	Brinell Hardness (HBW)	103
4.7.6	Effect of Heat on Microstructure and grain size	104
4.8	Comparison on (R_e), (R_m) and BHW Vs Temperature for air and water cooled rebars from Mills A	106
4.9	Charpy V-notch impact tests	106
4.10	Fatigue Testing	108
4.10.1	Comparison with AASHTO Fatigue Design Criteria	110
4.10.2	Comparison of fatigue properties of the ribbed 12 mm rebars with standards	111
4.11	Estimating the fatigue strength for rebars based on low-cost test	112

4.11.1	Dependent correlation of impact toughness, hardness, and tensile strength	113
4.11.2	Dependent correlation of toughness, chemical com- position and tensile strength	113
4.11.3	Dependent correlation of the toughness, strength ra- tio and hardness	114
	Conclusions and Recommendations	129
5.1	Introduction	129
5.2	Conclusions	129
5.3	Recommendations	131
	References	133
5.4	Definitions of terms related to fatigue	0
	Glossary	0
	Questionnaire to steel rolling mills	3
	Questionnaire to KEBS	17
	Tabulated results on the Effect of Heat on Mechanical Properties and Microstructure - Air cooling	27

Tabulated results on the Effect of Heat on Mechanical Properties and Microstructure - Water quenching	30
Determining Sample Size for rebars	33
E.1 Using Published Tables	33
E.2 Using formulas to calculate a sample size	34
E.2.1 Formula for calculating a sample for proportions . .	65
E.3 Selecting a Sampling Plan for Reinforcement Bars	65
Published Papers	67
F.1 Paper I	67
F.2 Paper II	67
Appendices	3

LIST OF TABLES

Table 2.1	Steel production by process	42
Table 3.1	Sample Frequency	53
Table 4.1	A summary of responses from the questionnaires on quality control of rebars	81
Table 4.2	A summary of responses from the questionnaires on production methods of rebars	82
Table 4.3	A Summary of responses from KEBS on quality con- trol	84
Table 4.4	Chemical Composition of 12 mm rebar from mill A (wt. %)	85
Table 4.5	Chemical Composition of 16 mm rebar from Mill A (wt. %)	85
Table 4.6	Chemical Composition of 16 mm rebar from mill B (wt. %)	86
Table 4.7	Charpy V-Notch (CVN) test in Joules for 12 and 16 mm rebars	107
Table 4.12	Output data for the correlation of toughness, yield- tensile ratio and Brinell hardness	114

Table C.1	Mechanical properties of 10 mm rebar cooled in air from mill A	27
Table C.2	Mechanical properties of 10 mm rebar cooled by air from mill B	27
Table C.3	Mechanical properties of 12 mm rebar cooled in air from mill A	28
Table C.4	Mechanical properties of 12 mm rebar cooled by air from mill B	28
Table C.5	Mechanical properties of 16 mm rebar cooled in air from mill A	28
Table C.6	Mechanical properties of 16 mm rebar cooled in air from mill B	29
Table D.1	Mechanical properties of 10 mm rebar quenched in water from mill A	30
Table D.2	Mechanical properties of 10 mm rebar quenched in water from mill B	30
Table D.3	Mechanical properties of 12 mm rebar quenched in water from mill A	31
Table D.4	Mechanical properties of 12 mm rebar quenched in water from mill B	31

Table D.5	Mechanical properties of 16 mm rebar quenched in water from mill A	31
Table D.6	Mechanical properties of 16 mm rebar quenched in water from mill B	32
Table E.1	Guidelines for the selection of the minimum number of specimens and the associated degree of replication	34
Table E.2	Chemical composition (maximum % by mass)	66
Table E.3	Test stress ranges for nominal bar sizes	66

LIST OF FIGURES

Figure 2.1	Standard fatigue specimen (dimensions in mm)	20
Figure 2.2	Typical S-N curves	22
Figure 2.3	Ratio of endurance limit to tensile strength Vs tensile strength for various metals	23
Figure 2.4	Electric arc furnaces (EAF)	43
Figure 3.1	Grain Analysis via the Intercept method.	59
Figure 3.2	Standard full size Charpy V-notch specimen	68
Figure 4.1	Yield Stress Vs Temperature for air cooled rebars from Mills A and B	89
Figure 4.2	Tensile Strength Vs Temperature for air cooled re- bars from Mills A and B	115
Figure 4.3	Brinell Hardness Vs Temperature for air cooled re- bars from Mills A and B	116
Figure 4.4	Yield stress Vs Temperature for air cooled rebars .	117
Figure 4.5	Tensile strength Vs Temperature for air cooled rebars	117
Figure 4.6	Elongation ratio Vs Temperature for air cooled rebars	118
Figure 4.7	Modulus of Elasticity Vs Temperature for air cooled rebars	118
Figure 4.8	Brinell hardness Vs. Temperature for air cooled rebars	119

Figure 4.9	Optical micrographs (400x) of various heated and air cooled rebars.	120
Figure 4.10	Yield Stress Vs Temperature for water quenched rebars from Mills A and B	121
Figure 4.11	Tensile Strength Vs Temperature for water quenched rebars from Mills A and B	122
Figure 4.12	Brinell Hardness Vs Temperature for water quenched rebars between Mills A and B	123
Figure 4.13	Yield stress Vs Temperature for water quenched rebars	124
Figure 4.14	Tensile strength Vs Temperature for water quenched rebars	124
Figure 4.15	Elongation ratio Vs Temperature for water quenched rebars	125
Figure 4.16	Modulus of Elasticity Vs Temperature for water quenched rebars	125
Figure 4.17	Brinell hardness Vs Temperature for water quenched rebars	126
Figure 4.18	Optical micrographs (400X) of various heated and water quenched rebars.	127
Figure 4.19	Micrographs (400X)	128
Figure 5.1	Load cycle diagram	1

Figure 5.3	Important dimensions of ribbed bar	1
Figure 5.4	Ribbed bar, α - Transverse rib angle; β - angle between the rib and the axis of bar; h -height of midpoint of a bar; l -rib distance; b - rib top width; f_1 - rib spacing	1
Figure 5.2	Ribbed bar	2

LIST OF PLATES

1	Electric Furnace	55
2	Wet cutting machine Jean Wirtz CUTO 20	57
3	UTM being calibrated before use	61
4	Grips of the UTM with specimen	62
5	Rebars samples used in the study	63
6	Universal hardness tester	67
7	Charpy-V Impact tester	67
8	The servohydraulic testing machine with clamped test specimen	76
9	The MTS 810 fatigue machine with a specimen fractured at the centre	77
10	Research and Development Centre of Wuhan Iron and Steel China	78
11	Test specimen covered by aluminum in the two ends	78

LIST OF APPENDICES

Abbreviations

AASHTO	American Association of State Highways and Transportation Officials
ACI	American Concrete Institute
AISI	American Institute of Steel Industry
ASTM	American Society of Testing and Materials
BOF	Basic Oxygen Furnace
BS	British Standard
COMESA	Common Market for Eastern and Southern Africa
DRI	Directly Reduced Iron
EAC	East African Community
EAF	Electric Arc Furnace
GIA	Global Industry Analysts
GoK	Government of Kenya
IEA	International Energy Agency
IISI	International Iron and Steel Institute
ISO	International Organization for Standardization
JKUAT	Jomo Kenyatta University of Agriculture and Technology
KEBS	Kenya Bureau of Standards
KS	Kenya Standard
MTS	Material Testing Systems

NDT	Non Destructive Testing
OECD	Organisation for Economic Co-operation and Development
OHF	Open Hearth Furnace
OMM	Optical Metallurgical Microscope
Rebar	Reinforcing steel bar
UoN	University of Nairobi
UTM	Universal Testing Machine
USGS	United State Geological Survey

Notations

A_{gt}	Percentage total extension at maximum force
CVN	Charpy V-Notch impact toughness [Joules]
C_p	Chemical composition
d or D	Nominal diameter of the bar [mm]
d_n	Grain Size (μm)
E	Modulus of Elasticity [GPa]
EL	Elongation (%)
f	Frequency of load cycles in the fatigue test [Hz]
h	Rib height [mm]
HBW	Brinnell hardness number
K_t	Stress concentration factor
M	Population proportion
n	Sample Size
N	Number of cycles
N_f	Cycles to failure
r/h	Ratio of base radius of rebar to height of rolled-on transverse deformations
R	Stress ratio
$R_{P0.2}$	0.2 % proof strength, non proportional extension [GPa]
R_e	Yield stress [GPa]

\mathbf{R}_m	Ultimate Tensile strength [GPa]
$\mathbf{R}_m/\mathbf{R}_e$	Ratio tensile strength/yield strength
\mathbf{R}_r	Relative rib area [mm]
\mathbf{T}	Temperature, °C
σ	Stress [GPa]
σ_a or \mathbf{S}	Stress amplitude [GPa]
σ_e	Endurance fatigue limit [GPa]
σ_m	Mean stress (MPa)
σ_{max}	Maximum stress in a stress cycle [GPa]
σ_{min}	Minimum Stress in a stress cycle [GPa]

ABSTRACT

Fatigue performance of ribbed reinforcing bars (rebars) in concrete structures is of great interest to designers. This is because structures are becoming more slender, the traffic volume is increasing, the axle loads are larger, and the traffic speed limits are higher, the margin of reserve strength is progressively being reduced and the loading cycles are becoming more severe. Also the deterioration of mechanical properties of rebars at elevated temperature is of primary concern to the design and analysis of steel structures exposed to fire.

However, data on fatigue performance and effect of heat on mechanical properties of rebars made from local metal scrap is unknown. Hence, a study was conducted to investigate fatigue strength and the effect of heat on mechanical properties of rebars made from local scrap metal against published standards.

Fatigue was investigated using as-received 12 mm rebar specimens with 370 mm length. Axial load fatigue tests in air were conducted at room temperature using a stress ratio of 0.2 and 25 Hz at maximum stress amplitudes of 132, 136, 140, and 144 MPa until failure occurred using a MTS machine and thereafter S-N curves were plotted.

Separately, experiments were conducted to establish the effect of heat on mechanical properties. Eighty four specimens were prepared from 10,

12 and 16 mm rebars since these sizes are widely used in Kenya. Six specimens each (two from each diameter size) were heated in an electric furnace to temperatures ranging from 22 to 1000°C for one hour. At the end of the curing processes, three heated specimens (one per diameter size) were cooled in air while the remaining three were quenched in water for 15 minutes. Thereafter, the changes in mechanical properties (Yield stress, Tensile Strength, Percentage Elongation and Modulus of Elasticity) were determined using a UTM. Brinell hardness testing was performed using a universal Hardness tester, while Charpy-V impact tests was investigated using a Wolpert impact tester. To correlate mechanical properties to microstructural characteristics, metallographic analysis and grain size determination was studied using an optical microscope. Curves of Yield stress, tensile strength, percentage elongation, Modulus of Elasticity and Brinell hardness versus temperature were plotted and compared with the results obtained from the as-received rebars. The results show that the 12 mm rebar had a fatigue life of 1.8×10^6 cycles at a stress amplitude of 132 MPa hence the rebar did not meet the requirements of the standards. Other results show that normal mechanical properties can be assumed after exposure to temperatures below 500°C for one hour. Yield stress, tensile strength, Modulus of Elasticity, Brinell hardness and ductility of the rebars decreased with air cooling.

However, with water quenching after heating from 500 to 1000°C, the Yield stress, tensile strength and Brinell hardness increased while ductility and Modulus of Elasticity decreased. Variation of the microstructure occurred as temperature increased from 22 to 1000°C, whereby the grain size reduced from 18.9 to 13.7 μm and from 18.9 to 12.0 μm for air and water cooled specimens, respectively. Different rebar sizes and different steel mills showed varied mechanical properties. The 12 and 16 mm rebars exhibited superior impact toughness properties and chemical composition was found not to have a remarkable effect on fatigue and mechanical properties.

The higher gripping pressure needed to prevent the rebars from slipping during fatigue testing caused some of the rebars to break in the grips but aluminium tubing was used to protect the gripped ends.

The study provides precise information to the steel producers, designers, building industry and finally to the standardization bodies both at the national and international level. The results may also be used to support other research projects aimed at studying the behaviour of rebar steel structures exposed to extreme temperatures.

CHAPTER 1

Introduction

1.1 Preface

This chapter examines background information on steel and its uses. It describes the sources of iron and steel scrap, heat treatment, effects of chemical composition on mechanical properties, steel market, scrap metal market and the benefits of using scrap metal. It further discusses the quality control in the steel industry, and the use of scrap in other economies. The problem statement, justification, objectives, scope of the study and the hypothesis are also stated.

1.2 Overview on steels

Steel is an alloy of iron with definite percentage of carbon ranges from 0.15-1.5% [1], plain carbon steels are those containing 0.1-0.25% [2] There are two main reasons for the popular use of steel: (1) It is abundant in the earth's crust in form of Fe_2O_3 and little energy is required to convert it to Fe. (2) It can be made to exhibit great variety of microstructures and thus a wide range of mechanical properties. Although the number of steel specifications runs into thousands, plain carbon steel accounts for

more than 90% of the total steel output. The reason for its importance is that it is a tough, ductile and cheap material with reasonable casting, working and machining properties, which is also amenable to simple heat treatments to produce a wide range of properties [3]. They are found in applications such as train railroads, beams for building support structures, reinforcing rods in concrete, ship construction, tubes for boilers in power generating plants, oil and gas pipelines, car radiators, cutting tools etc [2]

1.3 Uses of steel

Iron and steel are used widely in the construction of road structures, railways, buildings and manufacture of wire products such as barbed wire, chain link and nails. Most large modern structures, such as stadiums and skyscrapers, bridges, and airports, are supported by a steel skeleton. Even those with a concrete structure will employ steel for reinforcing. In addition, steel has widespread use in major appliances and cars. It is also used in making a variety of other construction materials such as bolts, nails, and screws. Other applications include ship building, pipeline transport, mining, construction, aerospace, white goods (e.g., washing machines), heavy equipment such as bulldozers, office fur-

niture, steel wool, tools, and armour in the form of personal vests or vehicle armour. In the construction industry, steel used is classified as either mild steel or high yield steel. Mild steel is normally used for manufacturing mild steel bars, cold worked steel bars and hot rolled steel sections.

1.4 Sources of Iron and steel scrap

The main sources of iron and steel scrap come from the construction and transportation sectors. Mechanical engineering applications such as tube and metal ware are also the other main sources of old scrap.

1.5 Heat treatment of steel

Heat treatment is a combination of timed heating and cooling applied to a particular metal or alloy in the solid state in such ways as to produce certain microstructure and desired mechanical properties (hardness, toughness, Yield stress, ultimate tensile strength, Young's modulus, percentage elongation and percentage reduction).

Annealing, normalising, hardening and tempering are the most important heat treatments often used to modify the microstructure and mechanical properties of engineering materials particularly steels. Anneal-

ing is the type of heat treatment most frequently applied in order to soften iron or steel materials and refines its grains due to ferrite-pearlite microstructure; it is used where elongations and appreciable level of tensile strength are required in engineering materials [4].

In normalising, the material is heated to the austenitic temperature range and this is followed by air cooling. This treatment is usually carried out to obtain a mainly pearlite matrix, which results into strength and hardness higher than in as received condition. It is also used to remove undesirable free carbide present in the as-received sample [3]. Steels are normally hardened and tempered to improve their mechanical properties, particularly their strength and wear resistance. In hardening, the steel or its alloy is heated to a temperature high enough to promote the formation of austenite, held at that temperature until the desired amount of carbon has been dissolved and then quench in oil or water at a suitable rate. Also, in the harden condition, the steel should have 100% martensite to attain maximum Yield stress, but it is very brittle too and thus, as quenched steels are used for very few engineering applications.

By tempering, the properties of quenched steel could be modified to decrease hardness and increase ductility and impact strength gradually. The resulting microstructures are bainite or carbide precipitate in a ma-

trix of ferrite depending on the tempering temperature.

1.6 Alloy steels

Steels are alloys of iron and carbon. They are widely used in construction and other applications because of their high tensile strengths and low costs [5]. Steel can be cast into bars, strips, sheets, nails, spikes, wire, rods or pipes as needed by the intended user [6].

The carbon in typical steel alloys may contribute up to 2.1% of its weight. Varying the amount of alloying elements, their formation in the steel either as solute elements, or as precipitated phases, retards the movement of dislocations that make iron so ductile and weak, or therefore controls qualities such as the hardness, ductility, and tensile strength of the resulting steel. Steel's strength compared to pure iron is only possible at the expense of ductility [5].

The carbon content of steel is between 0.002% and 2.1% by weight for plain iron-carbon alloys [7]. Carbon contents higher than those of steel make an alloy commonly called pig iron that is brittle and unmalleable. Alloy steel is steel to which alloying elements have been intentionally added to modify the characteristics of steel [7].

Common alloying elements include: manganese, nickel, chromium, molyb-

denum, boron, titanium, vanadium, and niobium. Additional elements may be present in steel: phosphorus, sulfur, silicon, and traces of oxygen, nitrogen, and aluminium [7].

Alloys with carbon content greater than 2.1%, depending on other element content and possibly on processing, are known as cast iron. Steel is also distinguishable from wrought iron which may contain a small amount of carbon but large amounts of slag [7].

1.7 The steel market

Steel is not a homogenous product. Due to impurities in the scrap, scrap-based routes are not always able to meet the same high quality standards as an ore-based process. Moreover, the capacity of electric arc furnace plants is normally not large enough for them to compete in certain product segments, such as the production of flat products. Hence, it is appropriate to treat BOF steel and EAF steel as differentiated products [8].

Price data on steel exports from different regions show substantial variations also within each of these product categories. This may indicate either that the quality of the steel product differs across regions or that there is regional specialization in different product segments. A natural

implication is to treat steel from different regions as imperfect substitutes.

Steel demand is recognized to be relatively irresponsive to changes in steel prices [9]. An increase in steel production costs can therefore to some extent be passed on to steel consumers. However, price increases are constrained by the competition from substitute materials, such as concrete, aluminium, wood, etc. Climate policies will most likely also increase the production costs of some of the major competing materials [8].

1.8 Scrap Market Description

Iron and steel are manufactured from iron ore and scrap. Scrap has become increasingly important to the steel industry. Recycling steel is technologically possible and economically profitable. In consequence, a significant industry has developed to collect old and new scrap. Global Industry Analysts (GIA) [10] have reported that the global steel scrap market is projected to reach 631.5 million tons by 2015. Scrap metals can be recycled and used again for an indefinite period, resulting in protection and preservation of some of nature's most limited resources. It is always cheaper to recycle steel than to mine virgin ore and move

it through the process of making new steel. New scrap arises from pre-consumer sources and old scrap is generated from post-consumer sources. New scrap comes from all stages of industrial processing. It is generated within steel mills and foundries or industrial plants while making iron and steel products. Old scrap comes from many different products, both consumer and industrial and is composed of objects that no longer have further use. The North American steel industry's overall recycling rate is around 55-60% [11]. The major consumers of scrap are steel mills and ferrous foundries [12]. Scrap has become increasingly important to the steel industry. In Kenya, the main sources of steel are recycled scrap and imports. The Government of Kenya banned the exportation of scrap steel in its 2009/2010 budget speech [13] and this has been followed by enacting of the Scrap Metal Act, 2014 [14]. This should spur recycling of local scrap metal in 40 steel rolling mills operating in Kenya. Government statistics indicated that Kenya's annual demand for steel is estimated at between 480 000 and 600 000 tons a year [15]

1.8.1 Scrap Metal Act, 2014

The major purpose of the Bill is to make provision for the regulation of dealings in scrap metal as well as provide for the creation of a Scrap Metal Council and for connected purposes [14]. The Bill will stem the

tide against theft and vandalism of valuable public infrastructural assets like power cables, transformers, storm and sewer manhole covers.

1.8.2 Benefits of using scrap metal

Steel is the world's most recycled material [16]. This is done for economic as well as environmental reasons. Steel mill using scrap steel in place of virgin iron ore to make a new product gives the public outstanding value. Every tonne of new steel made from scrap steel saves 1,115 kg of iron ore, 625kg of coal, and 53kg of limestone [16]. Recycling conserves ever-diminishing landfill space and the surface biodiversity destroyed in mining of new raw materials from the ground. It closes the resources loop ensuring valuable resources are not lost, but are put back into good use. The metals made from these 'secondary resources' then make much less impact in the remanufacturing process the second time around.

Recycling is a true example of a 'sustainable' industry - a concept fundamental to our society's drive to reduce its environmental impact on the planet.

Metals' recycling protects the environment and saves energy. Using secondary raw materials means less use of natural resources which would otherwise be needed to make new metal compounds - such as iron ore in steelmaking; nickel in stainless steel; or alumina and bauxite in alu-

minium smelting.

There are also considerable savings in energy, and reduced CO₂ emissions, in production methods using recycled materials: The Environmental Protection Agency estimates that steel production using recycling scrap to make steel and aluminum uses about 74% less energy than the production of steel from iron ore [17]. European Union figures indicate that using recycled raw materials, including metals, cuts CO₂ emissions by some 200 million tonnes every year [16].

1.9 Quality Control in the steel industry

To specify the various physical and mechanical properties of the finished product, various tests, both destructive and nondestructive, are performed. Some of the major tests performed by quality control personnel include; metallurgical, hardness, hardenability, tension, ductility, compression, fatigue, impact, wear, corrosion, creep, machinability, radiography, magnetic particle, ultrasonic, and eddy current.

1.10 Use of scrap in other economies

Improving sales in the automobile industry and enhanced construction activity, the hardest hit segments due to recession, are expected to fuel

demand for scrap steel. Steel scrap's favorable impact on the economic is also expected to boost the consumption levels in steel making industry. Statistics show that metal and steel products are currently Kenya's largest manufactured goods exported within the COMESA and the EAC [15]

1.11 Problem Statement

Under normal conditions, rebars are subjected to a range of temperature no more severe than that imposed by ambient environmental conditions. However, there are important cases where these rebars may be exposed to much higher temperatures (e.g., building fires, heat assisted bending, industrial applications in which the rebar is in close proximity to furnaces, and some nuclear power-related postulated accident conditions). The failure of the World Trade Centre is a good example of failure under fire conditions [18].

Deformed bars have ridges, projections or ribs on their surface to provide better anchoring for concrete. The ribbed surface provides a better bond with the concrete compared to the twisted bar where the concrete may slip causing cracks. Internationally, twisted bars have been phased out for use in structural reinforcement of concrete due to their poor bonding

and structural properties

The requirements for reinforcing bar deformation patterns used in the United States given in ASTM A615/615M [19], ASTM A996/A996M [20], and A706/706M [21] were established over fifty years ago based on work by Clark [22]. Although a great deal of work has been learned about the behaviour of reinforced concrete members since that time, the requirements have not been updated accordingly.

Also, many reinforced concrete structures such as storey building, highway pavements, highway bridges, railroad bridges, airport pavements and bridges, offshore structures and slender towers, etc., are subjected to dynamic loads. It is possible, for reinforcement bars to fail without any outward signs of structural distress except local cracking of the concrete. In the AASHO road experiment, fatigue fractures occurred in overload tests on concrete bridges [23]. Here reinforcement bars in the outer beams of two reinforced concrete structures were fractured after about 730 000 cycles at different loads and comparisons with laboratory data indicated that the lives were shorter than expected.

There have been excellent reviews of many aspects of the fatigue of reinforcement steel bars written mainly as aids to the design engineer [24–28]. In the review by Menzies [29], it was found that there was a scarcity of data for fatigue of British reinforcement bars and it was necessary to

base design proposals largely on data for European steels. Since this review, a considerable number of investigations have been reported and data have become available for British steels. A number of new investigations have been commenced albeit mainly concerned with marine environments [30].

Fatigue strength data of rebars made from local scrap metal that are used in these structures for obtaining their safe, effective and economical design are needed.

Another issue of primary concern is that, both concrete and steel undergo considerable change in their strength, physical properties, and stiffness after exposure to heat, and some of these changes are not recoverable after subsequent cooling [31].

In spite of the wide use of rebars in the construction industry in the country, no studies have been published on fatigue strength and the effect of heat on mechanical properties of rebars made from recycled local scrap metal. The current study therefore is timely as it provides data in regard to fatigue strength and the effect of heat on mechanical properties (Yield stress, tensile strength, percentage elongation and Modulus of Elasticity) of rebars made from local scrap.

1.12 Justification of the study

This study provides information to the steel producers, designers, building industry and to the standardization bodies both at the national and international level on the fatigue performance of rebars made from local metal scrap in order to have safe, economical, and easily applicable design methods for reinforcement steel members subjected to building fires, which normally reach temperatures of about 1000°C. The results may also be used to support other research projects aimed at studying the behaviour of rebar steel structures exposed to extreme temperatures.

1.13 Objectives of the study

1.13.1 Main Objective

- To investigate the fatigue strength and the effect of heat on rebars made from local scrap metal and heated to various temperatures, and thereafter, cooled in different media (air and water).

1.13.2 Specific objectives/tasks

- To obtain information on quality control and production methods of the rebars used in the construction industry.

- To determine the chemical composition of the rebars to be tested.
- To determine the fatigue strength of the as received rebars.
- To study the effect of the microstructure on the strength of the rebars.
- To determine the effect of heat on mechanical properties and microstructure.

1.14 Scope of the research

The research was carried out using 10, 12, and 16 mm nominal diameter hot-rolled ribbed bars made from local scrap metal. The rebar sizes chosen for this research represent the widely used rebar sizes in the construction industry in Kenya.

1.15 Research Questions

Does Heat affects the mechanical properties for rebars made from local scrap metal and cooled in air and quenched in water?

How do the fatigue strength and impact toughness of rebars made from local scrap metal compare with the standard values?

1.16 Outline of thesis

This thesis is organized in five chapters. Chapter one covers the introduction while chapter two is a critical literature review on fatigue strength of ribbed bars and effect of heat on other mechanical properties of the rebars. Chapter three describes the methodology that was adopted in carrying out the study. In chapter four the results and discussion from the study are presented. Lastly, chapter five is dedicated to the conclusions and recommendations.

CHAPTER 2

Literature Review

2.1 Introduction

This chapter presents a detailed literature review that covers the fatigue failure in various components, various definitions as applied in fatigue, factors affecting fatigue life, review of the previous work on fatigue in rebars through a range of research papers, reports and theses. Production processes of steel and review of the previous studies on the effect of heat on mechanical properties of rebars is also covered.

2.2 Fatigue failure

Long ago, it was discovered that if you repeatedly applied and then removed a nominal load to and from a metal part (known as a “ cyclic load ”), the part would break after a certain number of load-unload cycles, even when the maximum cyclic stress level applied was much lower than ultimate tensile stress, or even the yield stress of the material [32]. These relationships were first published by A. Z. Wöhler in 1858.

It was noted that as reduced the magnitude of the cyclic stress reduced, the part would survive more cycles before breaking. This behaviour be-

came known as “**FATIGUE**” because it was originally thought that the metal got “ *tired* ”.

The fact that the original bulk design strengths are not exceeded and the only warning sign of an impending fracture is an often hard to see crack, makes fatigue damage especially dangerous [32].

Various components in manufacturing equipment, such as tools, dies, gears, cams, shafts, and springs, are subjected to rapidly fluctuating (cyclic or periodic) loads, in addition to static loads [33]. Cyclic stresses may be caused by fluctuating mechanical loads, such as (a) on gear teeth or reciprocating sliders, (b) by rotating machine elements under constant bending stresses, as is commonly encountered by shafts, or (c) by thermal stresses, as when a die comes into repeated contact with hot work pieces and cools between successive contacts. Under these conditions, the part fails at a stress level below that at which failure would occur under static loading. Upon inspection, failure is found to be associated with cracks that grow with every stress cycle and that propagate through the material until a critical crack length is reached, when the material fractures. The fatigue failure phenomenon is responsible for the majority of failures in mechanical components [33].

2.2.1 How to determine the fatigue strength of a metal

The fatigue behavior of a specific material, heat-treated to a specific strength level, is determined by a series of laboratory tests on a large number of apparently identical samples of that specific material [34]. Figure 2.1 shows a standard fatigue specimen [34]. These laboratory samples are optimized for fatigue life. They are machined with shape characteristics which maximize the fatigue life of a metal, and are highly polished to provide the surface characteristics which enable the best fatigue life. Fatigue test methods involve testing specimens under various states of stress, usually in a combination of tension and bending. The test is carried out at various stress amplitudes (S); the number of cycles (N) it takes to cause total failure of the specimen or part is recorded.

The cyclic stress level of the first set of tests is some large percentage of the ultimate tensile strength (R_m), which produces failure in a relatively small number of cycles. Subsequent tests are run at lower cyclic stress values until a level is found at which the samples will survive 10 million cycles without failure. The cyclic stress level that the material can sustain for 10 million cycles is called the Endurance Limit [33].

Typical plots, called S-N curves, are shown in Figure 2.2. These curves are based on complete reversal of the stress, i.e., maximum tension, then

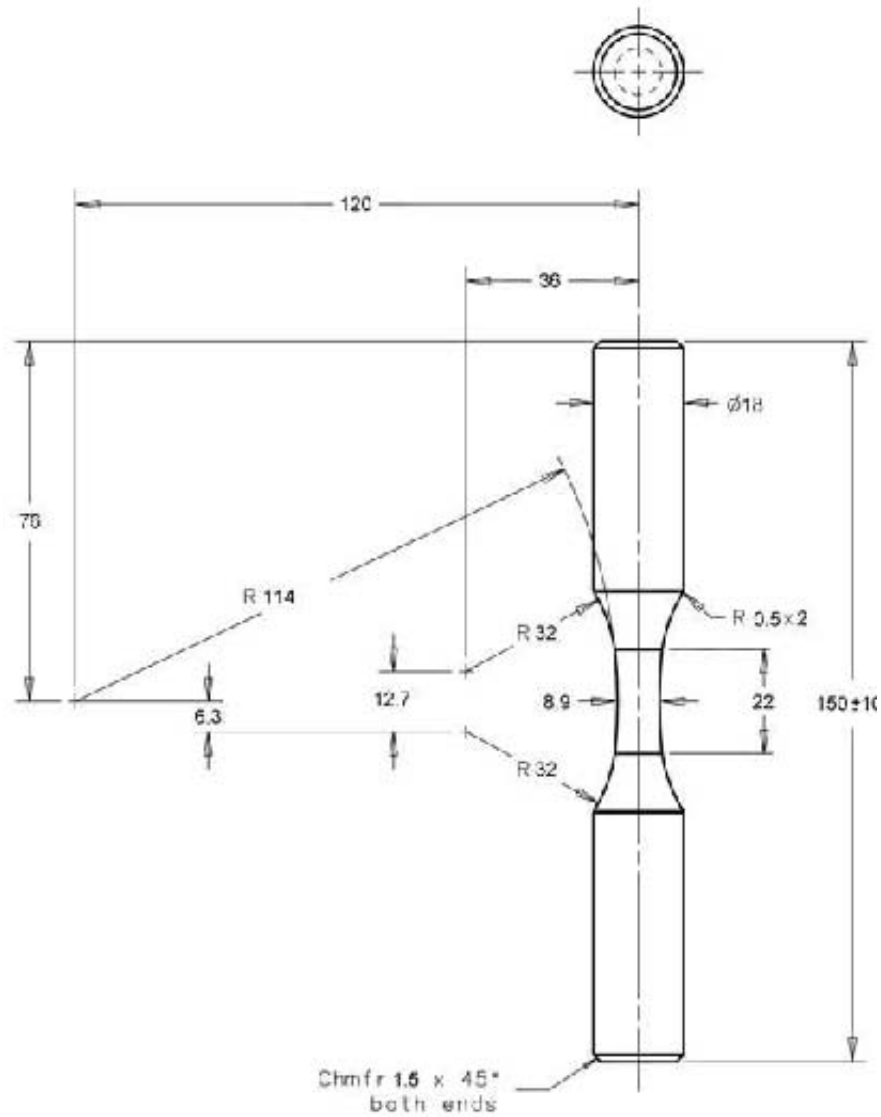


Figure 2.1: Standard fatigue specimen (dimensions in mm)

maximum compression, then maximum tension, etc, such as that imposed by bending a rectangular eraser or a piece of wire alternately in one direction and then the other.

The test can also be performed on a rotating shaft in four-point bending. With some materials, the S-N curve becomes horizontal at low stresses,

indicating that the material will not fail at stresses below this limit. The maximum stress to which the material can be subjected without fatigue failure, regardless of the number of cycles, is known as the endurance limit as shown in Figure 2.2 (a) [33].

Although many materials, especially steels, have a definite endurance limit, others, such as aluminum alloys as well as steels which have been case-hardened by carburizing, do not exhibit an infinite-life cyclic stress level, and the S-N curve continues its downward trend as shown in Figures 2.2 (a) and (b) [33]. For metals exhibiting such behaviour, the fatigue strength is specified at a certain number of cycles, such as 10^7 [33]. In this way, the useful service life of the component can be specified. The endurance limit for metals can be approximately related to their ultimate tensile strength (Figure 2.3). For carbon steels, the endurance limit is usually 0.4 - 0.5 times the tensile strength, although particular values can vary [33].

2.3 Definitions of terms related to fatigue

The definitions of the various terms related to fatigue are presented in Glossary of terms. The terms include fatigue, fatigue life, number of cycles, fatigue strength, fatigue limit, specimen, cyclic loading, stress

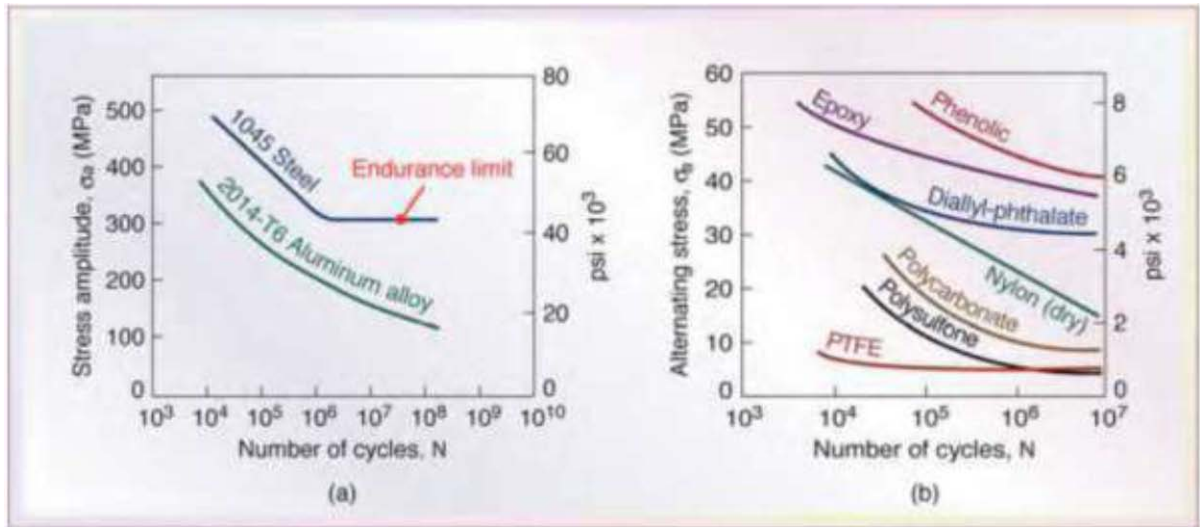


Figure 2.2: Typical S-N curves

range, stress amplitude, mean stress, stress Ratio (R), S-N curve, frequency, High Cycle Fatigue (HCF), Low Cycle Fatigue (LCF), stress concentration factor, stress raisers, notches and relative rib area.

2.4 Factors affecting fatigue life

The fatigue limit in a material can be obtained experimentally or estimated through the traditional approach of assuming its 50% of the tensile strength; for design purposes and in service, this value is recalculated as the effective or admissible fatigue limit, taking into account the effect of variables such as; average stress, surface finish, environment, stress concentrators, reliability, component size, grain size, heat treatment conditions, chemical composition, and level of inclusions. Listed below are

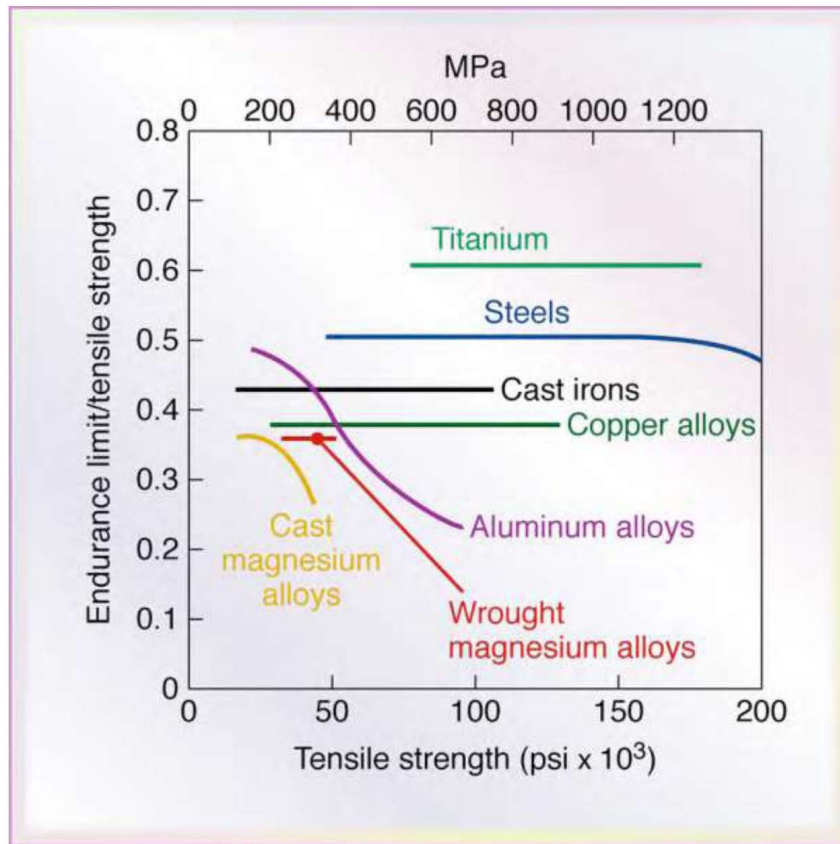


Figure 2.3: Ratio of endurance limit to tensile strength Vs tensile strength for various metals

the effects on fatigue performance that various factors cause [35].

2.4.1 Effect of average stress on fatigue

The contrast between the minimum and maximum load applied to the material has a key effect on the resistance to fatigue cracking; if the ratio is high, ($R = +1, 0$), fatigue endurance limit decreases, where R is the relationship between the minimum and maximum stress. The effect of increasing the mean stress is to reduce the allowable stress range for

a given number of cycles to failure. The introduction of a compressive phase in the cycling produces a disproportionate effect and endurances are longer for a given stress range. In studies of the effects of mean stress on the behaviour of Unisteel 60, it was shown that an increase in mean stress from 159 to 275 MPa caused a reduction of about 40 MPa in the stress range to give 10^6 cycles to failure [30].

2.4.2 Effect of stress concentrators

The resistance to fatigue cracking is severely reduced through the generation of specific stress concentrators caused by the presence of defects in the material, such as holes, pores, notches, nicks, and abrupt changes in geometry. In a study conducted by Smith et al [36], uniaxial fatigue tests were conducted to compare the fatigue life of nicks produced in the laboratory to Electrical Discharge Machining (EDM) defects. Defects made with EDM are used to simulate the effect of corrosion caused by pitting. For AA 7050 aluminum alloy, the notch produced by EDM resulted in a fatigue life similar to that obtained in the tests of samples containing “pitting” of similar size.

2.4.3 Effect of the level of inclusions

In a study conducted by Atkinson and Anderson [37], a correlation was developed of the maximum inclusion size in clean steels and the relationship to the mechanical properties. The important contribution of this research was the development of a new approach in design for fatigue using the generalized Pareto distribution. The Pareto distribution was used to predict the form of the size of the biggest inclusions and the volumetric fraction of the component in which the local fatigue stress exceeds a particular stress level. The new design method developed in this research allows one to analyze the effect of changes on the design stresses. Yang and Zhang [38] investigated the behaviour of the inclusions on fatigue behaviour in the super-long-life regime in 42 CrMo steels. The analysis by electron scanning microscope showed that fatigue cracks start mainly from non-metallic inclusions due to interface debonding of the inclusion from the matrix. The high cycle fatigue behavior is presented in steels with very low content of inclusions (almost zero inclusions). The size of inclusions can affect the initiation of fatigue cracks, according to the research conducted by Juvonen [39], in which evaluation of the effect of the level of inclusions on the fatigue behavior of different carburization conditions in AISI SAE 8620 steel was done. The relevant conclusion

was that the average size of inclusion for the start of fatigue cracks had an effect on the relationship between the fatigue limit and the mechanical resistance when the size of the inclusions ranged between 70 - 90 microns

2.4.4 Effect of grain size and grain direction

Materials with fine grain size exhibited higher fatigue properties than materials with coarse grain size. It is based on the observation that grain boundaries impede dislocation movement and that the number of dislocations within a grain have an effect on how easily dislocations can traverse grain boundaries and travel from grain to grain. So, by changing grain size one can influence dislocation movement and Fatigue strength. Research carried out by Di Schino and Kenny [40] on type 304 stainless steels studied the effect of the grain size of austenite (1 - 47 microns) on behavior in tension and fatigue. The relevant results of this investigation showed an increase in tensile stress and fatigue properties through refining the grain size.

In research carried out by Subramanya et al. [41], the speed of crack growth caused by fatigue was evaluated under the Paris regime for two microalloyed steels with ferrite and pearlite microstructures. The results obtained from testing crack growth rate showed no differences in the

response in the region of fatigue crack propagation in the two materials evaluated. These materials had showed differences with respect to the yield stress of the order of 170 MPa and in the size of pearlite colonies of 7 microns. The previous austenite grain size is directly related to the refining elements of the grain size.

2.4.5 Effect of the microstructure on fatigue strength

The microstructure of tempered martensite obtained from a heat treatment of quenching and tempering exhibits fatigue behavior superior to that of any other microstructure [35]. Tempered martensite in steels increases the fatigue limit because it is a structure in which the mobility of dislocations is minimal, resulting in an increased load level necessary to be applied in order to displace the dislocations [42].

2.4.6 Initiation of microcracks

In the presence of cyclic loads at the tip of a geometric or a metallurgical discontinuity, a phenomenon of cyclic elasto-plastic deformation occurs, in which the initiation of the fissure takes place.

2.4.7 Crack propagation

The surface condition and the nature of the medium play an important role in the fatigue strength; this determines the number of cycles required for the crack to appear [43].

According to Takuhiro [44] there is a correlation between the speed of crack propagation and the tensile strength in pre-deformed materials. Under conditions of large deformation there is a defined correlation between the two variables; when they have low deformations, the correlation is not strong compared to conditions of high deformation.

2.5 Review of the previous work on fatigue in rebars

Considerable research has been performed since the early 1950's on the fatigue behaviour of deformed and plain reinforcing bars, singly or embedded in concrete, especially in North America, Europe, and Japan [45]. The review has provided valuable information on the factors that influence the fatigue behaviour of rebars.

Tilly [30] summarized the factors that influence the fatigue life of reinforcing bars and grouped them under the important factors and the minor factors. Tilly indicated that the important variables included stress range, minimum stress, and deformation geometry of a bar, ra-

dius of bends, welding, and corrosion. Factors that have minor effects on fatigue strength include bar size, bar orientation, Yield Stress, and chemical composition. The conclusion was that the bar deformation geometry was insignificant factor that affects the fatigue life.

Burton [46] reported the results of fatigue tests on reinforcing bars embedded in concrete. The tests were conducted using three stress ranges namely, 214, 241, and 269 MPa, with a minimum tensile stress of 35 MPa, on concrete beams reinforced with single 25 mm reinforcing bar conforming to ASTM A615/A615M [47] for grade and deformations. One deformation pattern produced by fresh rolls, partially worn rolls, or fully worn rolls at the time of manufacture was used. The longitudinal ribs were placed in a horizontal plane (perpendicular to the plane of flexure) in half of the beams and vertically in the remainder. A total of thirty six 203 mm wide by 356 mm deep beams were tested. Three major variables, namely; position of the longitudinal ribs, surface geometry due to different conditions of the rolls at the time of manufacture, and stress range were investigated.

From the test results, Burton reported that stress range is the primary factor influencing fatigue strength. As the stress range increased, fatigue strength decreased. The maximum stress concentration occurred at the junction between the transverse and longitudinal ribs instead of at the

root of a lug. Burton also concluded that conditions of wear for the rolls had a minor effect on the fatigue life of the bars in the study.

Pasko [48] performed fatigue tests on 16 mm, Grade 60 (414 MPa) deformed reinforcing bars conforming to ASTM A615 [47], welded to 10 mm plain transverse bars. The fatigue strength of the reinforcing bars was reduced by one third when they were tack welded, compared with non-welded bars [46]. Butt welding has been proved to have no effect on fatigue strength [49].

Pfister and Hongstad [50] studied the fatigue behaviour of reinforcing bars embedded in concrete. The study covered three grades and four deformation patterns and included 181 reinforced concrete beams with straight or cold bent bars. It was found that Yield Stress, test beam cross section, and minimum stress level do not significantly affect the fatigue strength of bars up to 2 million cycles. However, the fatigue strength of one deformation pattern was 35% lower than that of the other, indicating that surface geometry has a strong effect on the fatigue performance. It was also observed that the fatigue strength of bars cold bent to 45 degrees was only 50% that of straight bars. By examining the locations where the fatigue cracks initiated, it was concluded that all fatigue cracks initiate at the root of a lug.

MacGregor et al. [51] reported fatigue tests on reinforced concrete beams

containing 16 mm, 25 mm, and 32 mm reinforcing bars with Yield Stresss of 276 MPa, 414 MPa, and 517 MPa, respectively. They concluded that fatigue strength of reinforcing bars was relatively insensitive to the tensile strength of the bar metal. However, the fatigue strength of the bars was appreciably lower than that of the base metal. This difference results from the stress concentration at the base of the deformations.

McDermott [52] performed fatigue tests on 13 and 36 mm A432 reinforcing bars with the DI-LOK pattern (the transverse ribs crossed midway between the two longitudinal ribs and met at the longitudinal rib - often referred to as an X-pattern). The 13 and 36 mm bars had average Yield Stresss of 481 and 457 MPa and average tensile strengths of 757 and 692 MPa, respectively. The tests were conducted under axial loading in air with a stress ratio (ratio of minimum stress to maximum stress in a load cycle) between zero and ± 0.03 . It was concluded that the fatigue strength was about 269 MPa corresponding to 3 million cycles for the 13 mm bars and about 131 MPa corresponding to 6 million cycles for the 36 mm bars. The size effect was explained by the fact that the 13 mm bars had a smoother transition between the transverse lug and the barrel of the bar. It was found that fatigue cracks initiate at the intersection of the transverse lugs. The test results suggested that using a fillet rather than a sharp angle at the root of a lug and tapering (gradually terminat-

ing) the transverse deformations before they meet the longitudinal ribs would increase fatigue strength. The procedures used for preparing the bar and gripping the bar during the test was described, which included complete removal of the transverse ribs in the regions in which the bars were gripped.

Hanson et al. [53] described the effect of deformation patterns on the fatigue behaviour of 25 mm reinforcing bars in concrete beams. American-made bars (Series 1) had crescent-shaped transverse lugs, while European-made bars (Series II) had inclined transverse lugs. All the bars had transverse lugs that did not merge into the longitudinal ribs. The beams were 203 mm wide by 356 mm deep reinforced with one 25 mm bar. Fourteen beams in Series 1 and 12 beams in Series II were tested. It was found that the fatigue strength corresponding to 2 million cycles for Series 1 and Series II bars were 179 and 258 MPa, respectively. By comparing the results with previous tests of American-made bars with transverse lugs that merge into the longitudinal ribs, they found that fatigue strength is not necessarily improved by terminating the transverse lugs before they meet the longitudinal rib, in contradiction to the conclusion by McDermott [52]. It was observed that fatigue cracks initiated at the base of the crescent-shaped lugs in the Series I bars and adjacent to the sharp side of a lug in the Series II bars (see Figure 5.4 in the Glossary of terms).

The fracture surface of Series I bars was a plane normal to the axis of the bar, while the fracture surface of Series II bars was a plane inclined at an angle of about 45 degrees to the axis of the bar.

McDermott [54] studied fatigue characteristics in air of 25 mm A615 Grade 60 reinforcing bars with different deformation patterns. Bars with the DI-LOK pattern, others with seven different experimental patterns, and four domestic competitors' bars were included in the program. All tests were conducted under zero-to-tension axial load. Sinusoidal load variation was selected, with a frequency of 7 Hz. The purpose of the tests was to establish the best deformation pattern for further development. From the test results, it was found that bars with a four-start-helix transverse deformation pattern (a long-pitch spiral pattern in which a transverse cross-section of the bar crosses four transverse deformations) had the best fatigue behaviour of the bars tested. By examining the details of the deformation patterns, it was found that decreasing the angle between the transverse lug and the longitudinal rib avoiding the intersection of two transverse deformations resulted in an increase in fatigue strength. This report also described test specimen preparation. The deformations were only partially removed from the portions of the bar, instead of completely machined off as described in the 1965 report [52], to avoid removing too much of the cross-sectional area in the grip region.

At both ends of the specimen, a copper tubing was used with fine white sand bonded to the inside surface with USS Nexus adhesive S-7001.

Studies have shown that width, height, angle of rise, and base radius of a protruding deformation of a reinforcing bar affect the magnitude of stress concentration [55,56], Fatigue strength of reinforcing bars may also be influenced by the orientation of the longitudinal rib. Several studies have also indicated that there are small differences between the fatigue strength of bars made with old or new rolls at steel mills.

McDermott [57] provided more information on the fatigue behaviour of the four-start-helix bars described in the 1969 report [54] and compared the fatigue behaviour of the helix bars with that of the DI-LOK bars in the 1965 report [52]. In this report, the fatigue strengths corresponding to 4 million cycles for 32 mm helix bars were 200 and 258 MPa, respectively. It was observed that larger bars had lower fatigue strength and explained it by the notch effect resulting from surface imperfections at the ribs, which are more pronounced in the larger bars. It was concluded that the 32 mm helix bars had better fatigue performance than the 36 mm DI-LOK bars. The 13 mm helix bars, however, do not appear to give similar results as the earlier 13 mm DI-LOCK bars. In general, it was felt that the results for larger bars can be conservatively applied to all bars and used as the basis for design criteria. Overall, McDermott

confirmed in the 1969 [54] conclusions that the fatigue characteristics of the four-start-helix deformation pattern are superior to those of the DI-LOK pattern. The test specimen preparation was the same as that described in the 1969 report [54] except that this time only copper tubing was used, instead of using the copper with sand bonded to the inside surface.

Hanson et al. [58] studied the fatigue behaviour of Grade 60, 25 mm bars on which the transverse lugs, inclined at an angle of about 45 degrees to the bar axis, forming helixes around the bar. The investigation consisted of 24 fatigue tests on bars embedded in T-shaped reinforced concrete beams. The minimum stress was 41 MPa tension throughout the tests. Based on the test results, it was concluded that the mean stress range causing fatigue failure in 5 million cycles was 192 MPa. The fracture surface was examined and it was found that 60 percent of the cracks began at the base of transverse lugs, while the other cracks began at the edge of the bar identification marks.

Jhamb and MacGregor [59] studied the effect of surface geometry on the fatigue strength of rebars. The study included eighty 25 mm bar specimens and 32 plain machined bar specimens tested in air under repeated axial loading to determine the effects of the deformations, decarburization of the surface, rust and mill scale and grade of steel. It was con-

cluded that there is a significant decrease in fatigue strength due to the presence of deformations and decarburization of the surface. Rust and mill scale do not influence fatigue strength. The grade of steel had no influence on the fatigue strength of the deformed bars, while specimens machined from the centre of deformed bars showed a linear increase in fatigue strength with grade, matching the results of the 1971 report [51]. It was also observed that the strength of bars tested in air was lower than that of bars tested in concrete beams. On examining the fracture surface of the deformed bars, it was found that the fatigue failure originated at the base of a transverse lug. The fatigue fracture zone was a smooth surface surrounded by a rough and crystalline tension fracture zone.

Jhamb and MacGregor [55] also studied the stress concentrations on the surface of deformed bars. Typical hot rolled deformed rebars contain two longitudinal ribs and a regular pattern of equally spaced transverse lug, which cause stress concentrations. K_t values were determined using finite element analysis with a 762 mm length, 25 mm diameter specimen with electrical resistance strain gages. Based on the study, the authors [55] concluded that the ratio of the lug base radius (r) to the lug height (h) has the most pronounced effect on K_t . The values of K_t decrease with an increase in r/h value. The fatigue strength of the deformed bars de-

creased when the ratio of radius to lug height r/h is less than about 1.25 and is almost constant for r/h ratios greater than 1.25.

Wascheidt [60] found that the strength of 16 mm diameter ribbed bars was 18% lower than plain bars for axial tests in air. Snowdon [27] found a similar effect for bending tests on 5.18 m long concrete beams. Helgason et al. [61] reported tests on 25 mm diameter ribbed bars which were machined to give smooth axial specimens of 6 mm diameter. This produced a big improvement in fatigue strength; the stress range to give 10^6 cycles to failure increased from 190 MPa to 430 MPa. Not all of this increase could be attributed to the removal of ribs because reduction in diameter may also remove surface inclusions and other potential crack initiation sites. In addition, the as-received bars were tested in concrete beams.

Studies have been made on the effects of wear in the rolls at the steel mills because new rolls give sharper base radii to the deformations and this can reduce the fatigue strength [61]. American tests have exhibited a very small effect whereas Swedish tests exhibited a small effect for 13 mm bar and a very big effect for the 16 mm bar [61]. In all cases, the experiments confirmed that reinforcement produced using worn rolls has better fatigue strength. Effects due to different types of deformation are difficult to assess quantitatively because other variables such as chemical

composition, method of manufacture (whether hot rolled or cold worked) and degree of quality control also influence fatigue strengths. For bars having longitudinal ribs, it has been found that when tested in concrete beams, their disposition affects the fatigue strength [30].

Both Bannister [28] and Burton and Hognestad [62] found that with the ribs in a vertical plane, the fatigue strength can be as much as 40% lower than when placed in a horizontal plane. Manufacturers identification markings, which appear as raised features, are very potent stress concentrations and cause premature fractures. In cases where these have been filed off, the fatigue life was increased by about 100%.

It is generally recognised that fatigue strength decreases with increase in bar diameter [30]. For plain cylindrical specimens the effect is relatively small. Frost et al. [63] reviewed data for rotating bending for the range of sizes relevant to reinforcement, 12.5 - 38 mm, for which the biggest reduction in fatigue limit was only 5%. Size effects for ribbed reinforcement bars are much bigger. In a review of available data, it was noted that the stress range to give failure in 2×10^6 cycles for 32 mm diameter reinforcement was 7-20% less than for 16 mm diameter reinforcement [64].

Helgason et al. [61] tested beams having 16 mm and 35 mm bars and reported reductions in strength of about 10%. Soretz [24] found no dif-

ference for 8 mm to 26 mm diameter bars at endurances up to 2×10^6 cycles.

In one of the few systematic studies of size effects of butt welded joints tested axially in air, Harrison of the British Steel Corporation found that there were no significant differences for diameters ranging from 6 mm to 32 mm [30].

In general, size effects appear to be more pronounced for axial tests than for bending. The explanation usually given for size effects is that bigger sections have a statistically greater likelihood of containing large flaws. Another contributing factor may be that smaller diameter bars can be more effectively worked. In the size range in question, the most important factor is almost certainly the relative contributions of crack initiation and propagation. For plain specimens most of the life is in initiation and the differences in propagation time for different diameter sections are minimal. For ribbed bars the initiation phase is reduced due to the presence of local stress concentrations at the ribs [30]. Furthermore, Gurney [65] has shown that in the vicinity of a stress concentration, the minimum size of flaw to permit crack growth reduces with increased thickness of specimen. In consequence it can be argued that the initiation life of bigger diameter bars is reduced, and total life decreases.

Untill now, there is lack of data on the fatigue strength on ribbed reinforcing steel bars made from local scrap. The current study is therefore timely as it has investigated the fatigue strength of ribbed reinforcing steel bars made from local scrap.

2.6 Steel production processes

Although steel had been produced in bloomery furnaces for thousands of years, steel's use expanded extensively after more efficient production methods were devised in the 17th century for blister steel and then crucible steel [5]. With the invention of the Bessemer process in the mid-19th century, a new era of mass-produced steel began [5]. This was followed by Siemens-Martin process and then Gilchrist-Thomas process that refined the quality of steel. With the introduction of new production process, mild steel replaced wrought iron [5].

Further refinements in the process, such as Basic Oxygen Steelmaking (BOS), largely replaced earlier methods by further lowering the cost of production and increasing the quality of the metal. Today, steel is one of the most common materials in the world, with more than 1.3 billion tons produced annually [5]. Based on statistics from “*The 1992 Census of Manufacturing*” [66], 1,118 steel manufacturing facilities currently exist

in the United States. Steel production is a \$ 9.3 billion dollar industry and employs 241,000 people in the US [6].

Iron and steel are manufactured from iron ore and scrap in a number of different production processes [8]. A steel making process involves five basic steps according to the Organization for Economic Co-operation and Development / International Energy Agency (OECD/IEA) [67]: (1) treatment of raw materials, (2) iron making, (3) steel making, (4) casting, and (5) rolling and finishing.

Iron making (step 2), which is the most energy intensive step, usually takes place in the blast furnace process, with iron ore and coke as the main inputs. Some iron is also produced through a direct reduction process, in which case iron ore and natural gas are the main inputs. The dominating steel production processes (step 3) are the basic oxygen furnace (BOF) and the electric arc furnace (EAF). The open hearth furnace (OHF) has until recently also enjoyed a sizeable market share, but it has now been phased out completely in most countries because of their slow operation. Some new processes (e.g. the Corex process) have been introduced in some countries. Globally, the basic oxygen furnace accounts for nearly 60%, while the electric arc furnace accounts for 34% of total steel production as shown in Table4.2.1 [68].

Table 2.1: Steel production by process

Production method	Share of world production (%)
Basic Oxygen Furnace (BOF)	58
Electric Arc Furnace (EAF)	34
Open Hearth Furnace (OHF)	5
Other technologies	3

2.6.1 Steel Production from Iron Ore

Steel production at an integrated steel plant involves three basic steps. First, the heat source used to melt iron ore is produced. Next the iron ore is melted in a furnace. Finally, the molten iron is processed to produce steel. These three steps can be done at one facility; however, the fuel source is often purchased from off-site producers [6].

2.6.2 Steel Production from Scrap Metals

Steelmaking from scrap metals involves melting scrap metal, removing impurities and casting it into the desired shapes. Electric arc furnaces (EAF) as shown in Figure 2.4 are often used. The EAFs melt scrap metal in the presence of electric energy and oxygen. The process does not require the three step refinement as needed to produce steel from ore. Production of steel from scrap can also be economical on a much smaller scale. Frequently mills producing steel with EAF technology are

called mini-mills [6].

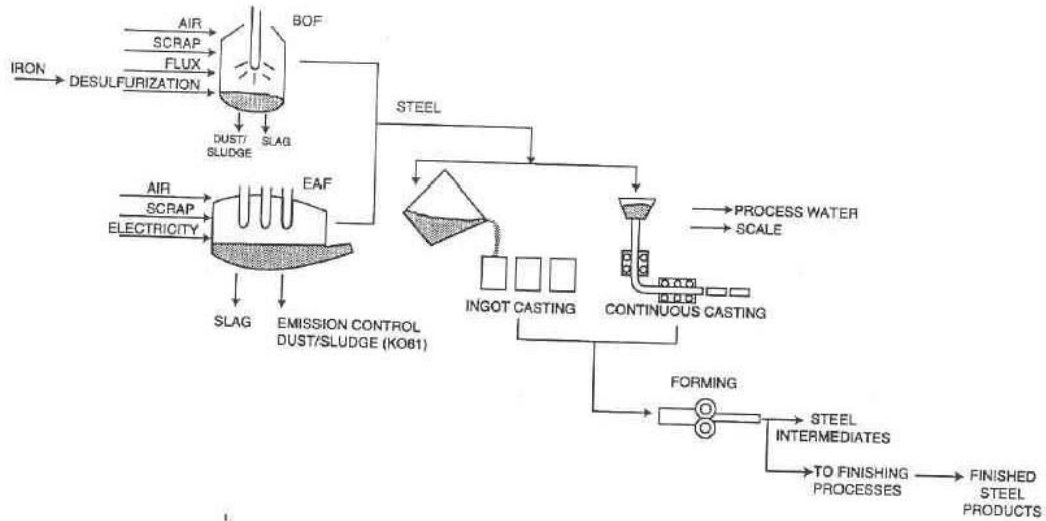


Figure 2.4: Electric arc furnaces (EAF)

2.7 Effects of Chemical Composition on Mechanical Properties

Various alloying elements are added so as to produce steel with the required properties. The most common alloying elements include increased amounts of manganese or silicon. Others may be elements not normally found in carbon steels such as nickel, chromium and vanadium [69]. Higher carbon contributes to the tensile strength of steel, that is, higher load bearing capacity and vice versa. Lower carbon content less than 0.1 percent will reduce the strength. Higher carbon content of 0.3 percent and above makes the steel bar unweldable and brittle. All commer-

cial steels contain some manganese, which is usually introduced during deoxidizing and de-sulfurizing. Steels with 1.0 to 1.5% are called carbon-manganese steels. Medium manganese steels have 2 to 9% manganese. Manganese increases the hardness and tensile strength of steel. High manganese steels, with 10 to 14% manganese content, are very hard and are machined with tungsten carbide or high speed steel tools. They are used in applications where wear resistance is a desirable property, such as in wear resistant castings [70].

Silicon is found in all commercial steels, usually 0.10 to 0.35% as a residue of the silicon used as a deoxidizer. However, the content may be increased as an alloying element, to between 3 and 5% to increase magnetic permeability. Silicon also improves wear resistance and acid resisting properties of steel. Silicon content of up to 1.75% increases the elastic limit and impact resistance without loss in ductility. Silicon increases electrical resistivity and decreases hysteresis losses, making silicon steel an important material for magnetic circuits where alternating currents are used [70].

Nickel is used to alloy steel, jointly with either chromium and/or molybdenum. Nickel-chromium steels are used where high tensile strength and high hardness are required. On the other hand, nickel-molybdenum alloy steels are characterized by high toughness and when case hardened,

tough cores are obtained. When both molybdenum and chromium are jointly used with nickel in alloy steels, improved impact and oxidation resistance are achieved [70].

Vanadium is usually used together with chromium to make strong, tough and hard alloy steels. It increases the tensile strength without lowering the ductility, and improves fatigue resisting qualities of steel [70].

2.8 Effect of heat on mechanical properties of rebars

The mechanical properties of steel continue to degrade with increasing temperatures, until near total strength and stiffness depletion occurs around 1,100°C [71]. Less than 20% strength and stiffness of steel are retained beyond about 700°C [71]. Beyond 870°C, metallurgical microstructure of steel undergoes a permanent transformation relative to its original chemical composition that result in grain coarsening and hardening, which, with the subsequent cooling, adversely affect its residual mechanical properties. This high level of heating for about 30 minutes or more and cooling, results in a reduced ductility and fracture toughness, as well as higher hardness and elevated yield and tensile strengths [71]. Temperature increase of the composite steel-concrete elements leads to a decrease of mechanical properties such as yield stress and Young's mod-

ulus [72]. The flexural strength for reinforced concrete beams exposed to fire at 550°C and 750°C for 60 and 120 minutes are less than that for the reference beam by about 35% and 44% respectively [73]. Also, at 950°C, the decrease in flexural strength is about 62% and 64% respectively [73]. Reinforced concrete beams on fire and heated at 750°C and cooled rapidly by quenching in water have a higher strength than those that are normally cooled in the atmospheric temperature [73]. Smith et al. [74] provided further confirmation data on steel properties after heating and cooling. Thus, load bearing of reinforcing steel decreases when steel or composite structure is subjected to a fire action.

In fire situations, the loss of strength for rebars at elevated temperatures may be significant and design requirements for fire are covered in Section 5 of AS 3600 [75] for rebars. The Yield Stress of steel is reduced to about half at 550°C. At 1000°C the Yield Stress is 10 percent or less [76]. Near total depletion of strength occurs at approximately 1204°C [77]. Due to its high thermal conductivity, the temperature of unprotected internal steelwork normally will vary little from that of the fire [76]. Young's modulus does not decrease with temperature as rapidly as does Yield Stress [76]. Cold-worked reinforced bars, when heated, lose their strength more rapidly than do hot-rolled high-yield bars and mild-steel bars. The differences in properties are even more important

after heating. The original yield stress is almost completely recovered on cooling from a temperature of 500 to 600°C for all bars but on cooling from 800°C, it is reduced by 30 percent for cold-worked bars and by 5 percent for hot rolled bars [76]. The loss of strength for prestressing steels occurs at lower stressing temperatures than that for rebars [76]. Cold-drawn and heat-treated steels lose a part of their strength permanently when heated to temperatures in excess of about 300°C and 400°C, respectively [76]. Under fire conditions, the temperatures in the steel will increase, resulting in both thermal expansion of the member and transient deterioration of its mechanical properties. The magnitude of these effects depends upon several factors, including the composition of the steel, the sizes and shapes of the parts and whether it was protected or not and the duration and nature of the fire [78]. These are important considerations if heat has been applied to assist bending or if the rebars have been subjected to a fire. If both the duration and the intensity of the fire are large enough, the load bearing resistance can fall to the level of the applied load resulting in the collapse of the structure [72]. However, the failure of the World Trade Centre (WTC) on 11th September 2001 and, in particular, of building WTC7 alerted the engineering profession to the possibility of connection failure under fire conditions [18].

As the heat of the fire intensified, the joints on the most severely burned floors gave way, causing the perimeter wall columns to bow outward and the floors above them to fall. The buildings collapsed within ten seconds, hitting bottom with an estimated speed of 200 km/h.

In addition, grain size has a measurable effect on most mechanical properties. For example, at room temperature, hardness, Yield Stress, tensile strength, fatigue strength and impact strength all increase with decreasing grain size [79]. Machinability is also affected; rough machining favours coarse grain size while finish machining favours fine grain size. The effect of grain size is greatest on properties that are related to the early stages of deformation. Thus, for example, yield stress is more dependent on grain size than tensile strength [79]. Fine-grain steels do not harden quite as much and have less tendency to crack than coarse-grain steels of similar analysis. Also, fine-grain steels have greater fatigue resistance, and a fine grain size promotes a somewhat greater toughness and shock resistance. Cold working frequently alters grain size by promoting more rapid coarsening of the grains in critically stressed areas. The original grain size characteristics, however, can usually be restored by stress relieving. Coarse grain steels have better creep and stress rupture properties because diffusion at high temperatures is impeded by sub grain low-angle boundaries present in coarse-grain steels [79]. Hence, the

response in mechanical properties of different structural steel grades at elevated temperatures should be well known in order to understand the behaviour of steel and composite structures when subjected to fire.

To study thoroughly the behaviour of certain steel structures at elevated temperatures, use of material data of the used steel material obtained by testing is necessary [80]. In addition, it is necessary to understand these changes in order to have safe, economical and easily applicable design methods for rebars subjected to fire.

In spite of the wide use of rebars in the construction industry in the country, no studies have been published on fatigue strength and the effect of heat on mechanical properties of rebars made from recycled local scrap metal

This thesis presents the details of an experimental study using test specimens obtained from rebars made from local scrap metal with nominal diameters of 10, 12, and 16 mm. They represent the commonly used rebar sizes for the local concrete reinforcement needs in Kenya. The specimens were subjected to seven different temperatures to determine the elevated temperature behavior. Fatigue strength and impact toughness were determined at ambient temperature using 12 mm and 12 and 16 mm rebars respectively. The rebars were sampled randomly from local steel rolling mills in Kenya. The current study therefore is timely

as it provides data in regard to fatigue strength and the effect of heat on the mechanical properties (Yield stress, tensile strength, percentage elongation, Modulus of Elasticity and Brinell hardness) and microstructure of rebars made from local scrap metal and heated to temperatures ranging from 22 °C to 1000 °C for one hour and then cooled in different media (air and water).

CHAPTER 3

Methodology

3.1 Introduction

The chapter presents the experimental set-up and testing conditions applied in the various experiments. The research work involved heating and cooling of the specimens, chemical composition analysis, microstructure examination, fatigue strength testing, Brinell hardness testing, Charpy impact testing and tensile testing to determine the effect of heat on the mechanical properties (Yield stress, tensile strength, percentage elongation and Modulus of Elasticity) of the ribbed rebars made from local scrap. A survey for the purpose of obtaining information on quality control and production methods of the rebars used in construction industry was also carried out.

3.2 Survey

A sample of five rolling steel mills was selected and a structured questionnaire distributed to them. A sample of the questionnaire is included in Appendix A. From the questionnaires, information expected included the production methods of rebars, quality control in the steel industry,

and standard sizes of reinforcing bars used in the local construction industry. A questionnaire (See Appendix B) was also sent to KEBS, as the national standards body to seek information on quality control of rebars in the country. Industrial visits to five rolling mills located in different countries (Kenya, China and Netherlands) were also made to get a firsthand experience of the production methods and quality control techniques. The specimens used in this study were also sampled during the industrial visits from two local steel rolling mills in Kenya.

3.3 Sampling and Number of Specimens

The test specimens were collected and sampled as detailed in each relevant standard. For fatigue testing, a test piece was selected for every 30000 kg, with at least three test pieces per test unit and nominal diameter [81]. Further, each test unit comprised ten test specimens. For each diameter, and from each test unit, five bars were selected for test. Guidelines on the minimum number of test specimens and the associated degree of replication in fatigue testing are shown in Table E.1 in Appendix G [82]).

For tensile testing, the sampling frequency is as shown in Table 4.3 [83].

For impact test, all specimens were taken from a single test coupon or

test location. Since a minimum average test result was required, three specimens were tested [84].

To account for variability among reinforcing bar producers, rebars were sampled randomly from two local steel companies based in Kenya, herein referred to as mill A and B. The test specimens selected did not exhibit isolated defects that were not characteristic of the product from which they were selected [81]. Mills A and mill B where the rebars were sampled from, command a large market share in Kenya hence the selected steels represent the general situation in the rebar market throughout the country.

Table 3.1: Sample Frequency

Nominal Size (mm)	Quantity (kg)
Under 10	1 sample for each 25000 kg or part thereof
10 - 16 inclusive	1 sample for each 35000 kg or part thereof
Over 16	1 sample for each 45000 kg or part thereof

3.4 Heating and cooling of the specimens

To examine the effects of heat on steel rebars obtained from local mills, six prepared tensile specimens each from different diameter rebars were cut into 450 mm length and heated in an electric furnace for one hour. The electric furnace had a maximum temperature of 1200°C and is shown

in Plate 1. After heating to the set temperature, the six samples were quickly taken out of the furnace and three samples quenched in water for 15 minutes while the other three were separately cooled in air to room temperature. Cold, still, clean tap water in a tank (25L) was used as the quenchant [85]. To commence the heating operation, the furnace was initially calibrated to determine the furnace operating temperature based on the pre-set furnace temperature. To determine this, the furnace was set to an initial temperature of 200°C and the furnace was switched on. This temperature was maintained with the aid of a thermostat that was used to control the furnace temperature. On attaining this temperature, a thermocouple was now introduced into the furnace chamber to measure and compare the temperature of the chamber. The furnace temperature was adjusted until it gave the same output temperature [86]. The specimens were then heated for one hour by placing them in the heating chamber and when the furnace reached the desired temperature, a calibrated stop watch was set on and the heating was stopped after one hour. To simulate temperatures likely to be experienced by the rebar during a fire, the rebars were heated to 100°C, 300°C, 500°C, 600°C, 900°C and 1000°C. The 100°C temperature was the lowest temperature tested, since the properties of the rebar steel are not significantly altered below this temperature and also to examine possi-

ble embrittlement behaviour, due to aging. The upper limit of 1000°C was chosen because, in a fire, the rebars of the construction elements are not usually subjected to temperatures higher than this and also the one hour time was sufficient for most metallurgical phenomena to be accomplished [87].



Plate 1: Electric Furnace

3.5 Chemical composition analysis

The chemical composition (product analysis) of the as-received, heated and cooled in both air and water specimens of the 12 and 16 mm rebars from mills A and B was determined spectrographically in accordance with ISO 15630-1:2002 [88] using spectroLAB LAVMII a spark immer-

sion analysis spectrometer located at KEBS.

3.5.1 Microstructure Characterization

The microstructure examination of the as-received, the heated and cooled in both air and water specimens were examined under an optical microscope type Leica as per the specifications in BS4449 [81]. Micrographs were captured with a digital camera connected to the microscope.

3.5.2 Metallographic Sample Preparation

Rebar specimens were cut into 15 mm length and sectioned using a diamond cutting wheel of a wet cutting machine, model Jean Wirtz CUTO 20 shown in Plate 2 which simultaneously lubricated and cooled using water-soluble coolant. The sectioned specimens were then cold mounted in epoxy to enhance handling of the small specimen with lengths of 15 mm during polishing. Following mounting, the specimens were mechanically wet ground starting with 120 grit silicon carbide (SiC) waterproof papers and progressively continued with finer grits (240, 400, 600, 800, and 1200). Specimens were rotated through 90 degrees after each grinding step. Rinsing between steps to remove previous grinding media was done. After final grinding on 1200 grit, the specimens were then dia-

mond polished using 6 and 1 μm rotating polishing cloth along with 1 μm alumina slurry. Finally, to reveal the microstructure of the polished surface for imaging, the specimens were etched in a 2% Nital solution (a reagent that is a solution mixture of 2 ml of Nitric Acid (HNO_3) and 98 ml of Ethanol ($\text{CH}_3\text{CH}_2\text{OH}$)) at room temperature, with cleaning and rinsing done with ethanol. Microscopic examination of the etched surface of various specimens was undertaken using a metallurgical microscope type Leica, with an inbuilt camera and computer system attached through which the resulting microstructure of the samples was all photographically recorded with a magnification of 400x.



(a) With safety lid open



(b) With safety lid closed

Plate 2: Wet cutting machine Jean Wirtz CUTO 20

3.5.3 Grain Size Measurements

The effective ferrite grain size was estimated in accordance with the ASTM E 112 [89]. The linear intercept method was used for the determination of the grain size, considering the steels to be of a two phase metal (i.e. ferrite and pearlite) [85].

Here, a pattern (i.e. circles, cross-and-circles, lines, etc) is overlaid atop the digital image (live or captured). Each time the overlaid pattern intercepts with a grain boundary, an intercept is drawn on the image and recorded (hence the name "Intercept Method"). Taking the system calibration into consideration, the image-analysis software automatically calculates the ASTM "G-Number" and mean intercept length, as a function of the intercept count and pattern length (See Figure 3.1). To ensure consistency in the results, these grain sizes were estimated from photomicrographs taken from areas at the mid radius of the specimens

3.6 Tensile testing

3.6.1 Test equipment

The tensile testing machine used in this study was a servo-hydraulic Universal Testing Machine (UTM) of 1000 kN capacity, shown in Plate

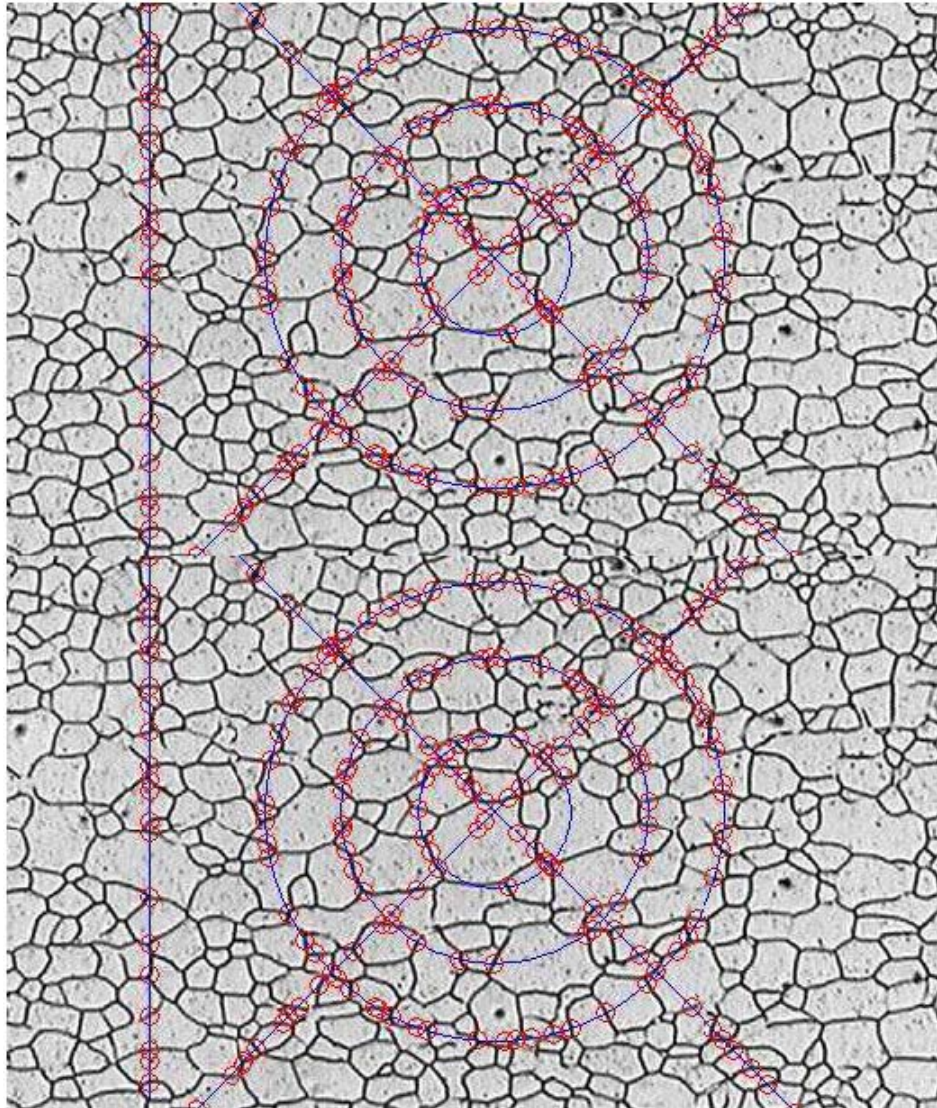


Figure 3.1: Grain Analysis via the Intercept method.

3. A cross head speed of 10 mm/min with the load axis parallel to the longitudinal axis of the rebar was observed during the test. Hydraulically operated grips using universal tapered 12.7 mm diameter collets were employed to secure the specimen ends in series with the load cell on the UTM, shown in Plate 4. The UTM, was calibrated in accordance with

ISO 7500-1 [90] before being used in testing (See Plate 3).

3.6.2 Test Specimens

The test specimens were obtained from as-received ribbed hot-rolled 10, 12, and 16 mm nominal diameter rebars obtained from local mills of the same composition. The specimens were cut off from full 12 m lengths of rebars sampled from steel mill A and B and prepared in accordance with ISO 6892-1 [91].

Two rebars of each nominal diameter were sampled and then divided into smaller pieces as shown in Plate 5 to produce all the required specimens for this investigations. The specimens were prepared after a series of cutting operations using a power saw. The specimens original gauge length was 5 times the nominal diameter. The specimens were marked with a center punch with equidistant gauge marks near the middle of the specimen. The distance between the marks was 5 mm. The purpose of the gauge marks was to provide reference points for determination of the percentage elongation. Punch marks were light, sharp, and accurately spaced.

The specimens were tested at room temperature (22°C) and after being heated to six elevated temperatures (100, 300, 500, 600, 900, 1000°C) and cooling, giving a total of seven temperatures. Six specimens, two

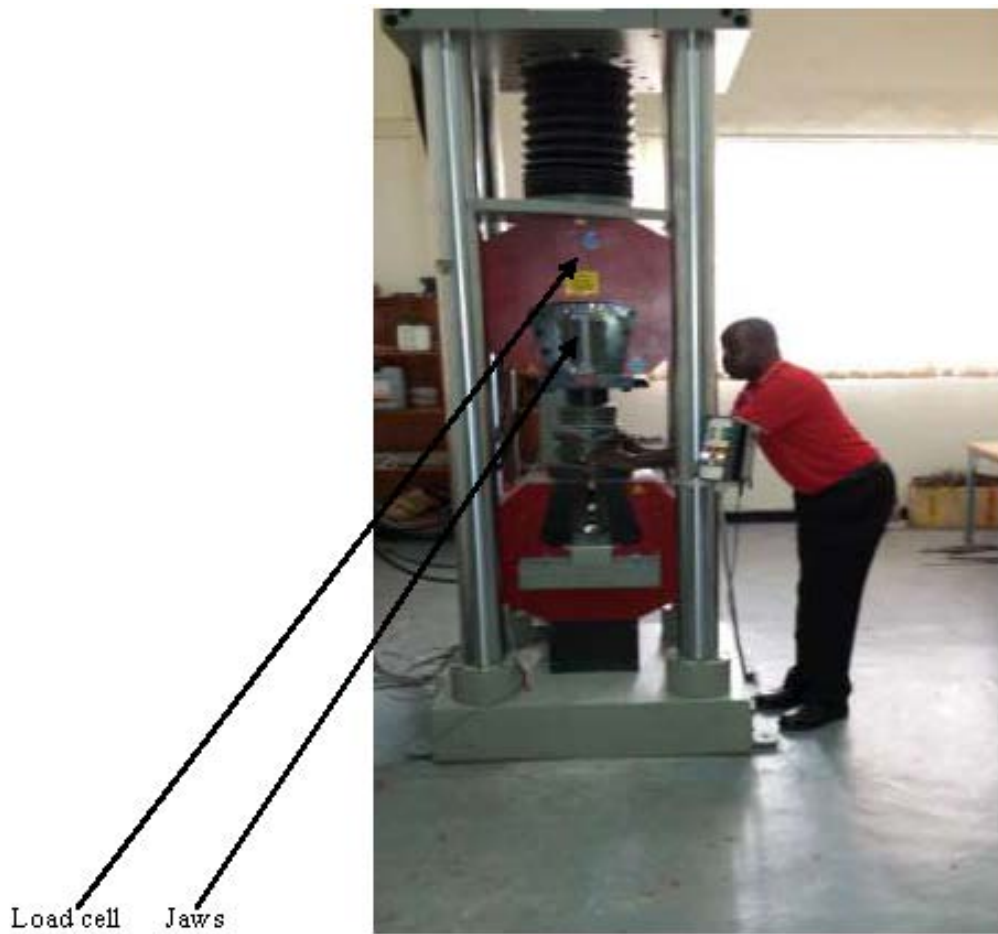


Plate 3: UTM being calibrated before use



Plate 4: Grips of the UTM with specimen

from each nominal diameter were heated at each set temperature, giving a total of 42 test pieces. From the six specimens, three were cooled in air (one each from 10, 12, and 16 mm) while the remaining three were cooled rapidly by quenching in water. This procedure was repeated for specimens from mill B, giving a total of 84 test pieces.



Plate 5: Rebars samples used in the study

3.6.3 Test Procedure

The tensile test was carried out in accordance with ISO 6892-1 [91]. Tensile tests were carried out on both the water quenched and air cooled

specimens using a UTM. The values obtained were compared with the as-received specimen values which had also been subjected to a similar tensile test. The initial diameter and initial gauge length for each sample were noted before the application of the uniaxial load. Each of the specimens was then loaded until it fractured, and the fracture load was recorded as well as the diameter at the point of fracture and the final gauge length. The values were recorded using the machine's own plotter and a computer connected to a data logger. Based on the data obtained from this test, major parameters that were determined from the stress-strain curve were the Yield stress or yield Point (R_e), Tensile Strength (R_m), Modulus of Elasticity (E), and Percentage Elongation ($\Delta L\%$).

3.7 Brinell hardness test (HBW)

3.7.1 Test equipment

Brinell hardness (HBW) was determined on a universal hardness tester, model INNOVATEST shown in Plate 6 with a standard steel ball of 1 mm diameter. The universal hardness tester was verified before use in accordance with ISO 6506-2 [92] and its load measuring device was found to be accurate to \pm one percent.

3.7.2 Test Specimen

The test specimens were obtained from as-received, heated and cooled 10, 12 and 16 mm rebar samples. The test pieces were cut into lengths of 30 mm. The test specimen surfaces were ground using a similar method to that described in the micrograph preparation up to the 1200 grit sandpaper to eliminate decarburized metal and other surface irregularities. The thickness of the specimen tested was 25 mm, which ensured that no bulge or other marking showed the effect of the load on the side of the specimen opposite the indentation.

3.7.3 Test Procedure

Brinell hardness (HBW) was determined in accordance with ISO 6506-1 [93]. Each of the test specimens was mounted on the anvil of the machine. The specimens were brought into contact with the steel ball indenter and allowed to rest for a dwell time of 15 seconds. A test force of 294.4 N and a steel ball of 1 mm in diameter were used in taking Brinell hardness readings. The distance from the center of any indentation to the edge of the test piece was at least two and one-half times the diameter of the indentation. The purpose for these distances is to ensure that any indentation made is not influenced by work hardening

and flow of material around the previous indentation. The edge distance requirement also ensures that the indentation's area of contact permits proper support. HBW values were determined from the arithmetic mean of the three hardness readings taken at different positions on the samples [4]. The final HBW values were obtained by averaging the arithmetic mean hardness values of 10, 12 and 16 mm test specimens.

3.8 Impact test

3.8.1 Test equipment

A Wolpert impact tester Plate 7 with Impact energy of 300 J and an impact velocity of 5.2 m/s was used in the study of charpy-V impact toughness of the 12 and 16 mm rebars under dynamic load.

3.8.2 Test specimens

Standard Charpy V-notch specimen sizes of 10 mm x 10 mm x 55 mm were machined and used in the testing of the 16 mm rebar (See standard Charpy V-notch specimen in Figure 3.2 [94]). Under-sized specimens of 10 mm x 7.5 mm x 55 mm were machined in the testing of 12 mm rebar specimens. This was because it was not possible to make the standard-



(a) Setting Up



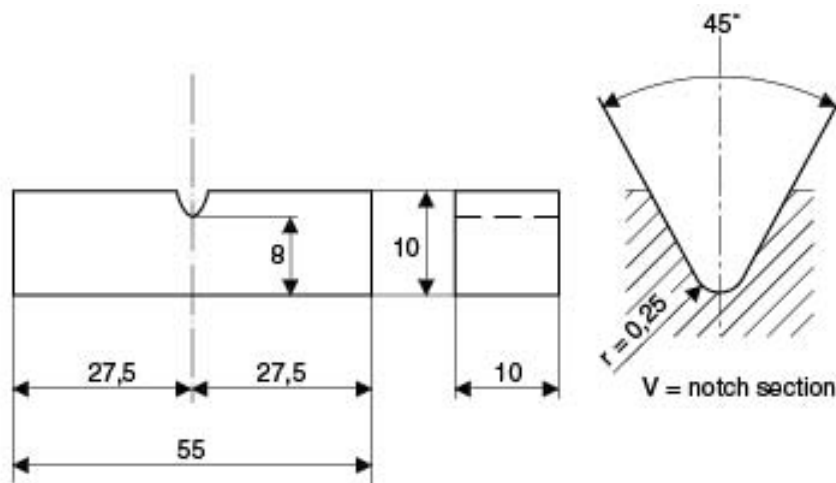
(b) With 12 mm rebar mounted

Plate 6: Universal hardness tester



Plate 7: Charpy-V Impact tester

size Charpy V-notch impact test specimens for 10 mm rebar because the thickness of the targeted steel bar was 12 mm. The Charpy V-notch specimens were machined from 12 and 16 mm rebar to the dimensional requirements of ISO 148-1 [95]. The machining was done by milling followed by surface grinding. V-notch was cut using a notching machine.



All dimensions in mm

Figure 3.2: Standard full size Charpy V-notch specimen

3.8.3 Test Procedure

The Charpy impact test, also known as the charpy V-notch test was carried out as per ISO 148-1 [95]. The test consisted of placing a notched specimen in an impact tester and breaking the specimen with a swinging pendulum. Minimum average test result was required in the charpy

impact, hence six specimens were tested [96] for both the 12 and 16 mm rebars.

3.9 Fatigue Testing

3.9.1 Introduction

This section deals with the fatigue tests of as-received 12 mm diameter hot-rolled ribbed rebars. As a result of the tests, the relationship between the number of cycles N and the stress amplitude σ_a of constant magnitude, which under the given conditions leads to fatigue failure, was found and shown in S-N curves. S denotes here the stress amplitude. Fatigue strength for rebars was also estimated based on low cost test.

3.9.2 Test equipment

Fatigue tests were conducted on a servo-hydraulic MTS 810 materials testing system. The 500 kN capacity MTS 810 machine used is found at Research and Development Centre of Wuhan Iron and Steel Corporation (WISCO) China. The MTS 810 machine, the experimental set-up (with specimen fractured in the grip) and experimental set-up (with specimen

fractured in the middle) are as shown in Plates 8 and 9 respectively. The testing machine was equipped with V-wedge hydraulic grips which made fastening of the test specimen to the testing machine simple and quick. The MTS machine force-measuring system was verified and calibrated statically in accordance with ISO 7500-1 [90] before use. Plate 10 shows the Research and Development Centre of Wuhan Iron and Steel Corporation (WISCO) China, where the fatigue testing was conducted.

3.9.3 Test specimens

The test specimens had a nominal diameter of 12 mm and a free length of $14d$, which was approximately equal to 170 mm according to ISO15630-1 [88]. All the test specimens were marked with a number for ease of identification and the overall length was 370 mm.

To avoid failure of the rebars where the grips of the testing machine clutch the rebars, all the rebars were covered with aluminium tubes at either end [97]. The dimensions of the aluminium tubes were 55 x 18 x 14 mm corresponding to the length, the outer and the inner diameter, respectively. The cavity between the rebar and the aluminium tube was filled with two component glue, Araldite 2011 (AVV106) + Araldite 2011B (HV 953U) [97].

For all the specimens, the surface of the free length between the grips was not subjected to surface treatment of any kind and did not contain identification marks as recommended in ISO15630-1 [88]. A sample test specimen covered by aluminum in the two ends is shown in Plate 11 and the nomenclature for a ribbed rebar test piece is as shown as Figures 5.4, 5.2 and 5.3 in Glossary of terms.

3.9.4 Test procedure

All test specimens were gripped axially in a MTS 810 machine [98, 99] and the testing was done at room temperature in accordance with ISO 15630-1 [88]. The tests were carried out in air using a stress ratio of 0.2, and different stress amplitude levels: 144(3), 140 (4), 136 (3), 132 (3) and 116 (2)kN, where the numbers in parentheses refers to the number of tests for the level concerned. A test frequency of 25 Hz was used to avoid heating of the specimens during cyclic loading. All of these tests were performed in lab air conditions. The application of load was sinusoidal wave as shown in Figure 5.1 and the minimum force for all the tests was 58 kN. The stress amplitude was determined as per the criteria given in Table E.3 in Appendix G. Testing was carried out under load control and stresses were calculated on the nominal cross-sectional area [99].

Constant cyclic stress amplitude was applied to a specimen and the

number of cycles to failure recorded.

Fifteen tests were conducted of which thirteen gave valid results. The thirteen results were used in the construction of a S-N curve.

3.9.5 Challenges in gripping of as received rebars

Unlike standard fatigue test specimens, the rebar diameter could not be reduced in the centre section before testing. This is because the deformations rolled onto the rebar surface have an effect on fatigue life, and must remain on the rebar during testing. Consequently, failure occurred at the grips. This would be expected because the bar has the same section inside and outside the grip area. As a result, any force exerted by the grips resulted in higher stress concentrations in the grip area, which in turn resulted in a high probability of failure at the grips. To ameliorate this situation, the force transmission areas at the ends of the rebars were strengthened by aluminum tubes to avoid fatigue failure due to shear stress at either end [97, 100] as shown in Plate 11. The tubes had a length of 55 mm, an outer diameter of 18 mm and an inner diameter of 14 mm. The cavity between the rebar and the aluminum tube was filled with two component glue, Araldite 2011 (AVV106) + Araldite 2011B (HV 953U) [97].

The test was carried out until failure of the test piece, or until reaching

5×10^6 load cycles as specified in BS 4449 [81] and Construction Standard [99], without failure. The frequency was chosen such as to induce failure due to the initiation and growth of cracks as opposed to internal friction causing large increases in temperature and consequent thermal breakdown [101]. During the testing, values of the minimum and maximum force were measured for every 1000 cycles [97].

If the fatigue failure occurred in the grips or within a distance of $2d$ of the grips or initiated at an exceptional feature of the test piece, the test was considered as invalid [88] and this was an undesired situation. The test was then automatically stopped by the testing machine. The test specimen was then replaced and the testing machine was started again. Tests in which fatigue failure occurred within the central portion of the bars were considered satisfactory. During the fatigue tests, the number of cycles required to cause failure of the specimens was recorded for later analysis.

3.9.6 Criterion of failure and test termination

The test was terminated when either the specimen failed or until reaching 5×10^6 load cycles as specified in BS 4449:2005 [81] and Construction Standard CS2 [99], without failure.

3.9.7 S-N Plots of Stress versus Fatigue Life

For the fatigue tests, the results are presented in plots of the stress amplitude versus the fatigue life of the specimen at that stress, commonly referred to as S-N curves. The S-N curve was smoothly drawn as an approximate middle line through the experimental points. A logarithmic scale was used for the number of cycles and the stress amplitude. The logarithm of the stress is presented on the ordinate in Cartesian coordinates, while logarithm of life is presented on the abscissa. It is the usual practice when data for multiple lots of material are presented to include the bands representing the majority of the data other than obvious outliers [102].

3.10 Data Acquisition

The data obtained from the fatigue test at minimum and maximum force was measured for every 1000 cycles and used for calculations in a MATLAB programme to generate fatigue strength curves (S-N curves).

Also load-elongation data was recorded and converted into stress-strain graphs during the tensile tests and results analyzed. The Yield stress (R_e), tensile strength (R_m), ratio of tensile strength/Yield stress (R_m/R_e), Modulus of Elasticity (E), and Percentage Elongation ($\Delta L\%$) were ana-

lyzed for the as-received and after a complete cycle of heating and cooling using tables and graphs.

Data obtained during Brinell hardness and impact toughness testing was recorded and analyzed using graphs and tables respectively.



Plate 8: The servohydraulic testing machine with clamped test specimen



Plate 9: The MTS 810 fatigue machine with a specimen fractured at the centre



Plate 10: Research and Development Centre of Wuhan Iron and Steel China



Plate 11: Test specimen covered by aluminum in the two ends

CHAPTER 4

Results and Discussion

4.1 Introduction

This chapter presents the outcomes of tests performed and discussion of the monotonic tensile, Brinell hardness, impact toughness and fatigue test results described in Chapter 3. The results of a survey conducted are also evaluated and discussed. Estimate of fatigue life using low cost tests is also presented.

4.2 Results from the Survey

Various issues were addressed through the questionnaire and the main ones are detailed below.

4.2.1 Quality Control

A summary of responses from the questionnaires on quality control of rebars from mill A and Mill B are as shown in Table 4.2.1 The quality control consisted of carrying out the chemical analysis using spark emission spectrometer before casting of ingot. Tensile testing, hardness, bending and rebend testing were carried out on the rebars in the

as rolled condition. The minimum yield strength specified by the Kenya Standard [83] is 460 N/mm^2 and percentage elongation was stated as 14%. The 10 and 16 mm as received rebars sampled and tested had a Yield stress of above 500 N/mm^2 . However the as received 12 mm rebars tested had a Yield stress of below 430 N/mm^2 . This was attributed to the low manganese and this was a good example of poor quality control at steel mills.

4.2.2 Production Methods

A summary of responses from the questionnaires on production methods of rebars from mill A and Mill B are as shown in Table 4.2. Two rolling mills responded to the questionnaire. The rolling mills were designated as Mill A and B. The rolling mills use three methods of production of rebars, namely the Quench and self-Tempering, Hot rolling and Cold Twisting process. Local scrap and imported billets are the raw materials for manufacturing twisted, round and ribbed bars. Scrap metal was sorted out through the use of visual inspection, conducting chemical analysis and by use of magnets before being used.

Table 4.1: A summary of responses from the questionnaires on quality control of rebars

No.	Variables	Supplier A	Supplier B
1	Do you carry out any quality control checks on the bars?		
	Yes	X	X
	No		
2	If yes, what quality checks do you carry out?		
	Tensile test	X	X
	Fatigue test		
	Impact test		
	Chemical analysis	X	X
	Other [] specify		
3	Which parameter/s are critical for a good quality bars?		
	Length	X	X
	Mass		
	Yield strength	X	X
	Tensile strength	X	X
	% Elongation	X	X
	Other [] specify		
4	How are the equipment used for quality checks verified?		
	By calibration checks	X	X
	By use of split samples		
	By use of Proficiency sample		
5	Do you carry out chemical composition analysis of the bars?		
	Yes	X	X
	No		
6	If you don't carry quality control checks, how do you verify the properties of the bars?		
	Send samples to be tested by KEBS	X	X
	Send specimens to be tested by ministry of works laboratories	X	X
	Send specimens to be tested by private laboratories		
	Other [] specify		
7	What is the minimum yield strength specified by the standards		
	250 N/mm ²		
	460 N/mm ²	x	x
	Other [] specify		
8	What is the minimum % Elongation expected ?		
	12		
	14	X	X
	Other [] specify		

Table 4.2: A summary of responses from the questionnaires on production methods of rebars

No.	Variables	Supplier A	Supplier B
1	Which type of steel reinforcement bars are manufactured by your factory?		
	Twisted bars		
	Round bars		
	Ribbed bars		
	All the above	X	X
	Other [] specify		
2	Which method of production for Rebars is used in your factory?		
	Work - hardening (cold - working)	X	X
	Microalloying		
	Quench and Self-Tempering	X	X
	Other [] specify		
3	Which raw materials do you use for manufacturing of the steel rebars?		
	local scrap metal	X	X
	Imported scrap metal		
	Imported billets	X	X
	Other [] specify		
4	Does your firm use scrap metal to manufacture reinforcing steel bars? (Yes or No)		
	Yes	X	X
	No		
5	If yes, How is the scrap sorted out?		
	Visual inspection	X	X
	Conducting chemical analysis	X	X
	Use of magnets	X	X
6	Which furnace is used for smelting the scraps?		
	Induction furnace	X	X
	Electrical Arc Furnace		
	Basic Oxygen Furnace		
7	What size of the rebar is most ordered for by the users?		
	8 mm	X	X
	10 mm	X	X
	12 mm	X	X
	16 mm	X	X
	20 mm		
	25 mm		

4.2.3 Survey results from KEBS

A Summary of responses from KEBS on quality control activities regarding locally manufactured rebars is as shown in Table 4.3. Tension, hardness (Rockwell, Brinell and Vickers), ductility, impact, radiography, magnetic particle, ultrasonic, eddy current, chemical composition analysis, bend and rebend testing are the main quality control methods performed by KEBS while analyzing the properties of rebars. KEBS quality assurance department is responsible for collecting test samples from the steel mills. The specimens are tested against a Kenya standard [83]. Those that meet the requirements were issued with a Standardization mark, else the manufacturer was required to destroy the rebars and make scrap metal.

4.2.4 Industrial Visits

Industrial visits were made to five steel rolling mills. Three mills are located in Kenya and the other two mills are based outside Kenya. The mills located in Kenya are Apex steel Ltd, Athi-River steel Ltd and Devki steel Ltd. Tata steels Ltd and Wuhan Iron and Steel corporation are based in the Netherlands and China respectively. Tempcore process and Cold Twisting processes were the methods used in the production

Table 4.3: A Summary of responses from KEBS on quality control

No.	Variables	KEBS
1	Do you carry out any quality control checks on the re-bars?	
	Yes	X
	No	
2	If yes, what quality checks do you carry out?	
	Tensile test	X
	Hardness test	X
	Fatigue test	X
	Impact test	X
	Chemical analysis	X
	Other [] specify	
3	Which parameter/s are critical for a good quality bars?	
	Length	X
	Mass	X
	Yield strength	X
	Tensile strength	X
	% Elongation	X
	Other [] specify	
4	Which equipment are used by KEBS for quality checks of rebars	
	Tensile machines	X
	Impact machines	X
	Hardness machines	X
	Bending machines	X
	Spectrometer	X
	NDT machines	
5	Do you carry out chemical composition analysis of the bars?	
	Yes	X
	No	
7	What is the minimum yield strength is specified by the standards for high strength rebars?	
	250 N/mm ²	
	350 N/mm ²	
	460 N/mm ²	x
	Other [] specify	
8	What is the minimum % Elongation expected after carrying out a tensile test?	
	10	
	12	
	14	X
	Other [] specify	

of rebars in the five steel mills visited.

Regarding quality control, tension, hardness (Rockwell, Brinell, Vickers), ductility, impact, radiography, magnetic particle, ultrasonic, eddy current, chemical composition analysis, bend and rebend testing were the main quality control methods used in the mills visited.

4.3 Chemical compositions

Tables 4.4 - 4.6 show the chemical composition (wt %) of the as-received specimens of the 12 mm rebars from Mill A, as-received, heated and cooled in (air and water) specimens of 16 mm rebar from mill A and mill B. In order to establish the combined effect of the alloying ele-

Table 4.4: Chemical Composition of 12 mm rebar from mill A (wt. %)

T°C	C	Si	Mn	P	S	Cu	Ni	Cr	Mo	Nb	V	C_P	C_{eq}
22	0.200	0.221	0.520	0.029	0.034	0.171	0.075	0.101	0.018	0.001	0.002	0.824	0.317

Table 4.5: Chemical Composition of 16 mm rebar from Mill A (wt. %)

T°C	C	Si	Mn	P	S	Cu	Ni	Cr	Mo	Nb	V	C_P	C_{eq}
22	0.203	0.220	0.528	0.032	0.032	0.172	0.075	0.098	0.020	0.001	0.002	0.929	0.332
500	0.184	0.216	0.537	0.036	0.029	0.168	0.071	0.095	0.020	0.001	0.002	0.927	0.313
900	0.197	0.227	0.544	0.039	0.031	0.168	0.072	0.097	0.020	0.001	0.002	0.954	0.327
1000	0.216	0.234	0.535	0.035	0.032	0.168	0.076	0.102	0.021	0.001	0.002	1.028	0.347

ments of the rebars, their carbon equivalent C_{eq} values were calculated

Table 4.6: Chemical Composition of 16 mm rebar from mill B (wt. %)

T°C	C	Si	Mn	P	S	Cu	Ni	Cr	Mo	Nb	V	C_P	C_{eq}
22	0.158	0.234	1.290	0.007	0.016	0.031	0.118	0.064	0.018	0.001	0.002	0.996	0.396
500	0.176	0.164	0.642	0.018	0.027	0.309	0.093	0.069	0.017	0.00	0.002	0.957	0.327
900	0.155	0.164	0.646	0.013	0.026	0.292	0.094	0.065	0.018	0.000	0.002	1.024	0.305
1000	0.172	0.244	1.280	0.006	0.016	0.032	0.076	0.118	0.010	0.001	0.002	1.141	0.417

using a well known equation (4.1) as given in standards [81,99]. The C_{eq} values thus obtained are presented in Tables 4.4- 4.6.

The carbon equivalent value (C_{eq}) was calculated using the following formula:

$$C_{eq} = C + \frac{Mn}{6} + \left(\frac{C_r + M_O + V}{5} \right) + \left(\frac{N_i + C_u}{15} \right) \quad (4.1)$$

where;

V is the percentage vanadium content;

Mo is the percentage molybdenum content;

Cu is the percentage copper content;

Ni is the percentage nickel content.

The C_{eq} calculated using equation (4.1) was observed to range between 0.36 to 0.40 which is considered very good for weldability [103]. The C_{eq} above 0.50 % can lead to brittle failures for high strength steels [103].

The sum of percentage of alloying elements (C_P), (C+Mn+Ni+Cr+Mo+V+Nb)

was also calculated. It is correlated to fatigue strength in subsequent sections. The calculated (C_P) was not constant and this was attributed to carburizing as the different sizes of the rebars were being heated to elevated temperatures. Diffusion of carbon atoms from the rebars with higher carbon content into rebars of low carbon content had occurred. It was observed that by heating the rebars, the mechanical properties changed without varying the chemical composition. The slight change in carbon content from 0.203 % to 0.216 % as the temperature increased from 22 to 1000 °C was due to carburizing.

4.4 Comparison of test results from Mill A and Mill B - Air cooling

The comparison on the effects of heat and air cooling on the Yield stress, Ultimate Tensile Strength and Brinell Hardness for rebars from mill A and mill B are presented graphically in Figures 4.1 - 4.3. It was observed that results on the effects of heat and air cooling on the Yield stress, Ultimate Tensile Strength and Brinell Hardness for rebars from mill A and mill B as shown in Figures 4.10-4.12 showed similar trends, hence results from mill A were used in the discussions. However, the yield stress of the as received 12 mm rebar from mill A was 430 MPa, which

was less than the expected 460 MPa by the standard [83]. This was due to the fact that it contained less manganese as compared to a similar rebar from mill B. It will be necessary to increase manganese contents to increase the Yield stress of the 12 mm rebars. The quality control departments of the industry should analyze more samples for chemical analysis. It is also recommended to send other samples to KEBS for chemical analysis. Results obtained by KEBS should be compared and appropriate actions taken to improve the quality of rebars produced.

4.5 Effect of Heat on Mechanical Properties and Microstructure - Air cooling

Tables C.1 - C.6 summarize the monotonic mechanical properties of the as-received, heated and air cooled 10, 12, and 16 mm rebars respectively extracted from tensile tests. The effects of heat and air cooling on the mechanical properties (Yield stress, Ultimate Tensile Strength, Percentage Elongation, Modulus of Elasticity, strain hardening ratio and Brinell Hardness) are presented graphically in Figures 4.4 - 4.9. The findings of effect of heat on mechanical properties and microstructure and air cooling have been published as paper I as indicated in Appendix F.

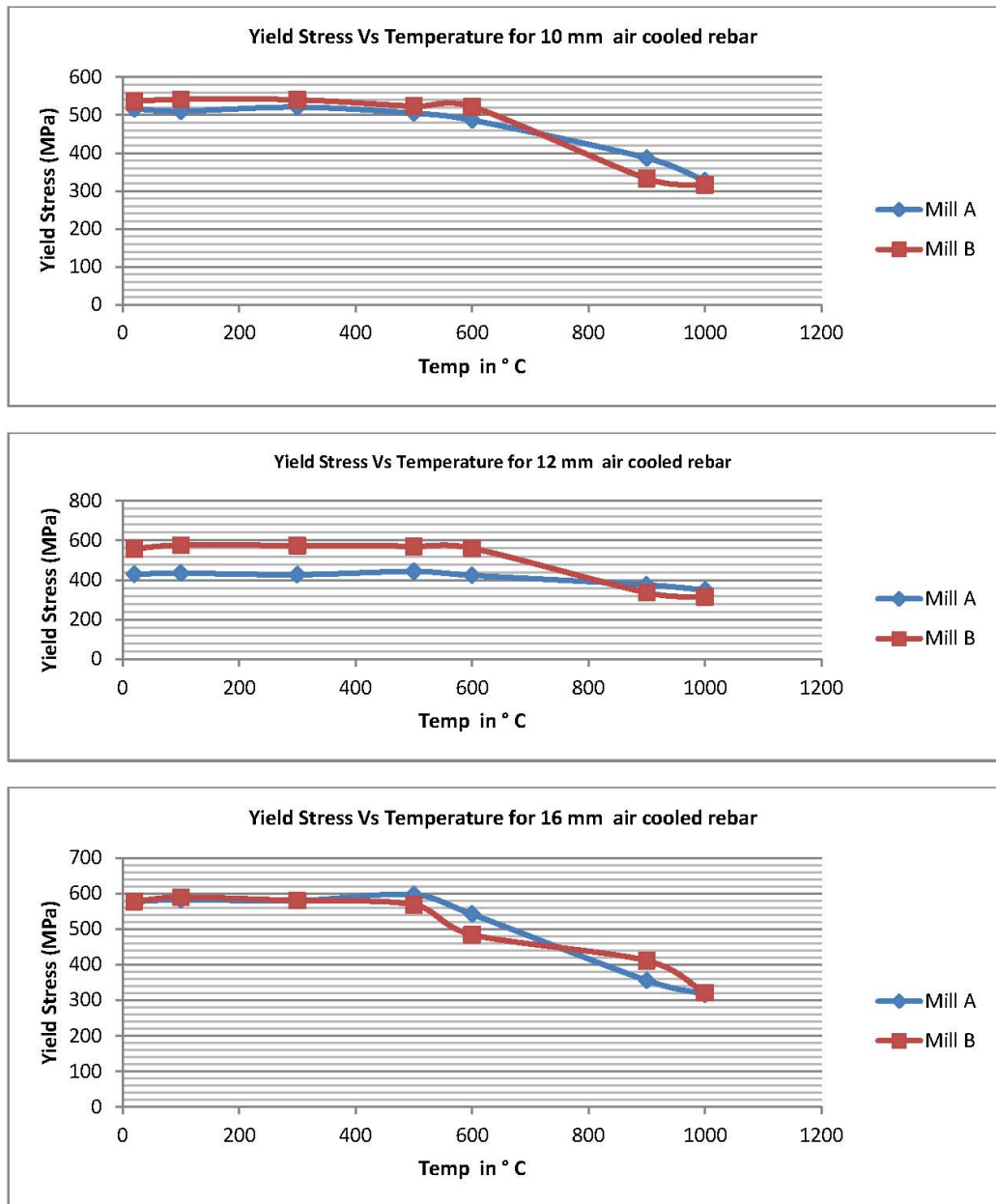


Figure 4.1: Yield Stress Vs Temperature for air cooled rebars from Mills A and B

4.5.1 Yield stress (R_e)

Yield stress of 10, 12 and 16 mm rebars was affected by the elevated exposure temperatures. It can be seen in Figure 4.4 that there was no

significant variation in Yield stress of rebars cooled by air below 500 °C. Plain rebars had experienced the strain hardening already for this temperature. According to Eurocode 3 [104], below 400 °C, there is no decrease in Yield stress, but above this temperature Yield stress decreases as temperature increases. The Yield stress losses for 10, 12 and 16 mm rebars were 25%, 12% and 38% for 900 °C exposure temperature, respectively when compared to that of the as-received rebars. For further increase of temperature up to 1000 °C, Yield stress decreased by 37%, 18% and 45%, for rebar 10, 12, and 16 mm, respectively. This decrease in R_e can be attributed to the nucleus of the iron atoms in steel rebar moving farther apart due to rising temperature in steel, leading to decreased bond strength, which in turn reduces the Yield stress [105].

It can also be observed that the as-received 16 mm rebar showed higher Yield stress than the as-received 10 and 12 mm rebars. This higher Yield stress for the 16 mm rebar was due to the chemical composition. The strengthening mechanisms was by solid-solution alloying. The 16 mm rebar contained a higher content of carbon and manganese than 10 mm and 12 mm rebars. These two elements are known to increase overall strength [106]. The Yield stress of the as-received 12 mm rebars was found to be 430 MPa. This value is lower than the standard allowed value of 460 MPa for high yield steel rebars [83]. It will be necessary to

increase the carbon and manganese contents to increase the Yield stress of the 12 mm rebar. The quality control departments of the industry should analyze more samples for chemical analysis. It is also recommended to send other samples to KEBS for chemical analysis. Results obtained will be compared and appropriate actions taken to improve the quality of rebars produced. It is also worth noting that yield stress decreased with the decrease in grain size as shown in Table C.5 (inverse Hall-Petch effect). This trend is less well established for finer grains. Some of the deviation from Hall-Petch strengthening could simply be due to pores in the material. Additional complications arise due to impurities at the grain boundaries like oxides and impurities inside the grain such as trapped or diffused gas [107].

4.5.2 Tensile Strength (R_m)

From Figure 4.5, it can be observed that the tensile strength remained high up to 500 °C for all the three sizes of rebars, after which it began to drop. After 500 °C, the residual tensile strength is lower than the tensile strength of the as-received rebars. The tensile strength losses for the 10, 12 and 16 mm rebars were 19%, 2% and 26% for 900 °C exposure temperature, respectively when compared to that of the as-received rebars. For the highest exposure temperature at 1000 °C, tensile

strength losses were 17%, 12% and 28%, respectively when compared to the as-received rebars. However, it should be noted that there is a possibility of complete strength loss of rebars at high temperatures when a structure is subjected to a high temperature fire. Consequently, the remaining strength of the rebars in structures is influenced by the exposure time and type of fire and will depend on the rate of heat transfer through the concrete cover to rebar steel [108].

4.5.3 Elongation

After the rebars cooled to room temperature, the retained ductility (elongation) after heating was measured as a ratio of the as-received room temperature elongation and the relationship is as shown in Figure 4.6. It can be seen in Figure 4.6 that there was no significant variation in ductility of rebars cooled by air up to 500°C. After 500°C, the residual elongation decreased with increasing temperature. The decrease for 10, 12 and 16 mm rebars was found to be 29%, 18% and 29% for 900°C exposure temperature, respectively. For further increase of temperature to 1000°C, elongation ratio decreases were 35%, 19% and 35%, respectively. The 10, 12 and 16 mm rebars showed similar elongation behaviour under elevated temperatures. These excess carbon, sulphur and phosphorus contents increase the strength and hardness of the rebars, and at

the same time decreased their ductility, making them brittle. Another relevant expression of ductility involves a stress ratio between the tensile strength (R_m) and the yield stress (R_e) of the rebar (R_m/R_e) [87]. The R_m/R_e ratio deduced from the stress-strain diagram could be used as an indirect means to express the extent of uniform elongation before fracture, i.e., the elongation up to the ultimate tensile strength. In all cases, it was higher than the minimum allowed value of 1.08 [83]. High R_m/R_e ratio and more percentage elongation signify that the steel is capable to strain harden, in the event of an earthquake. According to the latest ACI 318 code [109], reinforcement in members resisting earthquake-induced forces should have values of R_m/R_e not less than 1.25. Furthermore, the actual Yield stress should exceed the specified Yield stress by no more than 124 MPa. The 10 and 12 mm rebar meet these requirements, hence can be used for seismic applications.

4.5.4 Modulus of Elasticity (E)

The Modulus of Elasticity, E was determined from the stress - strain curve based on the tangent modulus of the initial elastic linear curve [110]. The result was expressed in gigapascals (GPa) and reported to three significant figures. The values of E obtained are presented in Figure 4.7. The test was considered invalid when the slope of this line differed

by more than 10 % from the theoretical value of the Modulus of Elasticity [88]. From Figure 4.7, it can be seen that E decreased with increase in temperature. This decrease can be attributed to the nucleus of the iron atoms in steel moving farther apart due to rising temperature in steel, leading to decreased bond strength, which in turn reduces the elastic modulus [105]. The slight increase in E between 500 and 600 °C requires further investigation. The relationship shown was nearly the same for all rebars tested. E does not decrease with temperature as rapidly as does Yield stress [76]. Also from the results in Tables C.1 and C.6, E varied with diameter. This variation of E was due to the differences in sample composition, the test method and the direction of the applied force with respect to the grain structure orientation (anisotropy) of the material. Measured steel modulus easily varies from 180-220 GPa [111].

4.5.5 Brinell Hardness (HBW)

The results of Brinell hardness measurements are as shown in Figure 4.8. The precipitation phenomena occurred at temperatures up to approximately 500 °C and are accompanied initially by a slight increase of hardness up to 100 °C, which thereafter becomes approximately constant up to 500 °C. Above 500 °C, hardness decreased with increase in temperature. The decrease in hardness can be associated with the

formation of soft ferrite matrix in the microstructure of the annealed sample by cooling [4]. The hardness values of 12 mm rebar was higher than the corresponding values of 10, and 16 mm rebars at temperatures from 100 up to 1000°C. The difference is attributed to their different chemical compositions. The 12 mm had more carbon, sulphur and phosphorus which are known to increase the strength and hardness of the steels. Further work on the rebar may be necessary to verify size effect on Brinell hardness.

4.5.6 Effect of Heat on Microstructure and grain size

The metallographic study showed that as-received rebar steel has a ferrite-pearlitic structure with Ferrite appearing as white and pearlite appearing as black, as shown in the micrographs in Figure 4.9. The microstructures of the samples heated to 100, 500, 600, 900 and 1000°C are shown Figure 4.9 (b) - (f) respectively. No significant microstructural changes occurred after heating the rebars up to 300°C. At 900°C (Figure 4.9 (e)) the deformed structure was fully homogenized and during the slow cooling from austenizing range to room temperature, the final microstructure consisted of fine ferrite grains in which the pearlite was more uniformly distributed. The grain size of the rebars was comparatively small and the d_n values for specimens was noted to decrease

from 18.9 to 13.7 μm as the temperature increased from 22 to 1000°C as shown in Table C.5. The grain refining effect was due to the presence of Vanadium, Titanium, and Niobium, which produced fine uniformly distributed nitro-carbides on the grain boundaries, that decreased the boundary migration. Vanadium, further had a relatively small solubility in austenite [112] hence leading to refinement of austenitic grains during hot rolling

4.6 Comparison of test results from Mill A and Mill B -Water Quenching

The comparison on the effects of heat and water quenching on the Yield stress, Ultimate Tensile Strength and Brinell Hardness for rebars from mill A and mill B are presented graphically in Figures 4.10 - 4.12.

4.6.1 Yield Stress Vs Temperature for water quenched rebars from Mills A and B

It's observed that results on the effects of heat and Water Quenching on the Yield stress, Ultimate Tensile Strength and Brinell Hardness for rebars from mill A and mill B as shown in Figures 4.10-4.12 showed similar trends, hence results from mill A were used in the discussions.

However, the yield stress of the as received 12 mm rebar from mill A was 403 MPa, which was less than the expected 460 MPa by the standard [83]. This was due to the fact that it contained less manganese as compared to a similar rebar from mill B. It will be necessary to increase manganese contents to increase the Yield stress of the 12 mm rebars. The quality control departments of the industry should analyze more samples for chemical analysis. It is also recommended to send other samples to KEBS for chemical analysis. Results obtained will be compared and appropriate actions taken to improve the quality of rebars produced.

4.7 Effect of Heat on Mechanical Properties and Microstructure - Water quenching

Tables D.1 - D.6 summarize the monotonic mechanical properties of the as-received, heated and water quenched 10, 12, and 16 mm rebars respectively extracted from tensile tests. The effects of heat and water quenching on the mechanical properties (Yield stress, Ultimate Tensile Strength, Percentage Elongation, Modulus of Elasticity, strain hardening ratio and Brinell Hardness) are presented graphically in Figures 4.13 - 4.18. The findings of effect of heat on mechanical properties and microstructure and water quenching have been published as paper II as

indicated in Appendix F.

4.7.1 Yield stress (R_e)

R_e was determined from the 0.2% proof strength ($R_{p0.2}$). The Yield stress of 10, 12 and 16 mm rebars as a function of temperature is presented in Figure 4.13. It can be seen from Figure 4.13 that there is no significant variation in Yield stress of rebars quenched after heating up to 500°C. The rebars had experienced strain hardening already for this temperature. According to Eurocode 3 [104], below 400°C, there is no decrease in Yield stress, but above this temperature a significant Yield stress increase occurs. The Yield stress increase of 10, 12 and 16 mm rebars were 118%, 180% and 10% for 900°C exposure temperature, respectively when compared to that of the as-received rebars. For further increase in temperature to 1000 °C, the corresponding Yield stress increases were 118%, 193% and 41%, respectively. The Yield stress increase for three sizes of rebars was due to accelerated cooling. When the alloy is cooled suddenly, the carbon atoms cannot make an orderly escape from the iron lattice. This cause "atomic bedlam" and results in distortion of the lattice, which manifests itself in the form of strength. If cooling is fast enough, a new structure known as martensite is formed, although this new structure (an aggregate of iron and cementite) is in the alpha

phase. The ability of obtaining different microstructures from tempered martensite on the surface to ferrite and pearlite in the core, as well as the grain refinement was among the other factors for the optimisation of strength [113]. The chemical composition, finishing temperature and cooling rates are the major three parameters that affect the properties of the rebars produced by water quenching cite Abdel. It can also be observed that the as-received 10 and 16 mm rebars showed higher Yield stress than the as-received 12 mm rebars. This higher Yield stress for the 10 and 16 mm rebars was due to the chemical composition. The 10 and 16 mm rebar contained higher content of carbon and manganese than 12 mm rebars. These two elements are known to increase the overall strength [106]. The 16 mm rebars also showed a brittle fracture. This was due to higher percentage carbon content of 0.216% [114]. The Yield stress of the as-received 12 mm rebars was found to be 403 MPa. This value is lower than the standard allowed value of 460 MPa for high yield steel rebars [83]. It will be necessary to increase the carbon and manganese contents to increase the Yield stress of the 12 mm rebar. The quality control departments of the industry should analyze more samples for chemical analysis. It is also recommended to send other samples to KEBS for chemical analysis. Results obtained will be compared and appropriate actions taken to improve the quality of rebars produced.

4.7.2 Tensile Strength (R_m)

From Figure 4.14, it is observed that there was no significant variation of tensile strength for 10, 12 and 16 mm rebars up to 500°C. Above 500°C, the tensile strength increased as compared to the as-received rebars. For the exposure temperature at 900°C, tensile strength increases were 134%, 160% and 16%, respectively. For the highest exposure temperature at 1000°C, tensile strength increases were 141%, 177% and 56%, respectively.

The ability of plastic deformation of the metal is depending on the ability of the dislocation motion. Since the strength of the rebars was also related to plastic deformation. The strengthening mechanisms obeyed a simple principle, the more restrict or hinder the dislocation motion makes a material stronger and harder. The increase in tensile strength for the three rebar sizes was also due to the formation of fine pearlite and martensite as a result of fast cooling due to smaller diameter size [115]. It can also be observed that the as-received 10 and 16 mm rebars showed higher tensile strength than the as-received 12 mm rebars. This higher tensile strength for the 10 and 16 mm rebars was due to the chemical composition. The 10 and 16 mm rebar contained higher content of carbon and manganese than 12 mm rebars. These two elements are known

to increase the overall strength [106]. The 16 mm rebars also showed a brittle fracture. This was due to higher percentage carbon content of 0.216% [114] and the presence of sulphur which are known to cause britleness.

4.7.3 Elongation

After the rebars cooled, the retained ductility was measured as a ratio of the retained elongation to original room temperature elongation and the relationship is as shown in Figure 4.15. The 10, 12 and 16 mm rebars showed similar elongation behaviour under elevated temperatures. The elongation retained decreased with increasing temperature until a minimum value was reached at 100°C and it remained constant up to 300°C. The initial decrease in ductility was caused by strain aging. After 300°C, elongation decreased with increasing temperature. This was due the formation of martensite due to fast cooling [114]. The decrease for 10, 12 and 16 mm rebars was found to be 24%, 28%, and 30% for 900 °C exposure temperature, respectively. For further increase in temperature to 1000°C, elongation ratio decreases were 29%, 29% and 72%, respectively. According to these results, the elongation capacity of 16 mm steel is lower than that of 10 and 12 mm steel under elevated temperatures. The 16 mm rebar showed brittle fracture behaviour under elevated tem-

peratures. This brittle behaviour is not suitable for rebars to be used in reinforced concrete structures [72]. As explained earlier in subsection 4.4.3 in the last paragraph, the results as presented in Table C.3 - C.5, 10 and 12 mm rebar meets the requirement, hence can be used for seismic applications.

4.7.4 Modulus of Elasticity (E)

The Modulus of Elasticity E , is about 210 GPa for a variety of common steels at room temperature. The variation of E with temperature for the rebars tested is presented in Figure 4.16 (Modulus at elevated temperature to that at room temperature). It can be seen that E increased with an increase in the temperature up to 100°C and thereafter, it remained approximately constant as temperature increased up to 500°C. After 500°C, the Young's modulus decreased when compared to the as-received rebars. For the exposure temperature at 900 °C, the decrease in Young's modulus compared to that of as-received rebars at room temperature for 10, 12 and 16 mm rebars, was found to be 4%, 2% and 1%, respectively. For the highest exposure temperature of 1000°C, the decrease in E was 2%, 2% and 2%, for 10, 12 and 16 mm rebars respectively. The relationship shown is nearly the same for all rebars. It has been reported [76] that Young's modulus does not decrease with tem-

perature as rapidly as does Yield stress. Also from the results in Tables D.1 - D.6, E varied with diameter. This variation in E was due to the differences in sample composition, the test method and the direction of the applied force with respect to the material's grain structure orientation (anisotropy). Measured modulus for steel easily varies from 180-220 GPa [111].

4.7.5 Brinell Hardness (HBW)

The Brinell hardness of the rebars increased gradually with temperature as shown in Figure 4.17. This behaviour is explained by the progressive decrease in grain size of the rebars with increase in temperature, which produces greater homogeneity and compactness of the deposited grains [105]. The precipitation phenomena occurred at temperatures up to approximately 500°C and are accompanied initially by a slight increase of hardness up to 500°C. Above 500°C, higher Brinell hardness was achieved. This was due to the faster cooling rate of steel resulting in highest free carbon in martensite [116]. Furthermore, the presence of fine dispersion of small particles in the pro-eutectoid ferrite and pearlitic ferrite, which will hinder the dislocation movement, may have also contributed to the higher Brinell hardness [117]. In general, the Brinell hardness increased because of the refinement of the primary phases after

rapid cooling in water [118]. It is well documented that the water quenching creates a supersaturated solid solution, and vacancies increase with carbon content in water quenched samples [119]. Thus, high hardness correlates with high resistance to slip and dislocation. It can be claimed that the increase in the Brinell hardness is due to the delay in the formation of ferrite which promotes the formation of pearlite and martensite at a higher cooling rate. Thus, the increase of Brinell hardness with the water quenched rebar steels can be explained by the increasing relative volume of pearlite and martensite after quenching [120].

4.7.6 Effect of Heat on Microstructure and grain size

The metallographic study showed that as-received rebar steel has a ferrite-pearlitic structure with Ferrite appearing as white and pearlite appearing as black, as shown in the micrographs in Figure 4.18 (a). Figure 4.19 (a) shows the ferrite and pearlite grain structure [121]. The microstructures of the samples heated to 100, 500, 600, 900 and 1000°C and quenched in water are shown in Figure 4.18 (b)-(f) respectively. After heating and quenching in water, the microstructure constituted martensite for 600 and 1000 °C as it can be seen in Figures 4.18 (d) and (f). Figure 4.19 (b) shows the martensite grain structure [121]. However, ferritic and bainitic zones can be observed too in the microstructure. At

900°C (Figure 4.18 (e)), all quenched samples consisted of martensite with proeutectoid ferrite along the grain boundaries which explains the higher hardness at temperatures above 500°C . In between the surface hardened into martensite and the core, fine circular ferrite with pearlite was formed, while in the core itself ferrite with pearlite was formed. Such microstructure distribution allows obtaining a high strength and good plastic properties. The grain size of the rebars was comparatively fine. The grain refining effect was due to the presence of Vanadium, and Niobium which produced fine uniformly distributed nitro-carbides on the grain boundaries, that decreased the boundary migration. Vanadium, further had a relatively small solubility in austenite [112] hence leading to refinement of austenitic grains during hot rolling. The d_n values for specimens was noted to decrease from 18.9 to 12.0 μm as the temperature increased from 100 to 1000°C as shown in Table D.5. The other reasons for the comparatively small grain size of tested steels may be the small diameter of the rebars and hence larger rolling reduction [122] and the presence of grain refiners such as vanadium and niobium in rebars tested. It has been found from the literature that other grain refiner elements like niobium and titanium have high potential in grain size refinement of rebar steel at high temperature and enhance the Yield stress of steel [121].

It is also worth noting that beyond 870°C, steel's metallurgical microstructure undergoes a permanent transformation relative to its original chemical composition that will result in grain coarsening and hardening, which, with the subsequent cooling, will adversely affect its residual mechanical properties. For example, the heating above 500°C for about 30 minutes or more and cooling resulted in a reduced ductility and Modulus of Elasticity, as well as higher hardness and elevated yield and tensile strengths [71].

4.8 Comparison on (R_e), (R_m) and BHW Vs Temperature for air and water cooled rebars from Mills A

The comparison on the effects of heat on air and water quenching on the Yield stress, Ultimate Tensile Strength and Brinell Hardness for rebars from mill A are presented graphically in Figure ??.

4.9 Charpy V-notch impact tests

Table 4.7 shows the results of the Charpy V-notch impact tests. The average values of the Charpy absorbed energy at room temperature were found to be 61 and 63 J for the 12 and 16 mm rebars respectively.

It has been generally recognized that a sufficient level of toughness is

required in order to avoid the initiation and propagation of cracks in the brittle fracture mode. Therefore, the 12 and 16 mm rebars conform to a minimum average CVN toughness value of 54 J at 22°C [123]. The Charpy absorbed energy was found not to depend on the type of the test specimens. Charpy results however cannot be considered to be directly relevant to structural behaviour. Materials that have high impact resistance generally have high strength, high ductility, and hence high toughness [123].

Refining the grain size is the best option for increasing the strength, because toughness is improved at the same time, but grain growth controllers are required in weldable steels. Increasing the alloy content of steel to increase its strength tends to reduce toughness, hence steel-makers offset this effect by grain size control during the manufacturing [124]. Steels that are produced by the normalization route, usually have a fine-grained ferrite and pearlite microstructure. The apparent changes in toughness that result from the geometry and strain rate are not quantified at all by the Charpy test, which always uses a standard small (10 mm thick) specimen under dynamic loading [124].

4.10 Fatigue Testing

The axial fatigue test results are displayed in Tables ?? and ?? and, the fatigue strength curve (S-N curves) are shown in Figures ?? and ??. Tests of thirteen specimens at five different stress amplitudes ranging from 132 to 144 MPa resulted in a fatigue life range of 3×10^5 to 1.8×10^6 cycles as shown in Table ??. The best fit curves for the bars were based on the average number of cycles at each stress range [45]. Based on the report by Jhamb and MacGregor [55], the best fit equation was chosen in the logarithm form for both the valid and invalid results. By linear regression, a straight line for the thirteen test results in Table ?? was calculated [97]. The equation for the straight line corresponding to Figure ?? is:

$$\text{Log}(\sigma_{max} - \sigma_{min}) = 2.399 - 0.0435 \text{Log}(N) \quad (4.2)$$

The ordinate axis is the logarithm to base 10 of stress amplitude, σ_a and the abscissa axis is the logarithm to base 10 of the number of cycles to failure, N.

Table ?? indicates that two specimens failed prematurely near the grips. The two axial premature failures fractured near the grip region with applied stress amplitude of 132 MPa. The direct cause of the premature

failures is thought to be linked to high tensile stress levels in the transition region resulting from residual stress and, therefore, lower strength at this section.

The equation for a straight line where all the 15 test results are included is:

$$\text{Log}(\sigma_{max} - \sigma_{min}) = 2.505 - 0.0628\text{Log}(N) \quad (4.3)$$

The 12 mm rebar appeared not to exhibit a fatigue limit below which fatigue failure is unlikely to occur when subjected to constant amplitude cyclic loading. The fatigue limit under constant amplitude loading conditions occurs for a few metals (notably low and medium strength steels) [125]. For a large number of steels, there is a direct correlation between tensile strength and fatigue strength; higher-tensile-strength steels have higher endurance limits. The endurance limit is normally in the range of 0.35 to 0.60 of the tensile strength [102].

Conventional steel reinforcing bars typically exhibit a fatigue life of 1×10^6 cycles at a stress amplitude of approximately 166 MPa [126]. In the current study, a fatigue life of 1.8×10^6 cycles is observed at a stress amplitude of approximately 132 MPa. Thus, the fatigue performance of the 12 mm rebar tested in this study was inferior to that obtained in the previous tests. One reason may be the fact that before the fatigue load was applied, tensile stresses were induced in the specimens when

the specimens were gripped. These tensile stresses result in an increased minimum stress, and a higher maximum stress level [45]. All of these factors are known to decrease fatigue strength [45]. Secondly, it may have resulted from slightly different metallurgy or manufacturing processes for the different batches of 12 mm rebar used in this study [127]. Generally smaller grain sized rebars at ambient temperature, have better fatigue resistance [125].

4.10.1 Comparison with AASHTO Fatigue Design Criteria

So far, no test has been standardized in the determination of the fatigue properties of rebars. Based on the equations developed by Helgason et al. [61], the AASHTO Bridge Specifications [23] provides a simplified design criterion for straight deformed hot rolled rebars embedded in concrete and according to that criterion, the design stress range is given;

$$f_f = 145 - 0.33f_{min} + 55r/h \quad (4.4)$$

where

f_f is the stress range, in MPa

f_{min} is the algebraic minimum stress, tension positive, compression negative, in MPa

r/h is the ratio of base radius to rib height, a value of 0.3 can be used

In the current tests, the minimum stress was 58 MPa. According to Equation 4.4, the design stress range should be 140 MPa. This means that for any stress range below 140 MPa, a bar in this experiment should sustain virtually an unlimited number of cycles without breaking. The 12 mm rebars were evaluated at a stress range of 132 MPa, and failed with 1.8×10^6 cycles, hence AASHTO fatigue criteria was not met.

4.10.2 Comparison of fatigue properties of the ribbed 12 mm rebars with standards

The 12 mm rebars tested failed after 1.8×10^6 cycles as shown in Table ??, specimen no. 6. Standards BS 4449 [81] and Construction Standard CS2 [99] both specify that test specimens should endure 5×10^6 cycles of stress in a fatigue test. Therefore the 12 mm rebar tested did not meet the specifications of the two standards. One reason was the fact that before the fatigue load was applied, tensile stresses were induced in the specimens when the specimens were gripped. These tensile stresses resulted in an increased minimum stress, and a higher maximum stress level [45]. All of these factors are known to decrease fatigue strength

[45]. Secondly, it may have resulted from slightly different metallurgy or manufacturing processes for the different batches of 12 mm rebar used in this study [127]. Generally smaller grain sized rebars at ambient temperature, have better fatigue resistance [125].

4.11 Estimating the fatigue strength for rebars based on low-cost test

Over the last few decades, many researchers have attempted to develop relations between monotonic tensile properties and uniaxial fatigue properties of engineering materials [128]. If reliable relations with reasonable accuracy can be established, they can serve to provide fast solutions to fatigue problems without time and cost involved in fatigue testing [128]. Based on a research by Martinez et al [35], it was shown that the V-Notch Charpy Impact toughness, the sum of percentage of alloying elements (C+Mn+Ni+Cr+Mo+V+Nb) and the mechanical properties have a positive linear effect in relation to the fatigue strength.

Considering this behaviour, correlations to predict the fatigue strength of the steel were developed based on Charpy impact energy, Yield stress, tensile strength, and Brinell hardness of the material.

These correlations with three variables that were generated using Mat-

lab mathematical software, using linear functions for data adjustments are stated as Equation 4.5, 4.6 and 4.7 and will be used to estimate the fatigue strength of the 12 mm rebar.

4.11.1 Dependent correlation of impact toughness, hardness, and tensile strength

The following expression relates the mechanical variables of toughness, hardness and tensile strength to the fatigue limit, and combines the toughness field that tends to oppose the resistance to the spread of fatigue cracking [35].

$$\sigma_e = 0.17CVN + 2.59HBW - 0.41R_m \quad (4.5)$$

4.11.2 Dependent correlation of toughness, chemical composition and tensile strength

The following expression relates the mechanical variables of toughness, tensile strength and chemical composition [35].

$$\sigma_e = 0.13CVN + 7.49C_P + 0.37R_m \quad (4.6)$$

4.11.3 Dependent correlation of the toughness, strength ratio and hardness

The following expression relates the mechanical variables of toughness, yield-tensile ratio and Brinell hardness [35].

Table 4.12

$$\sigma_e = 1.35CVN - 791.03 \frac{R_e}{R_m} + 3.27HBW \quad (4.7)$$

Rebar dia.
12

As shown in Tables ?? to 4.12, the three correlations, i.e. Equations 4.5, 4.6 and 4.7 used in estimation of the fatigue strength give higher values than experimental results for the 12 mm rebar. The three correlations show variations in fatigue strength of 32.5%, 81.8% and 290% respectively, compared to the experimental result. Dependent correlation of the toughness, tensile strength and hardness gave a fatigue strength estimate of 175 MPa which was nearer to the experimental result of 132 MPa. Based on this result, experimental results will continue to be relied more than estimates described above.

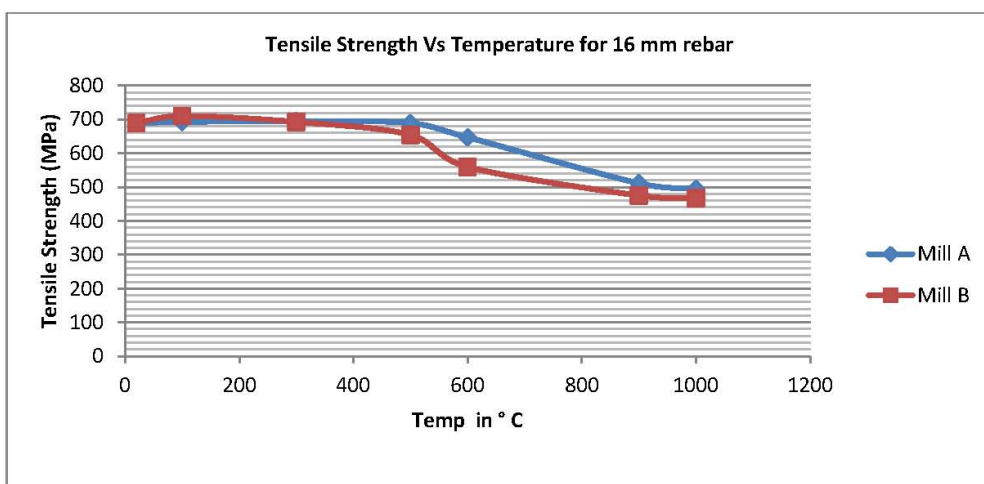
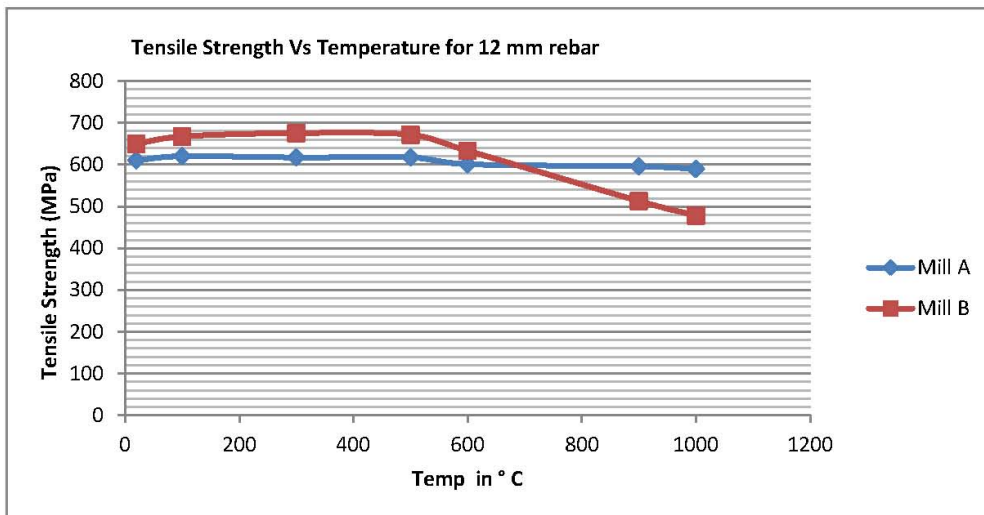
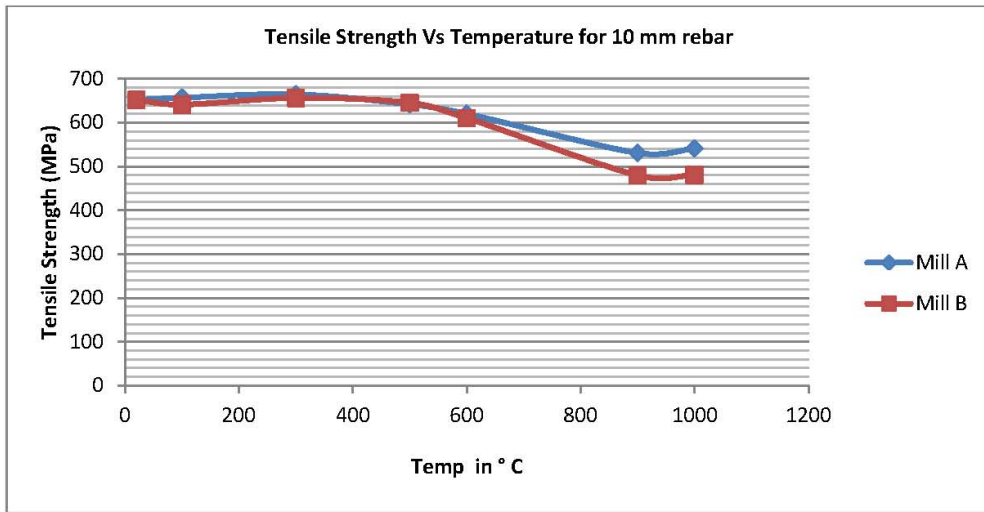


Figure 4.2: Tensile Strength Vs Temperature for air cooled rebars from Mills A and B

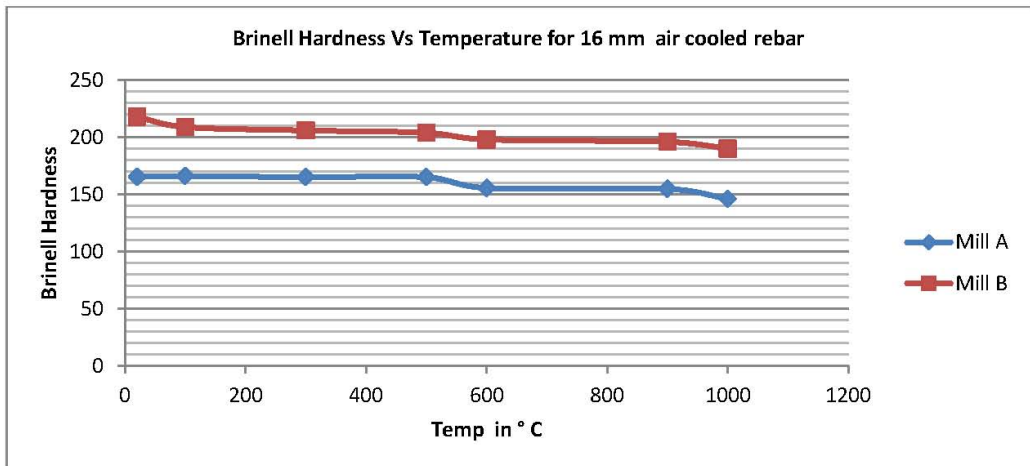
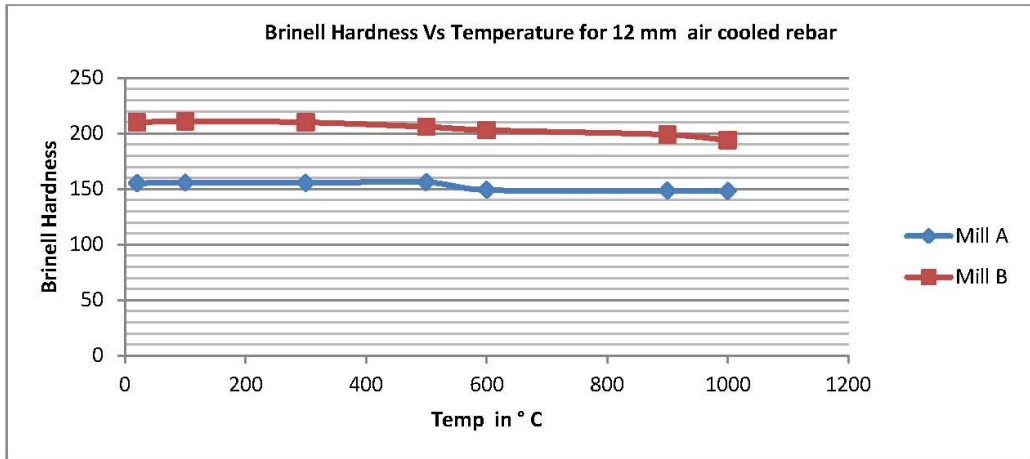
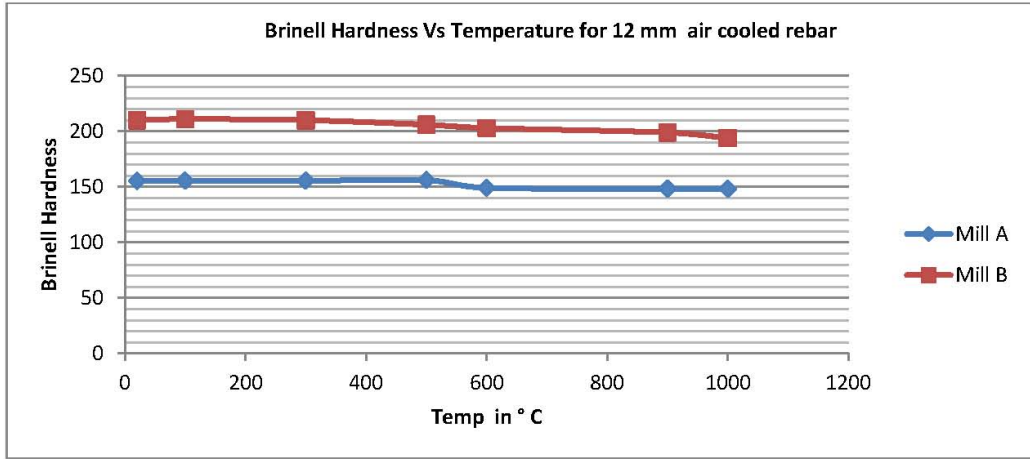


Figure 4.3: Brinell Hardness Vs Temperature for air cooled rebars from Mills A and B

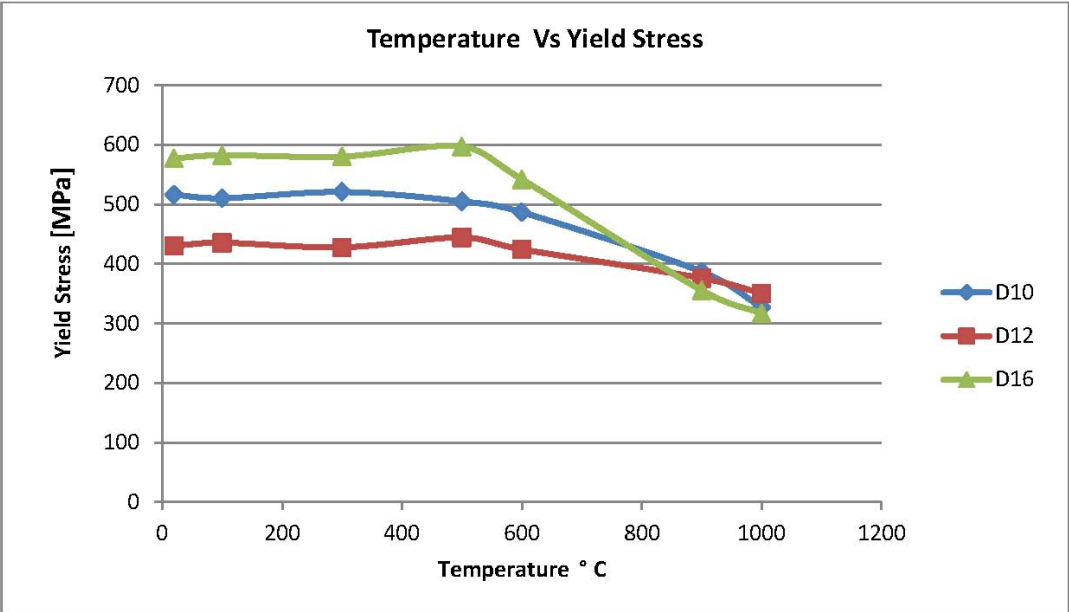


Figure 4.4: Yield stress Vs Temperature for air cooled rebars

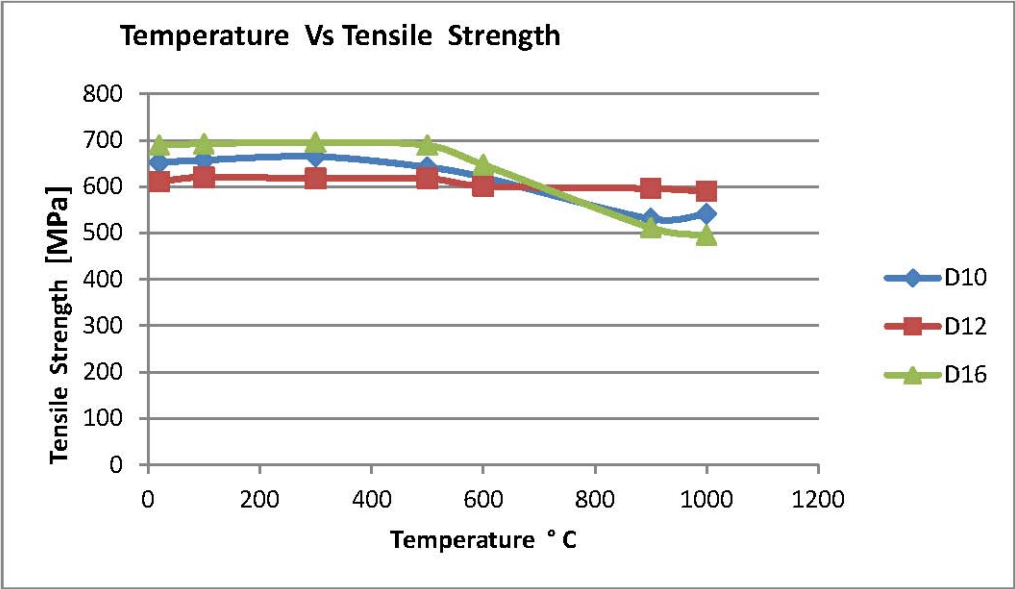


Figure 4.5: Tensile strength Vs Temperature for air cooled rebars

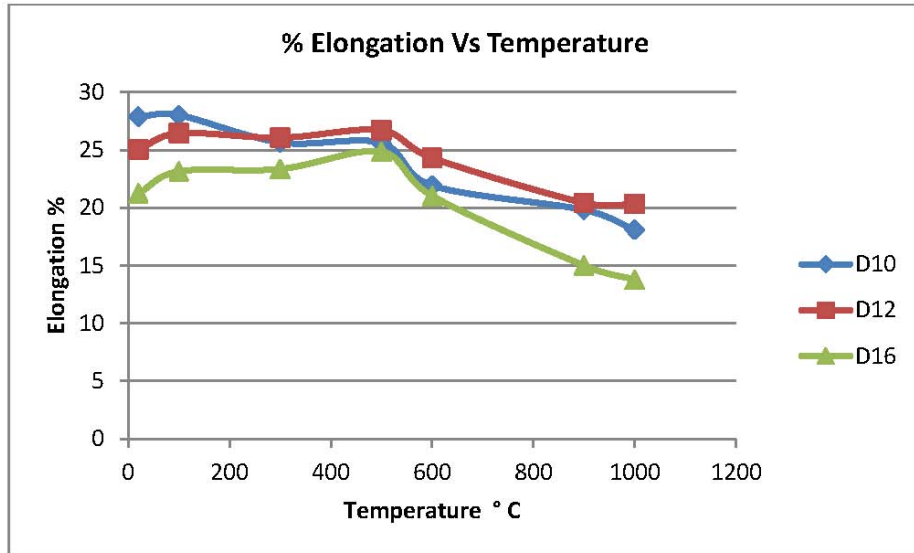


Figure 4.6: Elongation ratio Vs Temperature for air cooled rebars

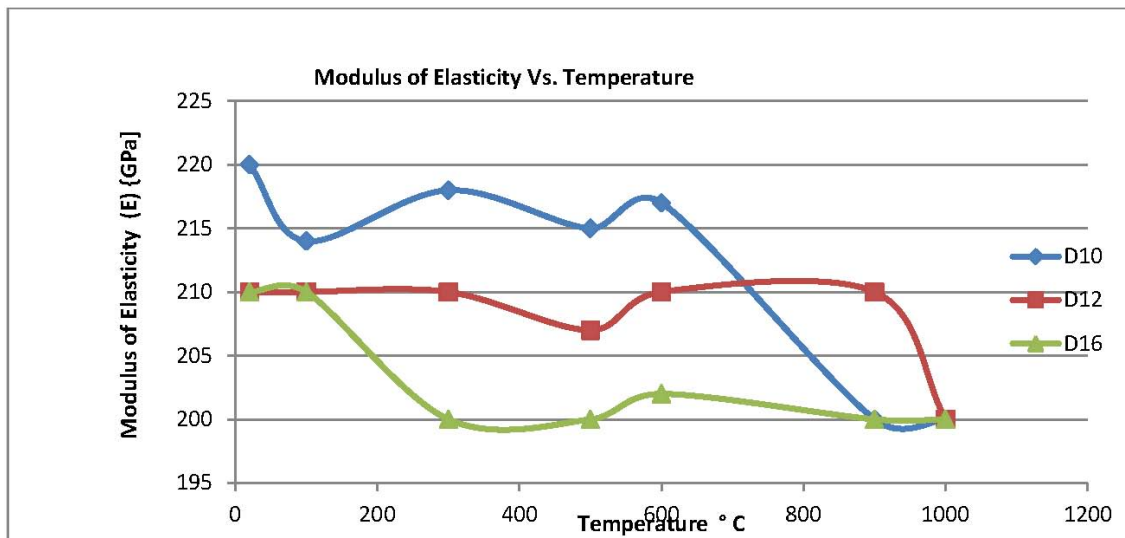


Figure 4.7: Modulus of Elasticity Vs Temperature for air cooled rebars

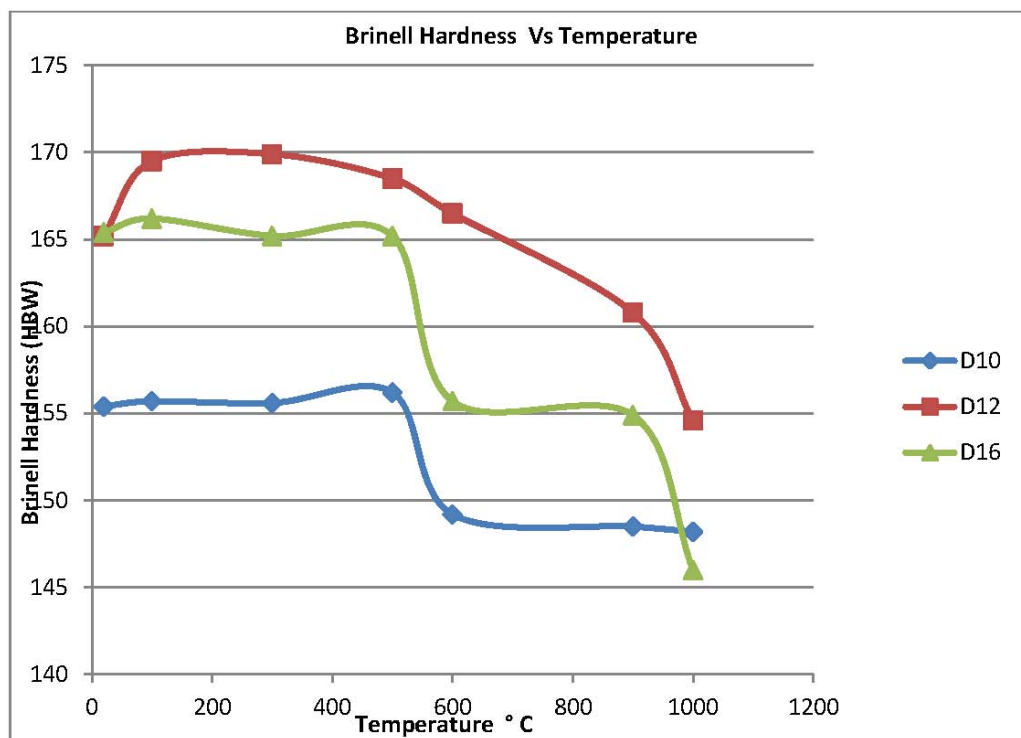


Figure 4.8: Brinell hardness Vs. Temperature for air cooled rebars

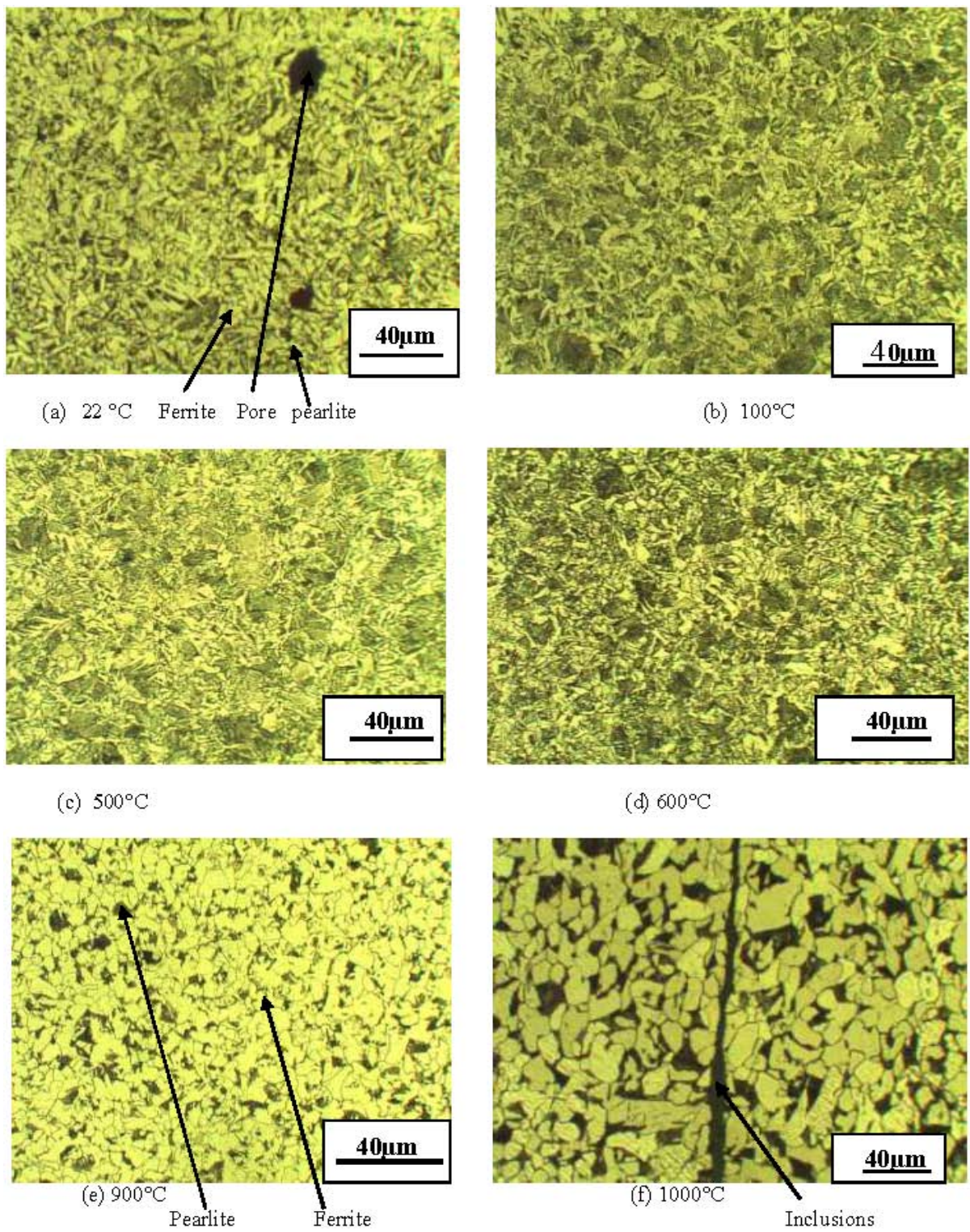


Figure 4.9: Optical micrographs (400x) of various heated and air cooled rebars.

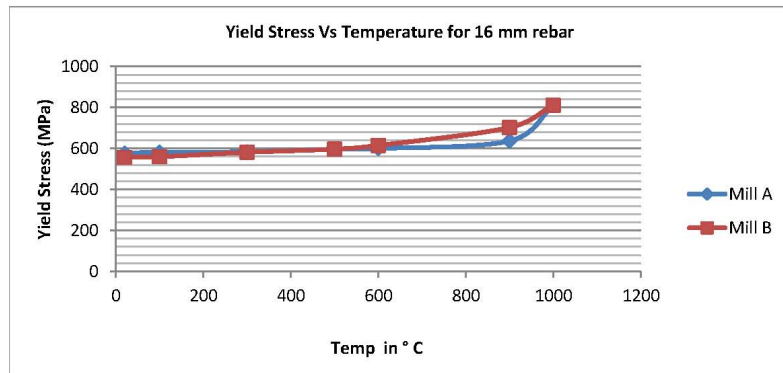
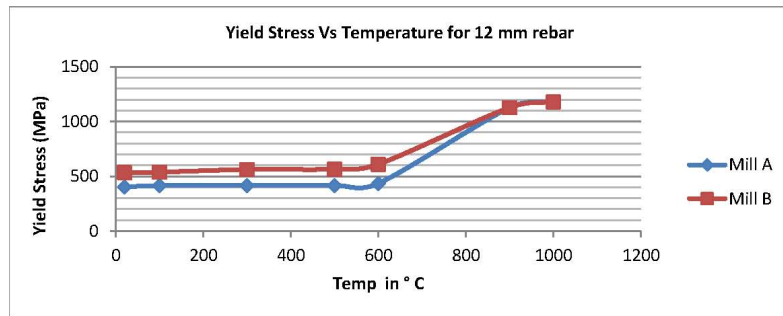
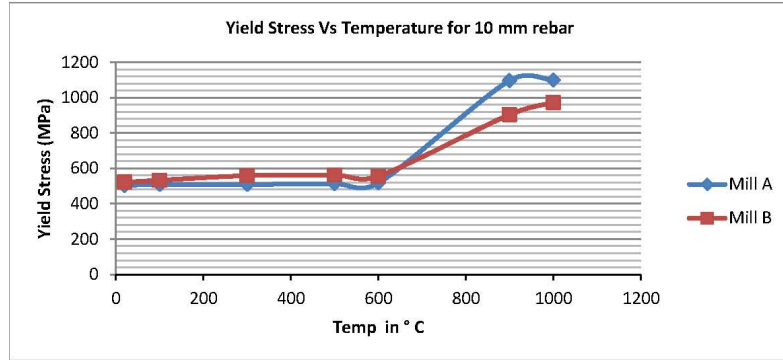


Figure 4.10: Yield Stress Vs Temperature for water quenched rebars from Mills A and B

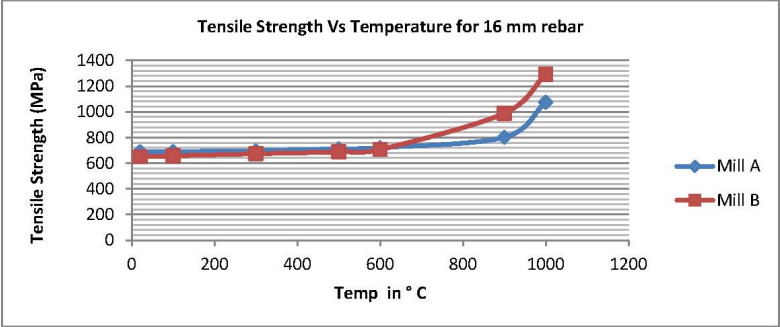
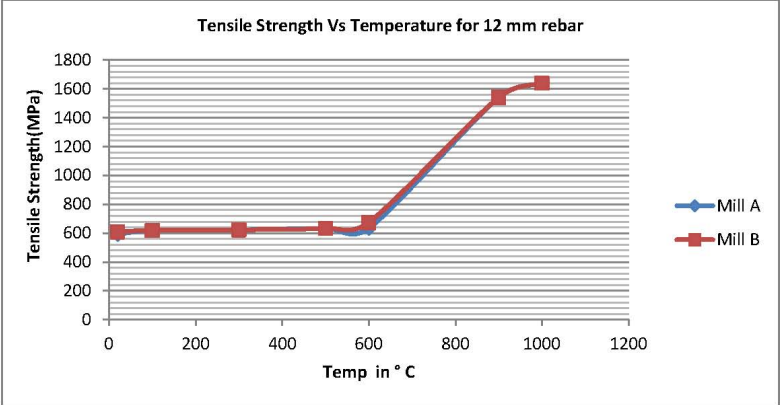
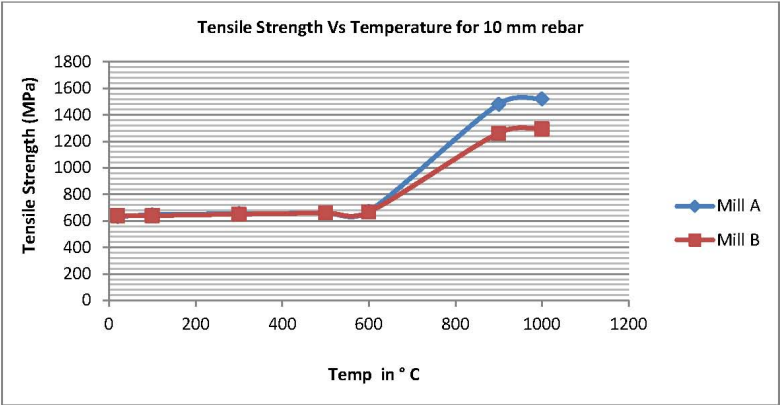


Figure 4.11: Tensile Strength Vs Temperature for water quenched rebars from Mills A and B

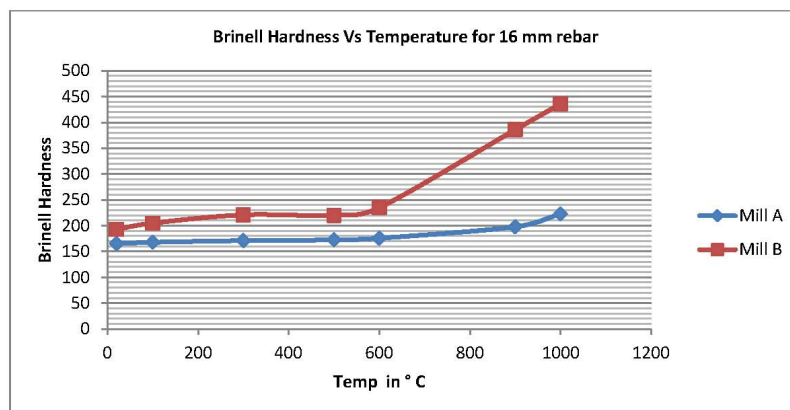
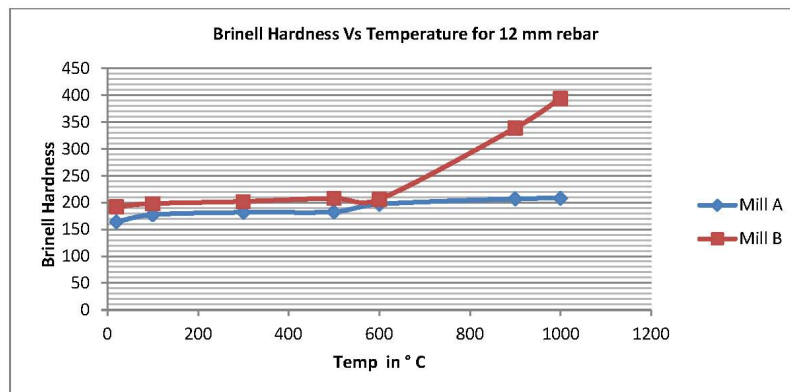
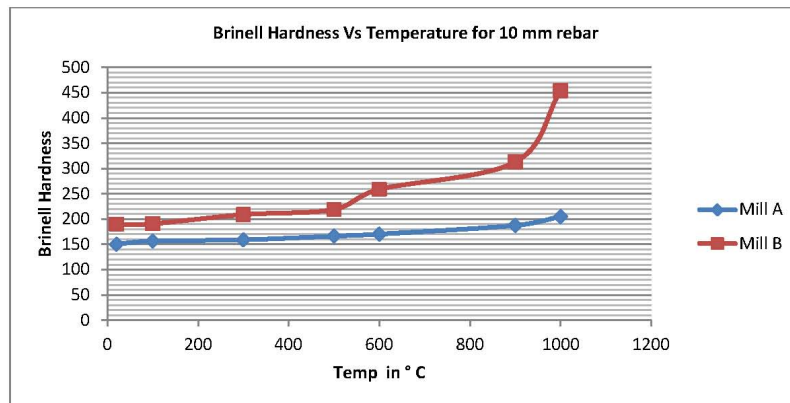


Figure 4.12: Brinell Hardness Vs Temperature for water quenched rebars between Mills A and B

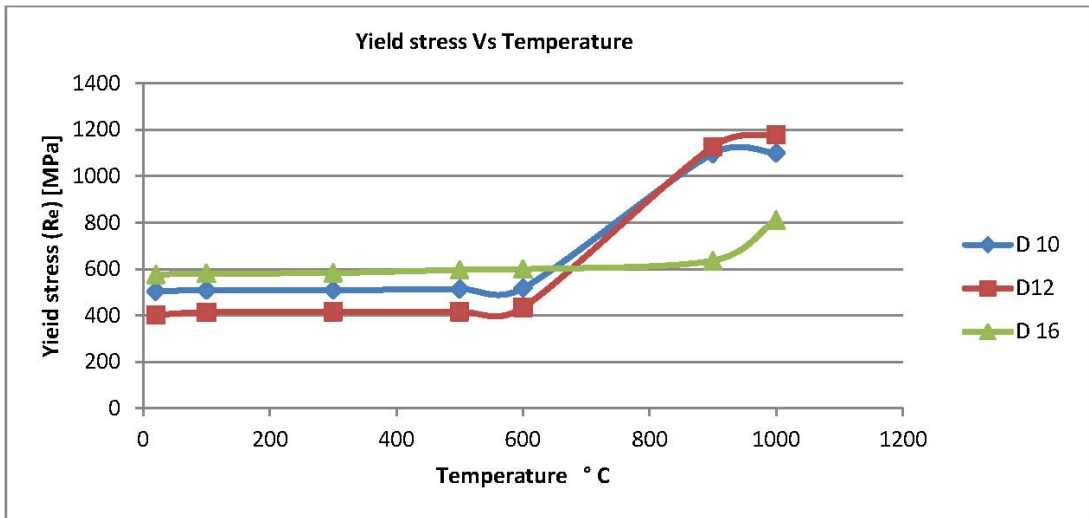


Figure 4.13: Yield stress Vs Temperature for water quenched rebars

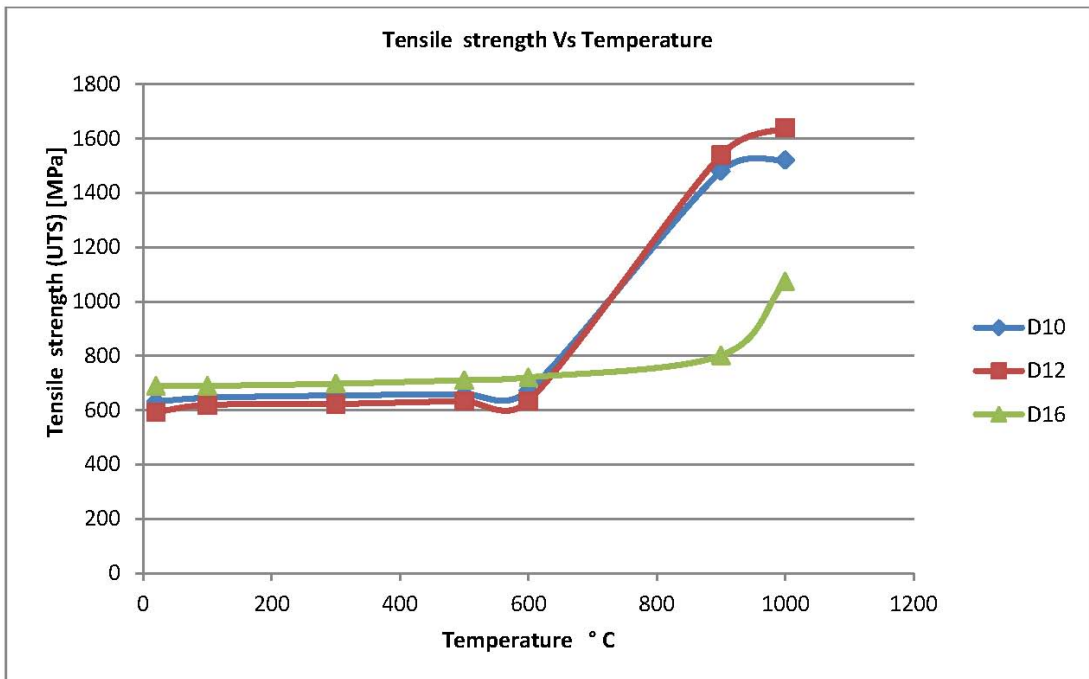


Figure 4.14: Tensile strength Vs Temperature for water quenched rebars

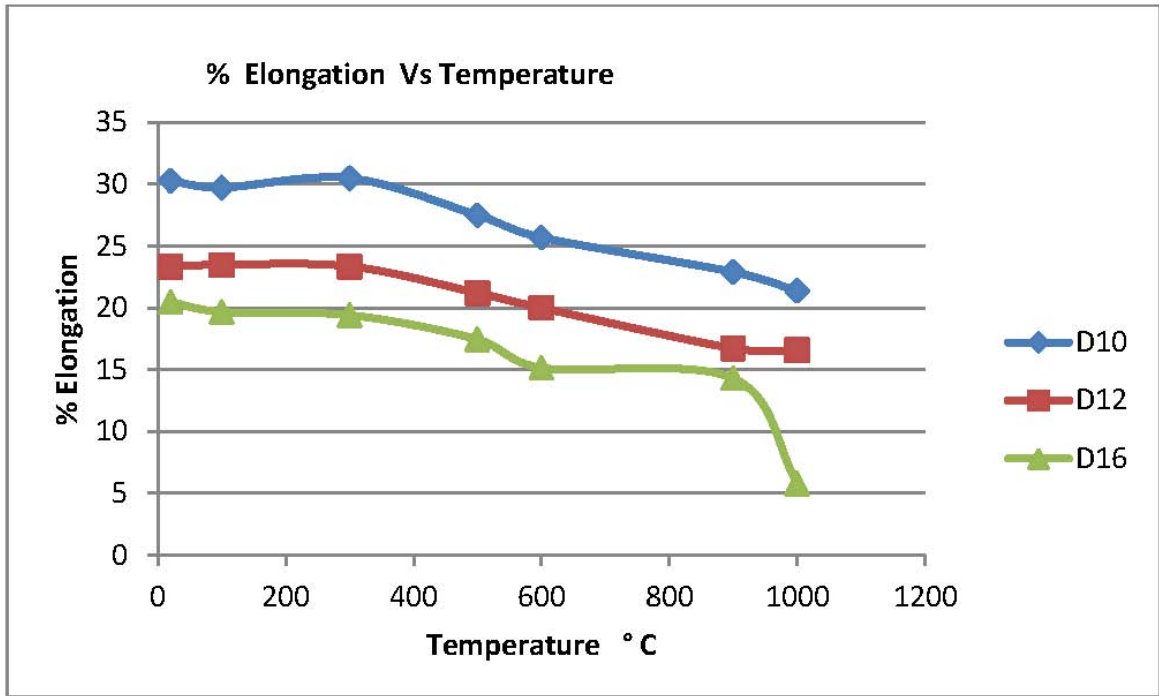


Figure 4.15: Elongation ratio Vs Temperature for water quenched rebars

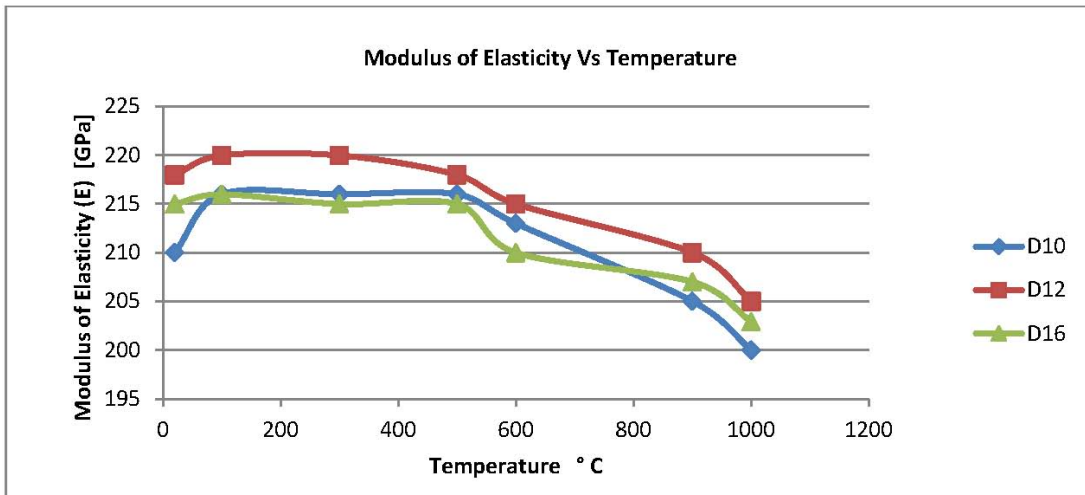


Figure 4.16: Modulus of Elasticity Vs Temperature for water quenched rebars

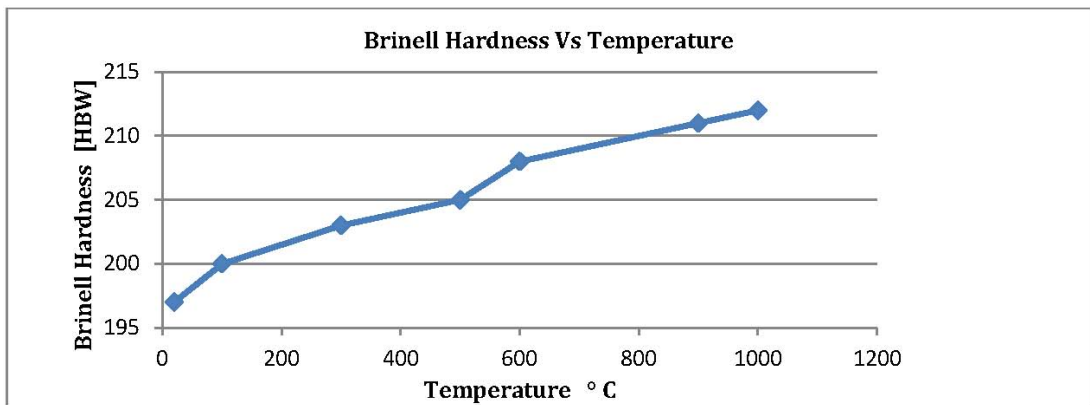


Figure 4.17: Brinell hardness Vs Temperature for water quenched rebars

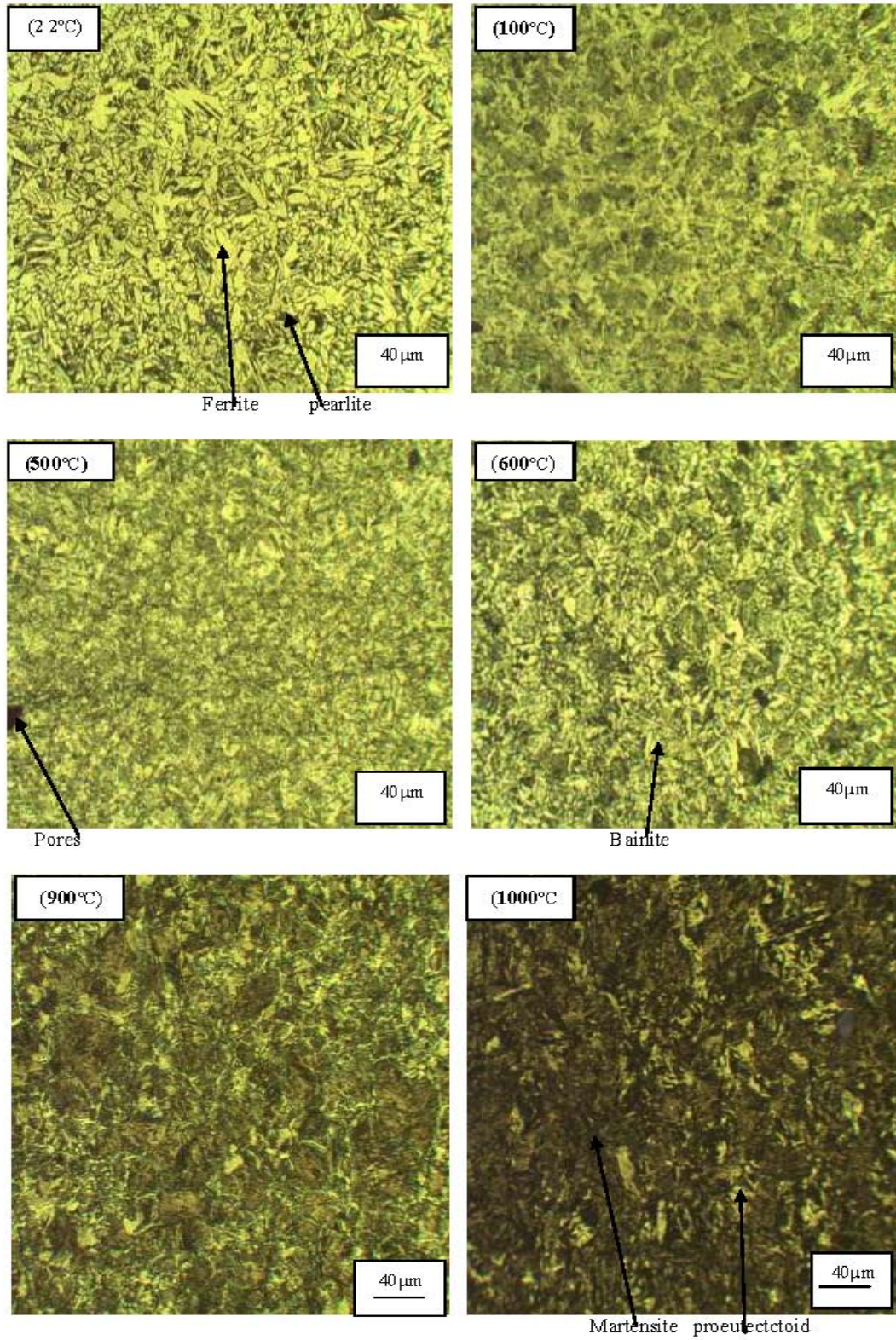
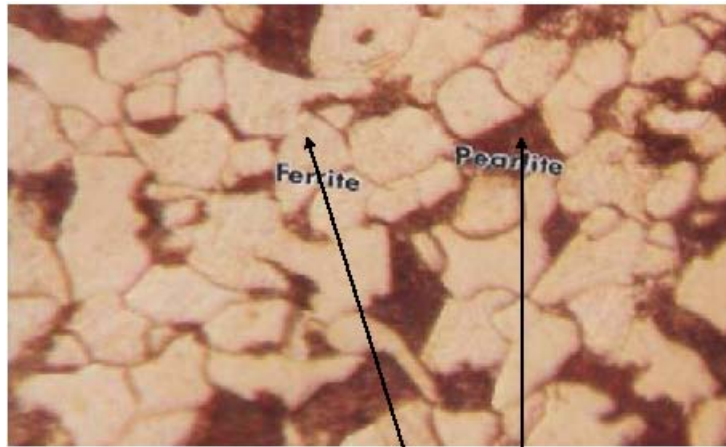


Figure 4.18: Optical micrographs (400X) of various heated and water quenched rebars.



(a) Ferrite and grain pearlite structure



(b) Martensite grain structure

Figure 4.19: Micrographs (400X)

CHAPTER 5

Conclusions and Recommendations

5.1 Introduction

This chapter presents the conclusions and suggests some recommendations.

5.2 Conclusions

The following conclusions can be drawn from this study:

- i The quality control tests carried out on rebars in the industry consisted of Chemical analysis, metallurgical, hardness, tensile, ductility, impact, NTD, bend and rebend testing .
- ii The two methods of production of rebars used in the industry are Tempcore and Cold Twisting processes.
- iii The chemical composition was found not to have a remarkable effect on the critical temperature above which the residual Yield stress becomes lower than the standard allowed value of 460 MPa. The temperature was found to lie between 500 and 600 °C for all rebars examined.

- iv A fatigue life of 1.8×10^6 cycles is observed at a stress amplitude of 132 MPa for 12 mm rebar in constant amplitude axial loading.
- v The rebars sampled showed stable mechanical properties and microstructure after heating up to 500 °C, and cooling in both air and water hence normal bar properties can be assumed after exposure to temperatures up to 500 °C for one hour.
- vi For higher temperatures between 500 to 1000 °C, the retained Yield stress as a proportion of normal rebar properties were: 600 °C - 0.9, 900 °C - 0.7, 1000 °C - 0.6 for air cooling and 600 °C - 1.1, 900 °C - 2.0, 1000 °C - 2.2 for water quenching.
- vii Yield stress, tensile strength, Modulus of Elasticity, Brinell hardness and ductility of the rebars decreased with air cooling whereas Yield stress, tensile strength, and Brinell hardness increased while ductility and Modulus of Elasticity decreased with water quenching as the heating temperature increased from 500 to 1000 °C.
- viii The effect of heating the rebars to temperatures from 22 °C to 1000 °C was a high R_m/R_e ratio (above 1.25) hence the 10 and 12 mm steel rebar are recommended in applications in earthquake prone areas.
- ix The toughness of the 12 and 16 mm rebars tested was 61 and 63 Joules respectively which was well in excess of the minimum average

CVN toughness specification requirements value of 54 Joules at 22 °C.

5.3 Recommendations

There were some interesting results and observations that came about while conducting this study; however, there are factors worth considering in order to develop a closer understanding of the fatigue performance and effect of heat on the mechanical properties of ribbed steel rebars made from local scrap.

In future research, the following recommendations need to be considered:

- To develop a more comprehensive fatigue testing program with as-received rebars in air that would allow evaluation of other effects such as rebar size, rib height and spacing, corrosion, and welding which were not considered in this present study would be useful.
- Other methods of gripping as-received specimens of large size rebar diameters (over 20 mm) and compared with the current method.
- It is necessary to test more specimens and generate more data on Low Cycle Fatigue (LCF) on rebars and compare the results with the High Cycle Fatigue (HCF) carried out during the present study.

- On Fatigue test methodologies between the as-received specimens used in this experiment and the standard test specimens should be developed in future research in order to compare with the results obtained in this study.
- A random loading can be applied to the steel specimens to simulate the behavior of the rebar under a load more representative of a real earthquake.

References

- [1] John, V. B., *Introduction to Engineering Materials, 2ⁿd Edition. Macmillan Publishing Company Ltd.*
- [2] Alawode, A.J., *Effects of Cold Work and Stress Relief Annealing Cycle on the Mechanical Properties and Residual Stresses of Cold-Drawn Mild Steel Rod - M. Eng Thesis.* Mechanical Engineering Department, University of Ilorin, Nigeria, 2002.
- [3] Dell, K.A., , *Metallurgy Theory and Practical Textbook.* American Technical Society, Chicago.
- [4] Fadare, D. A., Fadara, T. G., and Akanbi, O. Y., “Effect of heat treatment on mechanical properties and microstructure of nst 37-2 steel,” *Journal of Minerals Materials Characterization Engineering*, Vol. 10, pp. 299–308, 2011.
- [5] <http://en.wikipedia.org/wiki/Steel>, 2011.
- [6] <http://www.istc.illinois.edu/info/librarydocs/manuals>, 1998.
- [7] Ashby, Michael, F., Jones, and David, R. H., *An introduction to microstructures, processing and design* . Butterworth-Heinemann, 1992.

- [8] Mathiesen, L. and Maestad, O. , *Climate policy and the steel industry: achieving global emission reductions by an incomplete climate agreement.* [http://www.nhh.no/Files/Filer/institutter/sam/Discussion papers 20/2002/dp20.pdf](http://www.nhh.no/Files/Filer/institutter/sam/Discussion%20papers%202002/dp20.pdf), 2002.
- [9] Winters, A. L. , “Liberalizing european steel trade,” *European Economic Review*, Vol. 39 , pp. 611–621, 1995.
- [10] [http://www.strategyr.com/Steel Scrap Market Report.asp](http://www.strategyr.com/Steel%20Scrap%20Market%20Report.asp) (GIA report), 2014.
- [11] United States Geological Survey Minerals Yearbook-2001, *Recycling Metals*. USGS, 2001.
- [12] Albertson, K. and Aylen, J., “Forecasting using a periodic transfer function: with an application to the uk price of ferrous scrap,” *International Journal of Forecasting*, Elsevier,, Vol. 15(4), pp. 409–419, 1999.
- [13] GoK, *Budget Speech for the Fiscal Year 2009/2010*. GoK, 2009.
- [14] GoK, *Scrap Metal Act*. Printed and published by the government printer, Nairobi, 2014.
- [15] <http://www.engineeringnews.co.za/article/kenya-steel-plant>, 2014.

- [16] <http://www.norstar.com.au/Recycling/Processing/Benefits.aspx>, 2014.
- [17] <http://www.eia.gov/todayinenergy/detail.cfm?>, 2014.
- [18] Wald, F., Da Silva, L. S., and Moore, D. B., “Experimental behaviour of a steel structure under natural fire,” *Fire Safety*, Vol. 41, pp. 509–522, 2006.
- [19] ASTM A615 / A615M, *Standard Specification for Deformed and Plain Carbon-Steel Bars for Concrete Reinforcement*. American Society for Testing and Materials, West Conshohocken, PA, 2014.
- [20] ASTM A996 / A996M-14a , *Standard Specification for Rail-Steel and Axle-Steel Deformed Bars for Concrete Reinforcement* . ASTM International, West Conshohocken, PA, 2014, www.astm.org, 2014.
- [21] ASTM A706 / A706M-14, *Standard Specification for Deformed and Plain Low-Alloy Steel Bars for Concrete Reinforcement* . ASTM International, West Conshohocken, PA, 2014, www.astm.org, 2014.
- [22] Clark, A. P., “Comparative bond efficiency of deformed concrete reinforcing bars,” *ACI*, Vol. 43, pp. 381–400, Issue 11, 1946.

- [23] AASHO, *Road Test Report 4 Bridge Research. High way Research Board Special Report 61D, Washington.* 1962.
- [24] Soretz, S., “Fatigue behaviour of high yield steel reinforcement,” *Concrete Construct. Engng*, Vol. 60, pp. 72–280, 1965.
- [25] TRRL Leaflet LF 637, “Programme for fatigue testing for reinforcement bars,” tech. rep., 1978.
- [26] ACI Committee 439, “Uses and limitations of high strength steel reinforcement,” *ACI J*, Vol. 70 No.2, pp. 77–104, 1973.
- [27] Snowden, L. C., “The static and fatigue performance of concrete beams with high strength deformed bars,” *Building Research Station*, Vol. 70, 1971.
- [28] Bannister, J. L., “The behaviour of reinforcing bars under fluctuating stress,” *Concrete*, Vol. 3, pp. 405–409, 1969.
- [29] Menzies, J. B., “The fatigue strength of steel reinforcement in concrete,” *Building Research Station*, Vol. 71, 1971.
- [30] Tilly, G. P., “Fatigue of reinforced bars in concrete: A review,” *Fatigue of Engineering Materials and Structures, Oxford, England: Pergamon Press*, Vol. 2, pp. 251–268, 1979.

- [31] Chen, B. and Liu, J., “Residual strength of hybrid-fiber reinforced high-strength concrete after exposure to high temperatures,” *Cement and Concrete Research*, Vol. 34, pp. 1065–1069, 2004.
- [32] *www.nde-ed.org*, 2014.
- [33] Serope, K. and Steven, R. S., *Manufacturing, Engineering & Technology, Fifth Edition* . Pearson Education, Inc., Upper Saddle River, 2006.
- [34] *www.epi-eng.com/mechanical/engineering/basics/fatigue/in/metals.htm*. 2015.
- [35] Alexander, M., Alban, J., Anibal, S., and Ivan, U., “Development of a correlation to estimate the fatigue strength for steels based on low-cost test,” *J C.T.F Cienc. Tecnol. Futuro.*, Vol. 4, No.2 , 2010.
- [36] Smith, S., Newman, J., and Piascik, R. , *Simulation of Fatigue Crack Initiation at Corrosion Pits With EDM Notches*. NASA, 2003.
- [37] Atkinson, H., and Anderson, C. , *Estimation of the Maximum Inclusion in Clean Steels and the Relationship with Mechanical Prop-*

- erties*. Dept. of Mechanical Engineering, University of Sheffield, Sheffield, South Yorkshire, England, 2003.
- [38] Yang, Z., and Zhang, J. M. , “The fatigue behaviours of zero inclusion and commercial 42crmo steels in the superlong fatigue life regime,” *Acta Materialia*, Vol. 52, pp. 5235–5241, 2004.
- [39] Juvonen, P. , *Effects of non-metallic inclusions on fatigue properties of Calcium Treated Steels - PhD Thesis*. Helsinki University of Technology, Espoo, Finland, 2004.
- [40] Di Schino and Kenny, J. M. , “Grain size dependence of the fatigue behaviour of a ultrafine - grained aisi 304 stainless steel,” *Materials Letters*, Vol. 57, pp. 3182–3185, 2003.
- [41] Subramanya, V., Padmanabhan, K., and Jaeger, G. , “On the fatigue crack growth behaviour of two ferrite-pearlite microalloyed steels,” *Materials Letters*, Vol. 46, pp. 185–188, 2000.
- [42] Lampman, S., Davidson, G., and Reidenbach, F., “Fatigue and fracture,” *ASM Handbook*, Vol. 19, pp. 96–109, 1996.
- [43] Dowling, N. E. J., “Integral estimations for cracks in infinite bodies,” *Eng. Fracture Mechanic*, Vol. 1, pp. 1–8, 1998.

- [44] Takuhiro, M., “Method for the evaluation of mode i fatigue crack growth rate of prestrained materials,” *Inter. J. of Fatigue*, Vol. 29 (9-11), pp. 1737–1743, 2007.
- [45] Fei, J. and Darwin, D., “Fatigue of high relative rib area reinforcing bars,” tech. rep., 1999.
- [46] Burton, K. T., “Fatigue tests on reinforcing bars,” *ACI J*, Vol. 7, No.3, pp. 13–23, 1965.
- [47] ASTM 615/615M, *Standard Specification for Deformed and Plain Billet - Steel Bars for Concrete Reinforcement*. American Society for Testing and Materials, West Conshohocken, PA., 2012.
- [48] Pasko, T. J., “Effect of welding on fatigue life of high-strength reinforcing steel used in continuously reinforced concrete pavements,” tech. rep., 1971.
- [49] Sanders, W. W., Hoadley, P. G. and Munse, W. H. , “Fatigue behaviour of welded joints in reinforcing bars for concrete,” *The Welding Journal, Research Supplement*, Vol. 40, No. 12, pp. 529–535, 1961.
- [50] Pfister, J. F. and Hongstad, E., “High strength bars as concrete reinforcement, part 6: Fatigue test,” *PCA Research and Develop-*

- ment Laboratory*, Vol. 6 No. 1 (January), pp. 65–84, 1964.
- [51] MacGregor, J. G., Jhamb, I. C. and Nuttall, N., “Fatigue strength of hot rolled deformed reinforcing bars,” *ACI*, Vol. 68, pp. 169–179, 1971.
- [52] McDermott, J. F., “Fatigue tests of a 432 high-strength-steel reinforcing bars,” *Applied research laboratory*, 57.019-901 (5) , p. 23, 1965.
- [53] Hanson, J. M., Burton, K. T., and Hognestad, E., “Fatigue tests on reinforcing bars-effect of deformation pattern,” *PCA Research and development Laboratories*, Vol. 10, No.3, pp. 2–13, 1968.
- [54] McDermott, J. F., “Fatigue characteristics of reinforcing bars with various deformation patterns,” *Applied research laboratory*, 45.019-001 (1), p. 30, 1969.
- [55] Jhamb, I. C. and MacGregor, J. G., “Stress concentrations caused by reinforcing bars deformations. fatigue of concrete: Abeles symposium,” *American Concrete Institute (ACI)*, Vol. 41, pp. 168–182, 1974a.
- [56] Derecho, A. T., and Munse, W. H. , “Stress concentration at external notches in members subjected to axial loadings,” *Bulletin*

- No 494, Engineering Experiment Station, Urbana, IL: University of Illinois, 1968.*
- [57] McDermott, J. F., “Fatigue strength of grade 60 reinforcing bars with a spiral deformation pattern,” *Applied research laboratory*, 57.019-452 (2), p. 20, 1971.
- [58] Hanson, J. M., Helgason, T., and Ball, c., “Fatigue strength of experimental no. 8 grade 60 helix reinforcing bars,” *Research and development Laboratories, cement and concrete research institute, portland cement Association*, p. 29, 1972.
- [59] Jhamb, I. C. and MacGregor, J. G., “Effect of surface characteristics on fatigue strength of reinforcing steel, abeles symposium fatigue of concrete,” *American Concrete Institute (ACI)*, Vol. 41, pp. 139–150, 1974b.
- [60] Wascheidt, H., *Problems of fatigue strength of steel bars embedded in concrete - PhD thesis*. Mechanical Engineering, Aachen, Germany, 1965.
- [61] Helgason, T., Hanson, J. M., Somes, N. F., Corley, G. and Hognestad, E. , “Fatigue strength of high-yield reinforcing bars,” tech. rep., 1976.

- [62] Burton, K. T., “Fatigue tests on reinforcing bars,” *ACI J*, Vol. 7, No.3, pp. 13–23, 1965.
- [63] Frost, N. E, Marsh, K. J. and Pook, L. P., *Metal Fatigue*, pp 54-57, Clarendon Press, oxford. 1974.
- [64] ACI Committee 215, “Considerations for design of concrete structures subjected to fatigue loading,” *ACI J. Proc.*, Vol. 71, pp. 97–121, 1974.
- [65] Gurney, T. R., “The influence of thickness on fatigue strength of welded joints,” pp. 523–534, 1979.
- [66] United States Department of Commerce, *1992 Census of Manufacturers - Blast Furnaces, Steel Works and Rolling and Finishing Mills* . United States Department of Commerce, 1992.
- [67] OECD/IEA, “Recent trends in global greenhouse gas emissions: regional trends 1970-2000 and spatial distribution of key sources in 2000 environmental sciences,” *Environmental Sciences*, Vol. 2, pp. 2–3, 2005.
- [68] IISI, *International Iron and Steel Institute*. IISI, 2001.
- [69] Mantell, E., *Engineering Materials Handbook*. McGraw Hill Book Company, 1958.

- [70] Clauser, H. R. and Brandy, G. S., *Engineering Materials Handbook*. McGraw Hill Book Company, 1977.
- [71] Gewain, R. G, Iwankiw, N. R., and Alfawakhiri, F., *Facts for Steel Buildings-Fire*. American Institute of Steel Construction, 2003.
- [72] Topcu, I. B. and Karakurt, C., “Properties of reinforced concrete steel rebars exposed to high temperatures,” *Research Letters in Materials Science*, Vol. 10, Article ID 814137, 4 pages, 2008.
- [73] Chadha, R. P., and Mundhada, A. R., “Effect of fire on flexural strength of reinforced concrete beam,” *International Journal of Engineering Research Technology (IJERT)*, Vol. 1 Issue 3, 2012.
- [74] Smith, William, F., Hashemi, Javad , *Foundations of Materials Science and Engineering (4th ed.)*. McGraw-Hill. ISBN 0-07-295358-6, 2006.
- [75] AS 3600, *Australian Standard for Concrete Structures*. Australian Standard, 2009.
- [76] ASHI Reporter, *The Effects of Fire on Structural Systems*. American Society of Home Inspectors. American Society of Home Inspectors, 2007.

- [77] AISC, “Facts for steel buildings - fire,” *American Institute of Steel Construction*, Chicago, IL 60601-2000, 1973.
- [78] Rassizadehghani, J., Raygan, S., and Askari, M., “Comparison of the quenching capacities of hot salt and oil baths,” *Metal Sci. Heat Treat*, Vol. 48, pp. 5–6, 2006.
- [79] Herring, D. H., “Grain size and its influence on materials properties,” http://en.wikipedia.org/wiki/Deformation_engineering, 2005.
- [80] Outinen, J., “Mechanical properties of structural steel at elevated temperatures and after cooling down,” *Proceedings of the 10th International Fire and Materials Conference, San Francisco, USA*, pp. 125–126, 2007.
- [81] BS 4449, *Steel for the reinforcement of concrete- Weldable reinforcing steel-Bar, coil and decoiled product- Specification*. BSI, 2005.
- [82] ISO TR 12105, *Methods of Fatigue Testing: Guide to General Principles*. ISO, 2014.
- [83] KS 573, *Kenya Standard - High yield steel bars for the Reinforcement of concrete - Specification*. Kenya Bureau of Standards, 2014.

- [84] ASTM A370-97a , *Standard Test Methods and Definitions for Mechanical Testing of Steel Products* . ASTM International, West Conshohocken, PA, 2014, www.astm.org, 1997.
- [85] Matthew, A., *An Investigation of the Suitability of Using AISI 1117 Carbon Steel in a Quench and Self-Tempering Process to Satisfy ASTM A 706 Standard of Rebar - MSc thesis*. Graduate Department of Materials Science and Engineering, University of Toronto, 2011.
- [86] Senthilkumar, T., Ajiboye, T. K., “Effect of heat treatment processes on the mechanical properties of medium carbon steel,” *Journal of Minerals & Materials Characterization & Engineering.*, Vol. 11, No.2 , pp. 143–152, 2012.
- [87] Nikolaou, J., Papadimitriou, G. D., “Microstructures and mechanical properties after heating of reinforcing 500 mpa class weldable steels produced by various processes,” *Construction and Building Materials*, Vol. 18, pp. 243–254, 2004.
- [88] ISO 15630-1, *Steel for the reinforcement and prestressing of concrete-Test methods-Part 1: Reinforcing bars, wire rod and wire*. 2002.

- [89] ASTM E 112, *Standard Test Methods for Determining Average Grain Size*. American Society for Testing and Materials, West Conshohocken, PA, 2013.
- [90] ISO 7500-1, *Metallic materials - Verification of static uniaxial testing machines - Part 1: Tension /compression testing machines - Verification and calibration of the force-measuring system*. ISO, 2004.
- [91] ISO 6892-1, *Metallic materials-Tensile testing-part1: Methods of test at room temperature*. ISO, 2009.
- [92] ISO 6506-2, *Metallic materials - Brinell hardness test - Part 2: Verification and calibration of testing machines*. ISO, 2004.
- [93] ISO 6506-1, *Metallic materials - Brinell hardness test - Part 1: Test method*. ISO, 2004.
- [94] [http:// www1.veristar.com](http://www1.veristar.com), 2013.
- [95] ISO 148-1, *Metallic materials - Charpy pendulum impact test- Part 1: Test method*. ISO, 2006.
- [96] AASHTO T 244, *Mechanical Testing of Steel Products*. AASHTO, 2009.

- [97] Hansen, L. P., Heshe, G., “Static, fire and fatigue tests of ultra high-strength fibre reinforced concrete and ribbed bars,” *Department of Building Technology and Structural Engineering, Aalborg University, Denmark*, 1999.
- [98] Chad, M. P., *Axial and Torsion Fatigue of High Hardness Steels - MSc thesis*. Mechanical Engineering, University of Toledo, 2011.
- [99] CS2, *Steel Reinforcing Bars for the Reinforcement of Concrete*. The Government of the Hong Kong Special Administrative Region, 2012.
- [100] Reinhard, M., Klaus, B., Friedrich, D., Daniel, M., and Guido, H., “Interactive determination of the fatigue behaviour of reinforcing steel,” *fib Symposium PRAGUE.*, Session 2B-6: Construction Technology, 2011.
- [101] Selden, R., “Progress in rubber and plastics technology,” p. 56, 1995.
- [102] ASM International, *Elements of Metallurgy and Engineering Alloys* . ASM International, Materials Park, Ohio, USA, 2008.
- [103] Bruneau, M., Uang, C., Whittaker, A. S., *Ductile design of steel structures*. McGraw-Hill Professional, 1998.

- [104] CEN Eurocode 3, *prEN1993-1-2: Part 1.2: Structural Fire Design, Eurocode 3: Design of Steel Structures - Stage 49 Draft*. European Committee for Standardization, Brussels., 2003.
- [105] Salvador, B. R., Jilberto, P. F., Marcelo, J. V., Jacqueline, C. S. and Rodrigo, E. A., “Study of the effect of temperature on the hardness, grain size, and yield in electro deposition of chromium on 1045 steel,” *J. Chil. Chem. Soc.*, Vol. 53, No.1 , 2008.
- [106] Oyetunji, A., “Effects of microstructures and process variables on the mechanical properties of rolled ribbed medium carbon steel,” *Journal of Emerging Trends in Engineering and Applied Sciences (JETEAS)*., Vol. 3, No.3 , pp. 507–512, 2012.
- [107] Hofmann, H., “Mechanical Properties. pdf ,” *Advanced Nanomaterials*, 2011.
- [108] Topcu, I. B., and Isikdag, B., “The effect of cover thickness on re-bars exposed to elevated temperatures,” *Construction and Building Materials*. *In press*.
- [109] ACI 318, *Building Code Requirements for Structural Concrete and Commentary*. American Concrete Institute, 2011.

- [110] Chen, J. and Young, B., “Mechanical properties of cold-formed steel at elevated temperatures, proceedings of 17th international specialty conference on cold-formed steel structures,” *Recent Research and Developments in Cold-Formed Steel Design and Construction, University of Missouri-Rolla, USA*, pp. 437–465, 2004.
- [111] Gandhi, U., “Investigation of anisotropy in elastic modulus of steel,” *Workshop on Addressing Key Technology Gaps in Implementing Advanced High-Strength Steels for Automotive Light weighting, TRINA, TTC, 8/30/10, 2012*.
- [112] Jahazi, M., Eghbali, B., “The influence of hot forging conditions on the microstructure and mechanical properties of two microalloyed steels,” *Journal Material Process Technology*, Vol. 113(1-3), pp. 594 – 598, 2001.
- [113] Abdel-Aal, U., and El-Mohollowi, I., “Accelerated cooling of steel rebars establishment of technological and design parameters of the cooling unit by modelling and experimentation,” *Metallurgical Science and Technology*, Vol. 15 (1), pp. 1–24, 1997.
- [114] Odusote, J. K., Adebisi, J. A., Abegunde, M.A. and Adelele, A. A., “Effect of heat treatment on mechanical properties of reinforcing

- steel bars,” *Proceedings of 2013 Annual Conference and Technology Exhibition of Nigeria Society of Engineers*, pp. 10–16, 2013.
- [115] Ndaliman, M. B., “An assessment of mechanical properties of medium carbon steel under different quenching media,” *AU J.T.*, Vol. 15, No.4 , pp. 218–224, 2012.
- [116] Gunduz, S., and Capar, A., “Influence of forging and cooling rate on microstructure and properties of medium carbon microalloy forging steel,” *J. Mater Sci.*, Vol. 41, No.2 , pp. 561–564, 2006.
- [117] Odusote, J. K., Ajiboye, T. K., and Rabiou A. B., “Evaluation of mechanical properties of medium carbon steel quenched in water and oil,” *AU J.T.*, Vol. 15, No.4 , pp. 218–224, 2012.
- [118] Wang, X., Lu, H. M., Li, X. L., LI, L., Zheng, Y. F., “Microscopic phase-field simulation coupled with elastic strain energy for precipitation process of ni-cr-al alloys with low al content,” *Trans. Nonferrous Met. Soc. China.*, Vol. 17, No.4 , p. 122, 2007.
- [119] Oca D. G., Garcia, C., and Munoz-Morris M. A., *The Role of Carbon and Heat Treatment and Mechanical Properties of Carbon Steel*. Prentice-Hall, Inc., 2001.

- [120] Calik, A., “Effect of cooling rate on hardness and microstructure of aisi 1020, aisi 1040 and aisi 1060 steels.,” *International Journal of Physical Sciences.*, Vol. 4, pp. 514–518, 2009.
- [121] Munyazikwiye, B. B., *Investigation on Characterization and Variability of Mechanical properties of Reinforcing Steel Bars made from Scrap - MSc thesis.* Jomo Kenyatta University of Agriculture and Technology (JKUAT), Kenya, 2010.
- [122] Pang, G., Zhang, J., Zhang, H., Liu, C., Wang, R., Wan, Y.,, “The relationship of microstructure and mechanical properties of hot rolled nb-microalloyed high strength rebar steel,” tech. rep., 2005.
- [123] Axmann1, G., *Steels For Seismic Applications: ASTM A913 Grade 50 And Grade 65.* 2001.
- [124] Billingham, J., Sharp, J. V., Spurrier, J., and Kilgallon, P. J.,, *Review of the performance of high strength steels used offshore.* Cranfield University for the Health and Safety Executive, 2003.
- [125] Fatemi, A., *Fatigue Tests and S-N Approach .* University of Toledo, 2008.

- [126] MacGregor, J. G., and Bartlett, F. M., “Reinforced concrete: mechanics and design,” *1st Can. ed. Prentice Hall, Scarborough, ON*, Vol. 68, 2000.
- [127] Matthew, A., *Fatigue Behaviour of Reinforced Concrete Beams Strengthened with CFRP Laminates - PhD thesis*. Royal Military College of Canada, Kingston, 1997.
- [128] Kim, K. S., Chen, X., Han, C., Lee, H. W., “Estimation methods for fatigue properties of steels under axial and torsional loading,” *International Journal of Fatigue*, Vol. 24, pp. 783–793, 2002.
- [129] http://www.fea-optimization.com/ETBX/stresslife_help.html, 2014.
- [130] <http://www.wireweldingmachine.com/Ribbed-Bar.html>. 2011.
- [131] <http://www.steelasia.com/conw.htm>. 2009.
- [132] Thompson, M. K., Jirsa, J. O., Breen, J. E. and Klingner, R. E., *Anchorage Behaviour of Headed Reinforcement: Literature Review*. Center for Transportation Research Bureau of Engineering Research the University of Texas at Austin, 2002.

- [133] Israel, G. D., *Sampling The Evidence of Extension Program Impact. Program Evaluation and Organizational Development, IFAS*, University of Florida, 1992.
- [134] ASTM E739-10, *Steel Standard Practice for Statistical Analysis of Linear or Linearized Stress-Life (S-N) and Strain-Life (S-N) Fatigue Data* . ASTM International, West Conshohocken, PA, 2010, www.astm.org, 2010.
- [135] Nyamu, D. M., Maranga, S. M., Mutuli, S. M., “Selecting a sampling plan for reinforcement bars,” *Industrial Engineering Letters*, ISSN 2224-6096 (Paper) ISSN 2225-0581 (online) Vol. 3, No. 4 , 2013.

Glossary of Terms

5.4 Definitions of terms related to fatigue

Fatigue - The phenomenon of the progressive fracture of a metal by means of a crack which spreads under repeated cycles of stress.

Fatigue life (N_f) - It is the number of applied cycles to achieve a defined failure criterion.

Number of cycles (N) - Number of smallest segments of the force-time, stress-time, strain-time, etc., function that is repeated periodically (See Figure 5.1).

Fatigue strength - It is the stress to which the material can be subjected for a specified number of cycles. The term fatigue strength is used for materials such as most nonferrous metals that do not exhibit well-defined fatigue limits. It is also used to describe the fatigue behavior of carbon and low-alloy steels at stresses greater than the fatigue limit.

Fatigue limit - Fatigue strength at indicated life. This could be 5×10^6 , 10^7 , and 10^8 cycles, etc. Historically, this has usually been defined as the stress generating a life at 10^7 cycles.

Specimen - Portion or piece of material to be used for a single test determination and normally prepared in a predetermined shape and pre-

determined dimensions.

Cyclic Loading - Repetitive loading, as with regularly recurring stresses on a part, that sometimes leads to fatigue fracture. (2) Loads that change value by following a regular repeating sequence of change (See Figure 5.1).

Stress range - Arithmetic difference between the maximum and minimum stress ($\Delta\sigma = \sigma_{max} - \sigma_{min}$) (See Figure 5.1).

Stress amplitude, (σ_a) - One-half the algebraic difference between the maximum stress and the minimum stress in a stress cycle. Stress amplitude often is used to construct S-N diagram ($\Delta\sigma = \sigma_{max} - \sigma_{min}/2.$)(See Figure 5.1).

Mean stress, (σ_m) - is the algebraic mean of the maximum and minimum stress in the cycle ($\Delta\sigma = \sigma_{max} + \sigma_{min}/2.$) (See Figure 5.1).

Stress Ratio (R) - Ratio of minimum to maximum stress during any single cycle of fatigue operation (See Figure 5.1) [129].

S-N curve - Stress amplitude or stress range versus fatigue life plot, in semi-log or log-log basis (See Figure 2.2 and Figure 2.3).

Frequency - Number of force or strain cycles per unit time (second).

High Cycle Fatigue (HCF) - Fatigue testing carried out in the region where elastic behavior is dominant; fatigue life is relatively long and normally in the range 10^4 to 10^7 cycles.

Low Cycle Fatigue (LCF) - Fatigue testing carried out in the region where plastic strain is present; fatigue life is relatively short and normally in the range 10^2 to 10^5 cycles.

Stress concentration factor - Stress concentration factor is the ratio of maximum stress to nominal stress. It is greater than 1 and is a dimensionless parameter.

Stress raisers or stress risers - is a location in an object where stress is concentrated. An object is strongest when force is evenly distributed over its area. Fatigue cracks always start at stress raisers, so removing such defects increases the fatigue strength.

Notches - These are inevitable geometric discontinuities in structures. Stress-Life fatigue analysis assumes a smooth, unnotched specimen. However, in practice most fatigue failures occur at notches or stress concentrations.

Relative rib area - Ratio of projected rib area normal to bar axis to the product of the nominal bar perimeter and the center-to-center rib spacing (See Figures 5.4 [130], 5.2 [131] and 5.3 [132]).

i

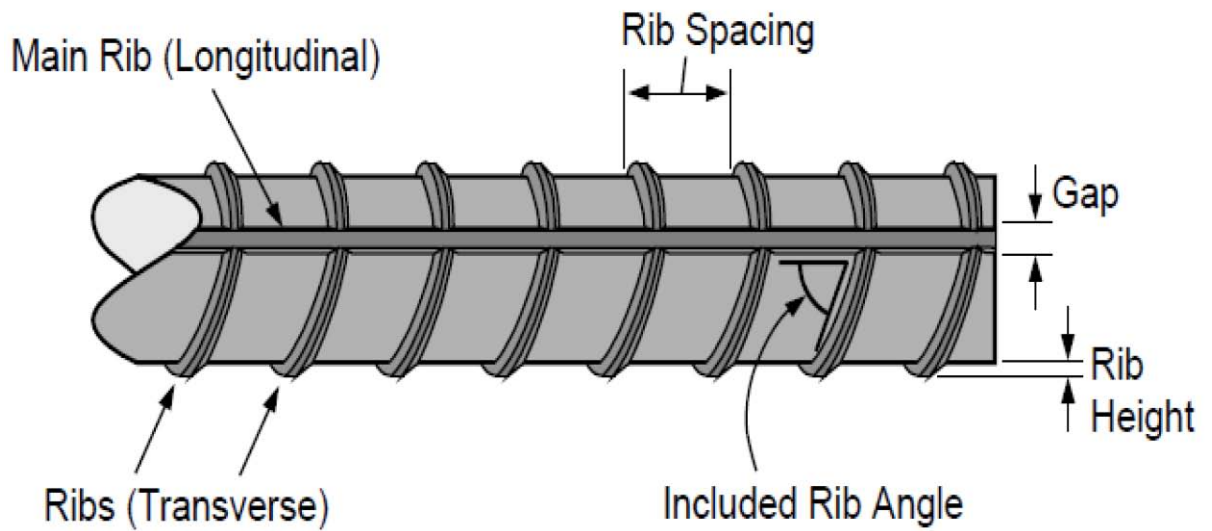


Figure 5.3: Important dimensions of ribbed bar

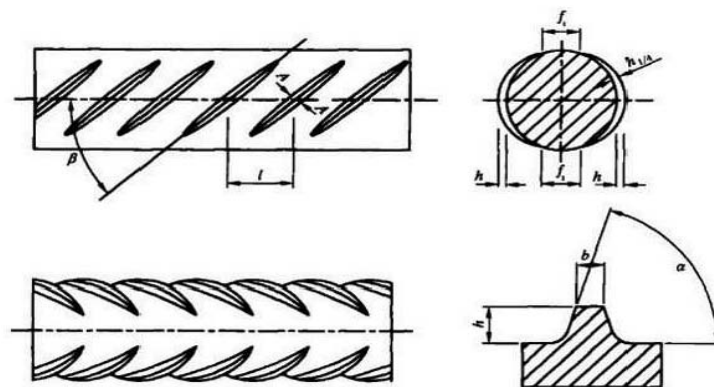


Figure 5.4: Ribbed bar, α - Transverse rib angle; β - angle between the rib and the axis of bar; h -height of mid-point of a bar; l -rib distance; b - rib top width; f_1 - rib spacing

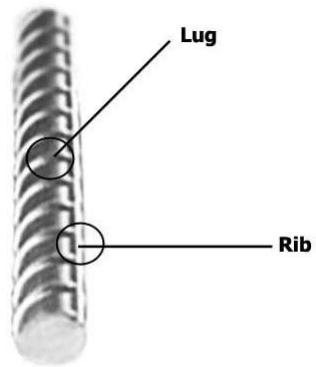


Figure 5.2: Ribbed bar

Appendix A

Questionnaire to steel rolling mills

RESEARCH TOPIC: EFFECT OF HEAT ON PROPERTIES OF REINFORCING
STEEL BARS MADE FROM SCRAP METAL

Department: Mechanical Engineering, Jomo Kenyatta University of
Agriculture and Technology (JKUAT)

Introduction

This survey is a part of MSc study in Design and Production Engineering by Mr. J. O. Bangi, under the supervision of Prof. S. M. Maranga, Prof. S. P. Ng'ang'a of Department of Mechanical Engineering, JKUAT and Prof. S. M. Mutuli Department of Mechanical & Manufacturing Engineering, University of Nairobi. The aim of this research is to study the Effect of Heat on Properties of Reinforcing Steel Bars made from Scrap Metal.

This questionnaire is composed of four sections:

Section 1: Production methods

Section 2: Quality Control

Section 3: Standard sizes of reinforcing bars and application

Section 4: Interest in the Research

Benefits of the study to your company

The results from this study would provide information on the Effect of Heat on Properties of Reinforcing Steel Bars made from Scrap Metal to steel producers, designers, building industry, and standardization bodies. The results may also be used to support other research projects aimed at studying the behaviour of rebar steel structures in fire.

Confidentiality

Your reply will be kept completely confidential.

Filling in the questionnaire

It is expected that the person in charge of quality, will respond to the questionnaire. Recognizing the respondent's valuable time, this questionnaire should require not more than 30 minutes to complete.

Follow-up industrial visits

The researcher of this study will make industrial visits in order to discuss with the appropriate persons the issues of quality control and production processes of the rebars in order to have a better understanding of the same. Your willingness to allow me to make the industrial visit to your factory to observe the quality and production processes will be

very much appreciated. For this purpose, please indicate your response in section 4 question 3 in the research interest section at the end of the questionnaire.

Contact person

Please return the completed questionnaire to:

Mr. Josephat Obwoye Bangi

Department of Mechanical Engineering, JKUAT,

P.O Box 62000, 00200, Nairobi.

Should you have any queries, please do not hesitate to contact me at:

E-mail: bangij@kebs.org

Mobile: 0722830965.

2

General information about the company

Name of the company:

Location: 1. NAIROBI [], 2. MOMBASA [], 3. NAKURU [], 4.

OTHER []

SPECIFY

Address:

Tel No:

Fax:

Email:

Contact person:

Section 1. Production Methods

1. Which method of production for Rebars is used in your factory?

(Please tick [] as appropriate)

a) Work-hardening (cold-working) []

b) Microalloying []

c) Quench and Self-Tempering []

d) Other [], specify

(i)

(ii)

(iii)

2. Which raw materials do you use for manufacturing of the steel re-

bars? (Please tick [] as appropriate)

a) Local scrap metal []

b) Imported scrap metal []

c) Imported billets []

d) Other [], specify

3

(i)

(ii)

(iii)

3. Which type of steel reinforcement bars are manufactured by your factory? (Please tick [√] as appropriate)

a) Twisted bars []

b) Round bars []

c) Ribbed bars []

d) All the above []

e) Other [], specify

(i)

(ii)

(iii)

4. Does the firm use scrap metal to manufacture reinforcing steel bars?

Yes [] No []

³Page 3 of 10 pages

5. If yes how does the firm sort out scrap?

- a) Visual inspection []
- b) Use of magnets []
- c) Conducting chemical analysis []

6. Which furnace do you use for smelting the scraps?

- a) Induction furnace []
- b) Electrical Arc Furnace []
- c) Basic Oxygen Furnace []

4

7. At what temperature do you smelt the scrap?

- a) 1350 °C []
- b) 1470 °C []
- c) Other [], specify
 - (i)

8. What temperature is required for rolling the ingot into bars?

⁴Page 4 of 10 pages

a) 1000 °C []

b) 1050 °C []

c) 1100 °C []

d) Other [], specify

(i)

Section 2: Quality Control

9. As a quality control check, are tests carried out to determine the mechanical properties of the rebars? Yes [] No []

10. If yes, please fill in the following details.

The type of rebar tested:

Test	Equipment used	Relevant Standard (e.g. Kenya Standard, ISO)
Tensile test		
Hardness test		
Fatigue test		
Bend test		
Other tests (specify)		

11. What parameter/s is mostly considered for a good quality of the bars? (Please tick [] as appropriate)

a) Length []

b) Mass []

c) Yield strength []

d) Tensile strength []

e) Elongation []

f) Fatigue []

g) Others [, specify

(i)

(ii)

(iii)

12. How are the testing equipment used for quality checks for the bars verified? (Please tick [] as appropriate)

a) Calibration checks []

b) Split samples []

c) Proficiency sample []

13. Do you carry out analysis on the chemical composition of the rebar?

Yes [] No []

If yes, please fill in the following details:

The type of rebar analysed:

Element	Equipment used	Relevant Standard (e.g. Kenya Standard, ISO)
Carbon		
Sulphur		
Phosphorous		
Silicon		
Manganese		
Other (specify)		

14. If you don't carry out quality control checks, how do you verify the properties of the bars? (Please tick as appropriate)

a) Send specimens to be tested by standard labs

b) Send specimens to be tested by Ministry of Infrastructure materials labs

6

c) Send specimens to be tested by private labs

d) Other specify

(i)

(ii)

15. How do you assure the quality of the results of the test you per-

⁶Page 6 of 9 pages

form?(Please tick [] as appropriate)

- a) internal quality control using secondary reference materials; []
- b) retesting of retained items; []
- c) correlation of results for different characteristics of a rebar
- c) proficiency-testing programmes; []

16. How often is the sampling of the rebars for the quality checks done to verify the properties of the bars? (Please tick [] as appropriate)

- a) One sample for every 25 tons []
- b) Samples are also taken for every 30 tons []
- c) Samples are also taken for every 35 tons []
- d) Other [], specify
- (i)

7

17. What is the minimum yield strength expected by carrying out tensile test?

- a) 250 N/mm² []
- b) 350 N/mm² []
- c) 460 N/mm² []

d) Other [], specify

(i)

18. What is the minimum % Elongation expected by carrying out tensile test?

a) 10 []

b) 12 []

c) 14 []

d) Other [], specify

(i)

Section 3: Standard sizes of reinforcing bars and application

19. What size of the rebar is most ordered for by the users? (Please tick [✓] as appropriate)

a) 8 mm []

b) 10 mm []

c) 12 mm []

d) 16 mm []

e) 20 mm []

f) Other [], specify

(i)

20. What is the estimated 10 mm bars produced by your factory in Tons per year? (Please tick [√] as appropriate)

a) Over 5,000 []

8

b) Over 10,000 []

c) Over 50,000 []

d) Other [], specify

(i)

21. What is the estimated 12 mm bars produced by your factory in Tons per year? (Please tick [√] as appropriate)

a) Over 5,000 []

b) Over 10,000 []

c) Over 50,000 []

d) Other [], specify

(i)

22. What is the estimated number of 16 mm bars produced by your factory in Tons per year? (Please tick [] as appropriate)

a) Over 5,000 []

b) Over 10,000 []

c) Over 50,000 []

d) Other [] specify

(i)

Section 4: Interest in the Research

23. Does your organization require the result from the questionnaire?

.....
.....

24. Explain the benefits your organization may achieve after the survey activity.

.....
.....

9

25. In regards to the above questionnaire, I wish to make a request for your

approval to make an industrial visit to your factory. Yes [] no []

26. Any other comment

.....
.....
.....

Name:

Designation:

Date:

Your time and effort in filling this questionnaire is greatly appreciated

10

Appendix B

Questionnaire to KEBS

RESEARCH TOPIC: EFFECT OF HEAT ON PROPERTIES OF
REINFORCING STEEL BARS MADE FROM SCRAP METAL

Department: Mechanical Engineering, Jomo Kenyatta University
of Agriculture and Technology (JKUAT)

Introduction

This survey is a part of MSc study in Design and Production Engineering by Mr. J. O. Bangi, under the supervision of Prof. S. M. Maranga, Prof. S. P. Ng'ang'a of Department of Mechanical Engineering, JKUAT and Prof. S. M. Mutuli Department of Mechanical & Manufacturing Engineering, University of Nairobi. The aim of this research is to study the Effect of Heat on Properties of Reinforcing Steel Bars made from Scrap Metal.

This questionnaire is composed of two sections:

Section 1: Testing of rebars for quality Control

Section 2: Interest in the Research

Benefits of the study to your company

The results from this study would provide information on the Effect of Heat on Properties of Reinforcing Steel Bars made from Scrap Metal to steel

producers, designers, building industry, and standardization bodies.

1

The results may also be used to support other research projects aimed at studying the behaviour of rebar steel structures in fire.

Confidentiality

Your reply will be kept completely confidential.

Filling in the questionnaire

It is expected that the person in charge of quality, will respond to the questionnaire. Recognizing the respondent's valuable time, this questionnaire should require not more than 30 minutes to complete.

Follow-up industrial visits

The researcher of this study also plans industrial visits in order to discuss with the appropriate persons the issues of quality control of the rebars in order to have a better understanding of the same. Your willingness to allow me to make the industrial visit to your Institute to observe the testing of the rebars for quality processes will be very much appreciated. For this purpose, please indicate your response in section 2 in the research interest section at the end

¹Page 1 of 7

of the questionnaire.

Contact person

Please return the completed questionnaire to:

Mr. Josephat Obwoye Bangi

Department of Mechanical Engineering, JKUAT,

P.O Box 62000, 00200, Nairobi.

Should you have any queries, please do not hesitate to contact me

at:

E-mail: bangij@kebs.org

Mobile: 0722830965.

2

General information about the company

Name of the company:

Location: 1. NAIROBI [], 2. MOMBASA [], 3. NAKURU [], 4.

OTHER []

²Page 2 of 7 pages

SPECIFY

Address:

Tel No:

Fax:

Email:

Contact person:

Section 2: Testing of rebars for quality Control

27. As a quality control check, are tests carried out to determine the mechanical properties of the rebars? Yes [] No []

28. If yes, please fill in the following details.

The type of rebar tested:.....

Test	Equipment used	Relevant Standard (e.g. Kenya Standard, ISO)
Tensile test		
Hardness test		
Fatigue test		
Impact test		
Bend test		
Chemical analysis		
Other tests (specify)		

29. which parameter/s is mostly considered for a good quality of the bars? (Please tick [√] as appropriate)

a) Length []

b) Mass []

c) Yield strength []

d) Tensile strength []

e) Elongation []

f) Fatigue []

g) Others [], specify

(i)

(ii)

(iii)

30. How are the testing equipment used for quality checks for the bars verified? (Please tick [√] as appropriate)

a) Calibration checks []

³Page 3 of 7 pages

- b) Split samples []
- c) Proficiency sample []

31. Do you carry out analysis on the chemical composition of the rebar?

Yes [] No []

If yes, please fill in the following details:

The type of rebar analysed:

Element	Equipment used	Relevant Standard (e.g. Kenya Standard, ISO)
Carbon		
Sulphur		
Phosphorous		
Silicon		
Manganese		
Other (specify)		

4

32. If you don't carry out quality control checks, how do you verify the properties of the bars? (Please tick [√] as appropriate)

- a) Send specimens to be tested by other standard labs abroad []
- b) Send specimens to be tested by Ministry of Infrastructure materials labs []

⁴Page 4 of 7 pages

c) Send specimens to be tested by private labs

d) Other specify

(i)

(ii)

33. How do you assure the quality of the results of the test you perform?(Please tick as appropriate)

a) internal quality control using secondary reference materials;

b) retesting of retained items;

c) correlation of results for different characteristics of a rebar

c) proficiency-testing programmes;

34. How often is the sampling of the rebars for the quality checks done to verify the properties of the rebars? (Please tick as appropriate)

a) One sample for every 25 tons

b) Samples are also taken for every 30 tons

5

c) Samples are also taken for every 35 tons

d) Other , specify

(i)

35. What is the minimum yield strength expected by carrying out tensile test?

a) 250 N/mm² []

b) 350 N/mm² []

c) 460 N/mm² []

d) Other [], specify

(i)

36. What is the minimum % Elongation expected by carrying out tensile test?

a) 10 []

b) 12 []

c) 14 []

d) Other [], specify

(i)

Section 4: Interest in the Research

37. Does your organization require the result from the questionnaire?

.....

.....

38. Explain the benefits your organization may achieve after the survey activity.

.....

.....

6

39. In regards to the above questionnaire, I wish to make a request for your

approval to make an industrial visit to your factory. Yes [] no []

40. Any other comment

.....

.....

.....

Name:

Designation:

⁶Page 6 of 7 pages

Date:

Your time and effort in filling this questionnaire is greatly appreciated

7

Appendix C

Tabulated results on the Effect of Heat on Mechanical Properties and Microstructure - Air cooling

Tables C.1 - C.6 summarize the monotonic mechanical properties of the as-received, heated and air cooled 10, 12, and 16 mm rebars respectively extracted from tensile tests.

Table C.1: Mechanical properties of 10 mm rebar cooled in air from mill A

Temp. °C	R_e [N/mm ²]	R_m [N/mm ²]	R_m/R_e	EL [%]	E [GPa]	HBW
22	517	652	1.26	30	220	155
100	511	657	1.29	30	214	156
300	521	665	1.28	30	218	156
500	505	642	1.27	30	215	156
600	487	620	1.27	28	217	149
900	387	531	1.37	24	200	149
1000	327	541	1.66	24	200	148

Table C.2: Mechanical properties of 10 mm rebar cooled by air from mill B

Temp. °C	R_e [N/mm ²]	R_m [N/mm ²]	R_m/R_e	EL [%]	E [GPa]	HBW
22	537	652	1.22	30	220	219
100	542	641	1.18	28	218	217
300	541	656	1.21	26	217	214
500	524	645	1.23	24	215	209
600	522	611	1.17	22	214	206
900	333	480	1.44	20	200	202
1000	316	481	1.52	18	200	194

Table C.3: Mechanical properties of 12 mm rebar cooled in air from mill A

Temp. °C	R_e [N/mm ²]	R_m [N/mm ²]	R_m/R_e	EL [%]	E [GPa]	HBW
22	430	611	1.42	25	210	165
100	436	621	1.42	26	210	170
300	428	618	1.44	26	210	170
500	445	618	1.39	27	207	169
600	424	601	1.42	24	205	167
900	376	596	1.58	20	205	161
1000	351	590	1.68	20	200	155

Table C.4: Mechanical properties of 12 mm rebar cooled by air from mill B

Temp. °C	R_e [N/mm ²]	R_m [N/mm ²]	R_m/R_e	EL [%]	E [GPa]	HBW
22	559	650	1.16	25	210	218
100	577	668	1.16	26	210	209
300	575	676	1.18	26	210	206
500	571	672	1.18	27	207	204
600	561	633	1.13	29	210	198
900	337	513	1.52	20	210	196
1000	315	478	1.52	20	200	190

Table C.5: Mechanical properties of 16 mm rebar cooled in air from mill A

Temp. °C	R_e [N/mm ²]	R_m [N/mm ²]	R_m/R_e	EL [%]	E [GPa]	HBW	d_n [μm]
22	577	690	1.19	21	210	165	18.9
100	583	692	1.19	23	210	166	17.8
300	580	696	1.20	23	200	165	16.6
500	597	689	1.15	25	200	165	15.3
600	542	647	1.19	21	202	156	15.3
900	356	512	1.44	15	200	155	14.3
1000	317	495	1.56	14	200	146	13.7

Table C.6: Mechanical properties of 16 mm rebar cooled in air from mill B

Temp. °C	R_e [N/mm ²]	R_m [N/mm ²]	R_m/R_e	EL [%]	E [GPa]	HBW	d_n [μm]
22	577	690	1.19	21	210	219	18.0
100	590	711	1.21	23	210	217	17.8
300	580	693	1.20	23	200	214	16.6
500	568	655	1.15	25	200	209	15.6
600	484	560	1.16	21	202	206	15.3
900	411	475	1.16	15	200	202	13.1
1000	321	467	1.46	14	200	194	13.0

Appendix D

Tabulated results on the Effect of Heat on Mechanical Properties and Microstructure - Water quenching

Tables D.1 - D.6 summarize the monotonic mechanical properties of the as-received, heated and air cooled 10, 12, and 16 mm rebars respectively extracted from tensile tests.

Table D.1: Mechanical properties of 10 mm rebar quenched in water from mill A

Temp. °C	R_e [N/mm ²]	R_m [N/mm ²]	R_m/R_e	EL [%]	E [GPa]	HBW
22	505	632	1.25	30	210	197
100	510	646	1.27	30	216	200
300	510	655	1.29	31	216	203
500	515	660	1.28	28	216	205
600	518	673	1.30	26	213	208
900	1098	1480	1.35	23	205	211
1000	1100	1521	1.38	21	200	212

Table D.2: Mechanical properties of 10 mm rebar quenched in water from mill B

Temp. °C	R_e [N/mm ²]	R_m [N/mm ²]	R_m/R_e	EL [%]	E [GPa]	HBW
22	523	640	1.22	25	210	192
100	534	640	1.20	19	204	198
300	560	651	1.16	21	199	211
500	564	661	1.17	19	197	216
600	557	668	1.20	14	194	233
900	905	1262	1.39	8	190	346
1000	974	1294	1.33	6	187	428

Table D.3: Mechanical properties of 12 mm rebar quenched in water from mill A

Temp. °C	R_e [N/mm ²]	R_m [N/mm ²]	R_m/R_e	EL [%]	E [GPa]	HBW
22	403	593	1.47	23	218	197
100	415	619	1.49	23	220	200
300	416	623	1.50	23	220	203
500	417	634	1.52	21	218	205
600	435	634	1.46	20	215	208
900	1128	1540	1.37	17	210	211
1000	1180	1640	1.39	17	205	212

Table D.4: Mechanical properties of 12 mm rebar quenched in water from mill B

Temp. °C	R_e [N/mm ²]	R_m [N/mm ²]	R_m/R_e	EL [%]	E [GPa]	HBW
22	535	609	1.14	21	216	192
100	538	619	1.15	18	214	198
300	562	623	1.11	17	201	211
500	565	634	1.12	17	199	216
600	610	674	1.10	15	196	233
900	1128	1540	1.37	6	193	346
1000	1180	1640	1.39	6	192	428

Table D.5: Mechanical properties of 16 mm rebar quenched in water from mill A

Temp. °C	R_e [N/mm ²]	R_m [N/mm ²]	R_m/R_e	EL [%]	E [GPa]	HBW	d_n [μm]
22	577	690	1.19	20	215	197	18.9
100	582	690	1.19	20	216	200	18.1
300	584	698	1.20	19	215	203	18.0
500	597	711	1.19	17	215	205	17.3
600	600	721	1.20	15	210	208	15.7
900	637	802	1.26	14	207	211	13.8
1000	812	1075	1.32	6	203	212	12.0

Table D.6: Mechanical properties of 16 mm rebar quenched in water from mill B

Temp. °C	R_e [N/mm ²]	R_m [N/mm ²]	R_m/R_e	EL [%]	E [GPa]	HBW	d_n [μm]
22	557	650	1.17	23	217	193	18.6
100	560	659	1.18	22	215	192	18.3
300	582	675	1.16	22	212	198	18.0
500	597	689	1.15	20	212	211	16.7
600	615	708	1.15	20	207	216	16.2
900	702	990	1.41	7	200	233	13.8
1000	812	1293	1.59	6	195	346	12.0

Appendix E

Determining Sample Size for rebars

The three criteria usually needed to be specified to determine the appropriate sample size is: the level of precision, the level of confidence or risk, and the degree of variability in the attributes being measured [133]. There are several approaches to determining the sample size. These include using a census for small populations, imitating a sample size of similar studies, using published tables, and applying formulas to calculate a sample size. The issue of sample size requirements is addressed in ASTM Specification E-739 recommendations [134]

E.1 Using Published Tables

Tables which provide the sample size for a given set of criteria were used, (See Table E.1 [82]) and two points are worth notings. First, this sample size reflects the number of obtained responses, and not necessarily the number of surveys mailed or interviews planned (this number is often increased to compensate for nonresponse). Second, the sample size presumes that the attributes being measured are distributed normally or nearly so. If this assumption cannot be

met, then the entire population may need to be surveyed.

Table E.1: Guidelines for the selection of the minimum number of specimens and the associated degree of replication

Test program classification	Minimum no. of specimens	Degree of replication
Exploratory tests	8 to 12	1.2 to 1.5
Research and development tests	8 to 12	1.5 to 2
Design data tests	12 to 24	2 to 4
Reliability tests	12 to 24	4 to 8
NOTE - in each case the lower minimum number refers to the situation where the general form of the S-N curve is known, and the higher minimum number to where it is not.		

E.2 Using formulas to calculate a sample size

Although tables can provide a useful guide for determining the sample size, it may be required to calculate a sample size for a different combination of levels of precision, confidence, and variability hence the application of one of several formulas.

Israel [133] provides a simplified formula to calculate sample sizes.

Formula (E.1) below was used to calculate the sample sizes at 95% confidence level and $P = 0.5$ are assumed,

where \mathbf{n} is the sample size, \mathbf{M} is the population size, and \mathbf{e} is the level of precision.

$$n = \frac{M}{1 + M(e)^2} \quad (\text{E.1})$$

E.2.1 Formula for calculating a sample for proportions

For populations that are large, Israel [133] developed Equation E.2 to yield a representative sample for proportions,

where

$$n_o = \frac{Z^2 pq}{e^2} \quad (\text{E.2})$$

The formula is valid where n_o is the sample size, Z^2 is the abscissa of the normal curve that cuts off an area at the tails ($1 -$ equals the desired confidence level, e.g., 95%), e is the desired level of precision, p is the estimated proportion of an attribute that is present in the population, and q is $1-p$. The value for Z is found in statistical tables which contain the area under the normal curve.

E.3 Selecting a Sampling Plan for Reinforcement Bars

Random sampling, though ideal, is difficult to achieve. The best and practical sampling method for rebars is systematic sampling as per the standards ASTM A615/615M [47] and BS 4449 [81]. Motivations of cost quite often indicate accidental sampling, or even doing away with testing altogether and having to be content with mill results analysis [135].

Table E.2: Chemical composition (maximum % by mass)

	C	S	P	N^b	Cu	<i>C_{eq}</i>
Cast analysis	0.22	0.05	0.05	0.012	0.8	0.5
Product analysis	0.24	0.055	0.055	0.014	0.85	0.52
^b Higher N contents are permissible if sufficient quantities of N binding elements are present.						

Table E.3: Test stress ranges for nominal bar sizes

Bar size mm	Stress range MPa
Up to and including 16	200
Over 16 up to and including 20	185
Over 20 up to and including 25	170
Over 25 up to and including 32	160
Over 32 up to and including 45	150

Appendix F

Published Papers

The following two papers were published based on the subject matter of this thesis:

F.1 Paper I

Bangi, J. O., Maranga S. M., Ng'ang'a, S. P. and Mutuli, S. M., Effect of Heat on Mechanical Properties and Microstructure of Reinforcing Steel Bars made from Scrap. *Journal of Research in Engineering* Volume 1 (2) 2014, pp 20-26.

F.2 Paper II

Bangi, J. O., Maranga S. M., Ng'ang'a, S. P. and Mutuli, S. M., Effect of Heat and Water Quenching on Mechanical Properties and Microstructure of Reinforcing Steel Bars made from Local Scrap, *International Journal of Engineering, Science and Technology*. Inpress (Accepted)